National Library of Canada
Bibliothèque nationale du Canada

Canadian Theses Service
Service des thèses canadiennes

Ottawa, Canada
K1A 0N4

NOTICE

The quality of this microform is heavily dependent upon the quality of the original thesis submitted for microfilming. Every effort has been made to ensure the highest quality of reproduction possible.

If pages are missing, contact the university which granted the degree.

Some pages may have indistinct print especially if the original pages were typed with a poor typewriter ribbon or if the university sent us an inferior photocopy.

Previously copyrighted materials (journal articles, published tests, etc.) are not filmed.

Reproduction in full or in part of this microform is governed by the Canadian Copyright Act, R.S.C. 1970, c. C-30.

AVIS

La qualité de cette microforme dépend grandement de la qualité de la thèse soumise au microfilmage. Nous avons tout fait pour assurer une qualité supérieure de reproduction.

S'il manque des pages, veuillez communiquer avec l'université qui a conféré le grade.

La qualité d'impression de certaines pages peut laisser à désirer, surtout si les pages originales ont été dactylographiées à l'aide d'un ruban usé ou si l'université nous a fait parvenir une photocopie de qualité inférieure.

Les documents qui font déjà l'objet d'un droit d'auteur (articles de revue, tests publiés, etc.) ne sont pas microfilmés.

La reproduction, même partielle, de cette microforme est soumise à la Loi canadienne sur le droit d'auteur, SRC 1970, c. C-30.

NL-339 (r. 88/04)

Canada

THE UNIVERSITY OF ALBERTA

Potential Rocksliding along Bedding Surfaces in Kananaskis Country

by

Hu, Xian-qin

(C)

A THESIS

SUBMITTED TO THE FACULTY OF GRADUATE STUDIES AND RESEARCH

IN PARTIAL FULFILMENT OF THE REQUIREMENTS FOR THE DEGREE

OF Master of Science

Geology

EDMONTON, ALBERTA

FALL, 1987

Permission has been granted to the National Library of Canada to microfilm this thesis and to lend or sell copies of the film.

The author (copyright owner) has reserved other publication rights, and neither the thesis nor extensive extracts from it may be printed or otherwise reproduced without his/her written permission.

L'autorisation a été accordée à la Bibliothèque nationale du Canada de microfilmer cette thèse et de prêter ou de vendre des exemplaires du film.

L'auteur (titulaire du droit d'auteur) se réserve les autres droits de publication; ni la thèse ni de longs extraits de celle-ci ne doivent être imprimés ou autrement reproduits sans son autorisation écrite.

ISBN 0-315-40948-7

THE UNIVERSITY OF ALBERTA

RELEASE FORM

NAME OF AUTHOR Hu, Xian-qin

TITLE OF THESIS Potential Rocksliding along Bedding Surfaces in Kananaskis Country

DEGREE FOR WHICH THESIS WAS PRESENTED Master of Science

YEAR THIS DEGREE GRANTED FALL, 1987

Permission is hereby granted to THE UNIVERSITY OF ALBERTA LIBRARY to reproduce single copies of this thesis and to lend or sell such copies for private, scholarly or scientific research purposes only.

The author reserves other publication rights, and neither the thesis nor extensive extracts from it may be printed or otherwise reproduced without the author's written permission.

(SIGNED) Xianqin Hu

PERMANENT ADDRESS:

Dept. of Geology
Lanzhou University
Lanzhou, Gansu, P.R. China

DATED July 27th 1987

THE UNIVERSITY OF ALBERTA

FACULTY OF GRADUATE STUDIES AND RESEARCH

The undersigned certify that they have read, and recommend to the Faculty of Graduate Studies and Research, for acceptance, a thesis entitled Potential Rocksliding along Bedding Surfaces in Kananaskis Country submitted by Hu, Xian-qin in partial fulfilment of the requirements for the degree of Master of Science.

.....

Supervisor

.....

.....

Date....July...10th....1987...

Abstract

The stability of 43 overdip slopes, where the bedding dips less steeply than but in the same direction as the slopes, in Kananaskis Country, Alberta, is controlled by frictional properties of the rocks, bedding dips and the rock mass strength rating which is a function of geological structure, intact rock strengths, weathering conditions, properties of the discontinuities and groundwater conditions.

Basic friction angles determined using tilting table tests are from 23° to 41° for pure crystalline carbonates with less than 10% impurity contents, less than 31.5° for impure crystalline carbonates and about 25° for quartz sandstones. Basic friction angles of quartz sandstones and dolostones decrease with displacements. Basic friction angles of pure crystalline carbonates decrease with dolomite contents and increase with grain sizes. Clay minerals and quartz might reduce basic friction angles of impure crystalline carbonates.

The overdip slopes are potential rock slides if the basic friction angles are less than the bedding dips. The minimum value of the apparent cohesion along the bedding surfaces at 11 out of 12 potential rockslide sites and 1 rockslide site in carbonate rocks is in the range of 30KPa to 50KPa. The cohesion prevents the potential rockslides from sliding at these sites. The profiles of many of the potential rockslides are convex or steplike with a dip slope

part or dip slope parts. If the bedding dips are much larger than the basic friction angles, overall dip slopes develop with some thin layers of rocks on the slope to form overdip scarps.

If the basic friction angles are larger than the bedding dips and the latter are between 20° and 30° and the slope is planar, the slope angles are dependent on the rock mass strength ratings. When the bedding dips are less than 20°, steep overdip slopes might develop from the joints perpendicular to bedding surfaces.

Acknowledgement

The author would like to thank my supervisor, Dave Cruden. His consistent guidance and help were essential for the completion of the thesis.

Support from the Department of Geology, University of Alberta, NSERC through an operating grant to D. Cruden and the Ministry of Education of PRC is appreciated.

I am grateful to the staff at the Kananaskis Environmental Research Center for their hospitality.

Special thanks is also to my field assistant, Kevin Lindstrom, whose input and many dedicated hours were indispensable to the thesis.

I am grateful to Tim Eaton, who gave a lot of help during the field investigation.

Mr. Alex Stelmach spent a lot of time helping me with the chemical analyses. His help is appreciated.

Table of Contents

Chapter — Page

Abstract iv

Acknowledgement vi

1. Introduction 1

1.1 General 1

1.2 Purpose and scope 2

1.3 Basic physical principles of rocksliding 4

2. Physical environments 7

2.1 Study area 7

2.2 Climate and drainage 7

2.3 Surficial geology 9

2.4 Bedrock geology 10

2.5 Slope types and potential rockslides 15

3. Site feature descriptions 19

3.1 Introduction 19

3.1.1 Previous work 19

3.1.2 Objectives and observations made in the field investigations 19

3.2 Area north of Mt. Lougheed 33

3.2.1 Site 1 33

3.2.2 Site 2 37

3.2.3 site 3 38

3.3 Area of Mt. Lougheed 39

3.3.1 Site 4 39

3.3.2 Site 5 and Site 6 42

3.4 Area of Mt. Sparrowhawk 43

3.4.1 site 7 43

3.4.2 Site 8 49

3.4.3 Site 9 51
3.4.4 Site 10 53
3.5 Quartzite Ridge Area 55
3.5.1 Site 11 56
3.5.2 Site 12 60
3.5.3 Site 13 60
3.6 Area of Mt. Buller and Mt. Engadine 62
3.6.1 Site 14 62
3.6.2 Site 15 67
3.6.3 Site 16 69
3.7 Area of North Ribbon Creek 71
3.7.1 Site 17 (Mt. Bogart) 71
3.7.2 Site 18 78
3.7.3 Site 19 78
3.7.4 Site 20 79
3.8 Area of Ribbon Creek 81
3.8.1 Site 21 81
3.8.2 Site 22 86
3.8.3 Site 23 87
3.9 Area of Mt. Kidd 87
3.9.1 Site 24 88
3.9.2 Site 25 91
3.10 Area of Galatea Creek 93
3.10.1 Site 26 96
3.10.2 Site 27 97
3.11 Area of Opal Range 98
3.12 Area of Mt. Inflexible 99

3.13 Area of Burstall Pass 103
3.13.1 Site 30 103
3.13.2 Site 31 110
3.13.3 Site 32 110
3.14 Area of Mt. Murray 112
3.15 Area east of Mt. Black Prince 113
3.16 Area of Aster Lake 116
3.16.1 Site 36 116
3.16.2 Site 37 123
3.16.3 Site 38 124
3.16.4 Site 39 124
3.16.5 Site 40 125
3.16.6 Site 41 127
3.17 Area of Highwood Pass 127
3.17.1 Site 42 131
3.17.2 Site 43 131
4. Basic friction angles and the factors influencing variation of basic friction angles 133
4.1 Tilting table tests and the results 133
4.1.1 Introducion to the tilting table tests .133
4.1.2 Sample preparation and testing procedure 135
4.1.3 Test results 137
4.2 Chemical Analysis of the carbonate rocks 144
4.2.1 Test procedure 146
4.2.2 Test results 148
4.3 Grain sizes of the samples 153
4.4 Relationship between basic friction angle, mineral composition and grain size 154

4.4.1 Basic friction angles of the pure carbonate rocks 154

4.4.2 The basic friction angles of the impure carbonate rocks 170

5. Stability analyses of the potential rockslides and other overdip slopes 172

5.1 Evaluation of the cohesion along the potential sliding surfaces 172

5.2 Stability of overdip slopes 182

5.2.1 Potential rockslides 182

5.2.2 Other overdip slopes 185

6. Conclusions 194

Bibliography 196

Appendix

Test Results 203

List of Tables

Table		Page
4.1	Rock samples and the sliding samples	138
4.2	Mean Initial and Final Sliding Angles of the Samples	140
4.3	Modified brittleness indexes for the sliding samples	145
4.4	Weights and Percentages of $CaMg(CO_3)_2$, $CaCO_3$ and Impurities of the Carbonate Samples	149
4.5	Rock types of the carbonate samples after the reclassification based on mineral compositions	150
4.6	Percentages of the Grain Sizes Larger Than 0.06mm for the Carbonate Samples	155
4.7	Dolomite Contents, Percentages of Grains Larger than 0.06mm and Basic Friction Angles of the Pure Carbonate Samples	157
4.8	Results of the simple regression of the basic friction angle on the dolomite content	158
4.9	Results of the regression of the basic friction angle on the dolomite content after deletion	161
4.10	Results of the simple regression of the basic friction angle on the percentage of grains larger than 0.06mm	162
4.11	Results of the simple regression of the basic friction angle on the percentage of grains larger than 0.06mm after deletion	166
4.12	Results of the Multiple regression of the Basic Friction Angle, the Dolomite Content and the Percentage of the Grain Size Larger than 0.06mm	167
4.13	Residuals of basic friction angls from the linear multiple regression equation	168
4.14	Mineral Compositions of the Impure Carbonate Samples and Their Basic Friction Angles	171

Table		Page
5.1	Results of the Lower Bounds of Apparent Cohesion along Bedding Surfaces at 18 Working Sites	178
5.2	Estimated Percentages of the Lower Bounds of Rock Bridges at 14 Working Sites	181
5.3	Potential rock slides in the study area	183
5.4	Rock mass strength ratings at 36 sites	187
5.5	Overdip slope sites except the potential rockslides	188
A.1	Tilting table test results	204
A.2	Results of chemical analyses of the carbonates	211
A.3	Results of indentation tests	212

List of Figures

Figure		Page
2.1	Study Area	8
3.1	Interpreted air photographs in the study area	30
3.2	Schematic drawing of examples of the locations of the centres of the working sites by an overlay on an air photograph	32
3.3	Geology and Working Sites North of Mt. Lougheed, Based on the Air Photograph AS 746 5043 108	35
3.4	Lithology around the potential sliding surface at Site 1	36
3.5	Cross section of the slope at Site 1	36
3.6	Geology and Working Sites in the Area of Mt. Lougheed, Based on the Air Photograph AS 745 5042 55	41
3.7	Geology and Working Sites in the Area of Mt. Sparrowhawk, Northern Part, Based on the Air Photograph AS 745 5041 11	45
3.8	Geology and Working Sites in the Area of Mt. Sparrowhawk, Southern Part, Based on the Air Photograph AS 746 5040 206	47
3.9	Lithology around the potential sliding surface at Site 7	48
3.10	Cross-section of the slope at Site 7	48
3.11	Lithology around the potential sliding surface at Site 8	50
3.12	Cross-section of the slope at Site 8	50
3.13	Cross-section of the slope at Site 9	52
3.14	Cross-sections of the slope at site 10	54
3.15	Geology and Working Sites in the Area of Quartzite Ridge, Based on the Air Photograph AS 746 5040 204	58
3.16	Cross-section at Site 11	59
3.17	Cross-section of the slope at site 12	61

Figure Page

3.18 Geology and Working Sites around Mt. Buller, Based on the Air Photograph AS 746 5039 155 64

3.19 Geology and Working Sites east of Mt. Engadine, Based on the Air Photograph AS 746 5038 109 66

3.20 Cross-section of the slope at Site 14 68

3.21 Cross-section of the slope at Site 16 70

3.22 Geology and Working Sites in the Area of North Ribbon Creek, 1, Based on the Air Photograph AS 746 5040 208 73

3.23 Geology and Working Sites in the Area of North Ribbon Creek, 2, Based on the Air Photograph AS 745 5041 12 75

3.24 Geology and Working Sites in the Area of North Ribbon Creek, 3, Based on the Air Photograph AS 745 5041 14 77

3.25 Cross-sections of the slope at Site 20 80

3.26 Geology and Working Sites in the Area of Ribbon Creek, West Part, Based on the Air Photograph AS 746 5039 157 83

3.27 Geology and Working Sites in the Area of Ribbon Creek, East Part, Based on the Air Photograph AS 746 5039 159 85

3.28 Geology and Working Sites in Mt. Kidd Area, Based on the Air Photograph AS 746 5039 161 90

3.29 Cross-section of the slope at Site 25 92

3.30 Geology and Working Sites in the Galatea Creek Area, Based on the Air Photograph AS 746 5038 113 95

3.31 Geology and the Working Site in the Area of Opal Range, Based on the Air Photograph AS 747 5034 161 101

3.32 Cross-section of the slope at Site 28 102

3.33 Lithology around the potential sliding surface at Site 28 102

Figure Page

3.34 Geology and Working Site in the Area of Mt. Inflexible, Based on the Air Photograph AS 747 5034 157 105

3.35 Cross-section of the slope at Site 29 106

3.36 Geology and Working Sites in the Burstall Pass Area, Based on the Air Photograph AS 747 5033 101 108

3.37 Cross-section of the slope at Site 30 109

3.38 Cross-sections of the slope at Site 31 111

3.39 Geology and Working Sites in the Area of Mt. Murray, Based on the Air Photograph AS 747 5032 56 115

3.40 Geology and Working Site East of Mt. Black Prince, Based on the Air Photograph AS 748 5030 213 118

3.41 Geology and Working Sites in the Aster Lake Area, Southern Part, Based on the Air Photograph AS 749 5024 162 120

3.42 Geology and Working Sites in the Aster Lake Area, Northern Part, Based on the Air Photograph AS 749 5025 215 122

3.43 Lithology around the Potential Sliding Surface at Site 39 126

3.44 Cross-section of the slope at Site 39 126

3.45 Lithology around the Potential Sliding Surface at Site 41 128

3.46 Cross-section of the slope at Site 41 128

3.47 Geology and the Working Sites in the Area of Highwood Pass, Based on the Air Photograph AS 748 5026 19 130

4.1 Calibrated standard relationship between the reading from the Perkin-Elmer#503 Atomic Absorption Instrument and the concentration for magnesium ion 151

4.2 Calibrated standard relationship between the reading from the Perkin-Elmer#503 Atomic Absorption Instrument and the concentration for calcium ion 152

Figure Page

4.3 Results of linear Regression between the Basic Friction Angle and the Dolomite Content 159

4.4 Results of Linear Regression between the Basic Friction Angle and the Dolomite Content after Deletion 163

4.5 Results of Linear Regression between the Basic Friction Angle and the Percentage of the Grain Size 164

4.6 Results of Linear Regression between the Basic Friction Angle and the Percentage of the Grain Size after Deletion 169

5.1 Relationship between the Apparent Cohesion and the Basic Friction Angle 179

5.2 Relationship between the Rock Mass Strength Rating and the Slope Angle 189

5.3 Relationship between the Slope Angle and the Bedding Dip 192

LIST OF SYMBOLS ON FIGURES:

Boundary of the study area

Boundary of geological formations (groups)

Axis of anticline

Axis of syncline

Axis of overturned syncline

Thrust fault, triangles on up-thrust side

Rockslide or rockfall deposit

Talus deposit, triangles pointing up-slope

Cross section

Boundary of working sites

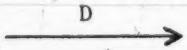

Dip slope

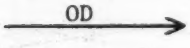

Overdip slope

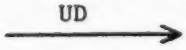

Underdip slope

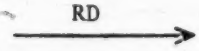

Anaclinal slope

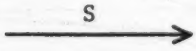

Orthoclinal slope

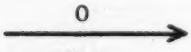

Plagioclinal slope

Rock glacier

SYMBOLS FOR GEOLOGICAL FORMATIONS (GROUPS)

Pleistocene and Recent	
Q	Quaternary
Lower Cretaceous	
Kbl	Blairmore Group
Cretaceous and Jurassic	
Jk	Kootenay Formation
Jurassic	
Jf	Fernie Group
Triassic	
Trs	Sulphur Mountain Formation
Permo-Pennsylvanian	
Prm	Rocky Mountain Group
Mississippian	
Mr	Rundle Group
Mb	Banff Formation (includes Exshaw Formation)
Devonian	
Dp	Palliser Formation
Df	Fairholme Group (includes Alexo-Sassenach and Yahatinda Formation)

SYMBOLS IN EQUATIONS

β	Dip angle of bedding surfaces
γ	Unit weight of rocks
σ	Normal stress acting on bedding surfaces
τ	Shear strength along bedding surfaces
ϕ	Friction angle along bedding surfaces
ϕ_b	Basic friction angle along bedding surfaces
c	Cohesion along bedding surfaces
i	Roughness angle along bedding surfaces
u	Pore pressure
A	Base area of potential sliding mass.
H	Thickness or average thickness of potential sliding mass
F	Safety factor
R	Resistant force which prevents potential sliding masses from sliding
T	Force which makes potential sliding masses slide
W	Weight of potential sliding mass

1. Introduction

1.1 General

Hazard mapping is a relative new undertaking to identify unstable slopes and to forecast the extent, the reach and the velocity of a certain rock mass once it starts accelerating. Pachoud (1975), Kohl (1976), Porter and Orombelli (1981), Carrara (1983, 1984), Whitehouse and Griffiths (1983) and Hansen (1984) provided examples of concerns, hazard models and hazard reports.

Eaton (1986) did detailed hazard mapping in Kananaskis Country of Alberta, Canada. In this reconnaissance of rockslide hazards in 880km², Eaton (1986, p. 64-65) found that dip slopes where the slope surfaces are bedding surfaces and overdip slopes where the bedding surfaces are less steeply than and dip in the same direction as the slopes are only 8% of all the slopes and glaciers. But the relative probability of major rockslides or rockfalls for dip slopes and overdip slopes is much higher than those for other slope types.

The research in this thesis is the continuation of the study of movements and stabilities of natural rock slopes in Kananaskis Country conducted by Eaton (1986). Only overdip slopes are studied in the thesis. All the overdip slopes identified by Eaton (1986) except a few which were inaccessible or small were investigated by the author. Another three overdip slopes adjacent to the study area of

Eaton (1986) were also identified and investigated. The stabilities of these overdip slopes are evaluated in this thesis.

The study area, Kananaskis Country, Alberta, Canada, is located in the Front Ranges of the Rocky Mountains and the rocks in the area are all sedimentary rocks. Because sedimentary rocks dominate Alberta bedrock except in the northeast of the province where Shield rocks are found and also sedimentary rocks cover large parts of the earth's surface, the results of the research may apply to other areas of sedimentary rocks.

1.2 Purpose and scope

The purpose of this research is to study the frictional properties of the sedimentary rocks in the study area, especially carbonate rocks, and to identify potential rockslides and to evaluate the stabilities of the potential rockslides and other overdip slopes by a limit equilibrium method or by the relationship between the rock mass strength rating and the natural slope angle. The cohesion along potential sliding surfaces is also estimated.

The basic physical principles of rocksliding are briefly reviewed in this chapter.

The study area, environmental conditions and general surficial and bedrock geology are described in Chapter 2. Slope types and the potential rockslides are also described and defined.

In Chapter 3, the previous work done in the Canadian Rockies is reviewed. Each of the working sites is described in detail. The descriptions include stratigraphy and geological structure around the working sites, dimensions of the potential rockslides and the factors influencing rock mass strength ratings.

In Chapter 4, the tilting table test and the test results on the rock samples taken from the study area are described and discussed. The procedures of chemical analyses for the rock samples are described and the mineral compositions attained from the analyses are presented. The grain sizes of the samples are examined and the results are given in this chapter too. Finally, the relationships among the basic friction angle, the mineral composition and the grain size of the carbonate rocks are studied and discussed.

In Chapter 5, cohesions along the potential sliding surfaces at potential rockslide sites are calculated by back-analysis using the data determined from the field investigations and from the test results in Chapter 4. The stabilities of all the working sites of overdip slopes are evaluated by the limit equilibrium method or by the relationship between the rock mass strength rating and the natural slope angle.

Conclusions are given in Chapter 6.

1.3 Basic physical principles of rocksliding

The systematic studies of rockslides can go back to 1932, when A. Heim, a geologist, described and analyzed all slides known to him and classified them into twenty types. He noted the very important distinction between slowly progressing slides, where conditions of stability are only slightly disturbed and the very rapidly accelerating slides, where concentrated energy causes rock masses to reach exceedingly velocities (Jaeger, 1979). Terzaghi (1962) suggested that rock slopes should be classified by the type of rock, the analysis of the mechanisms of rupture and the action of water in the pores, fissures and cracks. Müller (1959) and his co-workers emphasised that the behaviour of rock mass is dominated by discontinuities, such as faults, joints and bedding surfaces. The mechanical properties of discontinuities in rocks have been one of the major interests in rock mechanics for many years. The stabilities and movements of rock slopes are controlled by the mechanical properties of discontinuities in many situations. Eaton (1986, p.64) concluded that overdip slopes are the most active high magnitude rockfall and rocksliding zones.

The limit equilibrium method is used to evaluate the stabilities of potential rockslides and the Mohr-Coulomb law is used in calculation in this thesis. If the friction angle, the cohesion and the pore pressure are known, the stability of a slope can be evaluated. Also if the safety factor is specified and the friction angle and pore pressure

is given, the cohesion can be estimated.

The friction angle of a dry smooth rock surface is dependent upon its mineral composition, the texture and the displacement history of the rock. Coulson (1972) gave several profiles of rock surfaces with different surface roughnesses. He observed that the surface roughnesses of some limestone samples and sandstone samples were controlled by their porosity and individual grain sizes if the grain size of lapping compound was appreciably less than the grain size of the rock.

The basic friction angle is one of the most important friction angles and commonly used in stability analyses of rock slopes. Patton (1966a) suggested that the basic friction angle be measured on two rough-sawn surfaces. Coulson (1970) recommended that the basic friction be measured on surfaces rough-sawn and then lapped with #80 grit sandpaper. Bruce (1978, p. 184) noted that the basic friction angle is the sum of the mineral friction angle and the surface roughness produced by sandblasting. So the basic friction angle is determined from a smooth unpolished surface with microscopical roughness. Eaton (1986, p. 117-118) noted that the lower bound value of basic friction angles of dolomites is less than that of limestones and the lower bound value of basic friction angles of limestones is less than that of calcites. So basic friction angles of carbonate rocks seem to depend on the mineral compositions and grain sizes.

Selby (1980) developed a empirical relationship between the rock mass strength rating and the slope angle. If a slope profile is not controlled by the geological structure, is in a limit equilibrium state and without undercutting, the slope angle is only dependent on the rock mass strength rating. So it is useful to analyze the stabilities and the movements of overdip slopes not subjected to sliding by the relationship of Selby (1980). If the angle of a slope is not equal to the value predicted by the relationship, the slope angle may be subject to change due to erosion and weathering.

2. Physical environments

2.1 Study area

Field investigations were conducted over part of Kananaskis Country which is outlined in the Recreational Development Planning Base Map produced by the Alberta Department of Energy and Natural Resources (Alberta Goverment, 1981). In this thesis, the study area (Fig. 2.1) encompasses:

1. All of Peter Lougheed Provincial Park.
2. An area to the north of the provincial park, bounded on the east side by the divide of the Opal range, Evan Thomas Creek, Highway 40 and Lorette Creek, on the west side by Banff National Park, Spray Lakes Reservoir and the creek whose outlet is 2km northwest of outlet of Spurling Creek and on the north by latitude 51°00'.

The study area covers about 884 km². The elevations vary from about 1400m in the lower Kananaskis River valley to 3420m on the top of Mount Joffre situated in the southwest tip of the Provincial Park.

2.2 Climate and drainage

Climatological data from the study area is limited. The mean annual temperature from seven stations around the study area varies from 1.4° to 3.5° Celsius and the precipitation values range from 471 mm to 657 mm with about 45% falling in the form of snow (Environment Canada, 1981). It can be

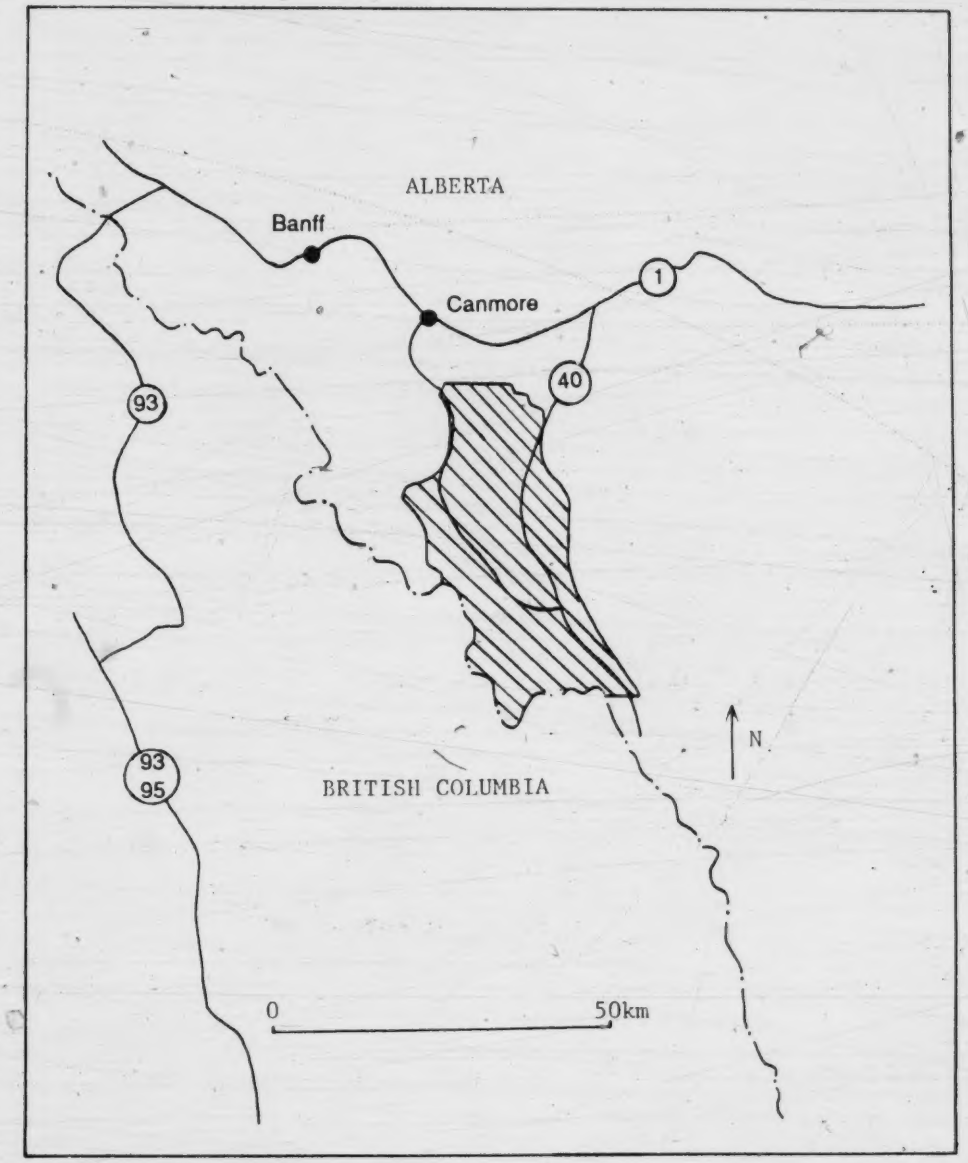

Figure 2.1 The Study Area

expected that freeze-thaw cycles occur everywhere in the study area during the spring and fall seasons. The area is covered by snow all through the year except June, July and August, when there are only some snow patches at higher elevations. Even in June, July and August, it snows in mountain valleys sometimes. The climate in the mountain area is changeable and unpredictable.

The largest river in the study area is the Kananaskis river which flows northward to enter Barrier Lake. There are many small creeks over the study area. The discharge rates of the Kananaskis river and all the small creeks vary greatly with time. The water is mainly from melted snow.

2.3 Surficial geology

Jackson (1976) mapped the surficial geology and made a terrain inventory in Kananaskis Country. Bayrock and Reimchen (1980) mapped surficial geology in Alberta Foothills and Rocky Mountains. Rockslides, slumps and landslides were included in the 29 surficial units. Greenlee (1981) conducted a soil survey around Kananaskis Lakes with interpretations for recreational use.

Four glacial episodes in the Quaternary have reshaped the mountains (Jackson, 1981). Wisconsin tills are represented in the study area by the Bow Valley till, the Canmore till and the Eisenhower Junction till, which are found on the bottom of the main trunk valleys of the study area (Jackson, 1981). The Bow Valley till, the Canmore till

and the Eisenhower Junction till were deposited by the Bow Valley Advance, the Canmore Advance and the Eisenhower Junction Advance (Rutter, 1972). The Bow Valley Advance was in Glacial Episode Three and at or earlier than the Early Wisconsin. The Canmore Advance and the Eisenhower Junction Advance were in Glacial Episode Four and at the Late Wisconsin (Jackson, 1981). Younger neoglacial tills can be found on the floors of many higher tributary valleys. All the tills have been reworked and some alluvial sediments have deposited on the floors of major rivers and valleys and around the outlets of small valleys. Bedrock slopes lie at high elevations. Talus from rockslope movements are found below and/or bedrock slopes.

2.4 Bedrock geology

The Rocky Mountains occupy a strip of land 700km long by 60km wide inside Alberta's border with British Columbia (including Banff and Jasper National Parks). The study area is in the Front Ranges of the Rocky Mountains.

A series of thrust faults strike northwest-southeast through the area. They are Bourgeau thrust fault, Sulphur Mountain thrust fault, Lewis thrust fault, Rundle thrust fault, Lac Des Arcs thrust fault, Exshaw thrust fault and McConnell thrust fault. The strong and old sedimentary rocks are uplifted by the thrust faults to form mountain ranges and the relatively weak and younger rocks floor the big valleys. Normal, reverse and tear faults occur on smaller

scales. Anticlines and synclines extend parallel to the strike of the thrust faults. The bedrock contains at least three joint sets. Two are perpendicular to the bedding and one is subparallel to the bedding. The number of joint sets perpendicular to the bedding can reach 4.

The working sites are in the Devonian Fairholme Group, the Devonian Palliser Formation, the Mississippian Banff Formation, the Mississippian Rundle Group, the Permo-Pennsylvanian Rocky Mountain Group and the Triassic Sulphur Mountain Formation.

The Fairholme Group consists of the Flume, Cairn and Southesk formations.

The Flume Formation (estimated thickness 75m) consists of lower light grey to black, finely and coarsely crystalline to sugary, medium to thickly bedded limestones and dolostones commonly characterizied by reefs of stromatoporoids and corals and upper argillaceous, dark grey, medium bedded, commonly fossiliferous limstones with several bands of dark black shale (Raymond, 1930).

The Cairn Formation (estimated thickness 150 to 335m) consists of two main facies, a lower limestone facies and an upper dolostone facies. The limestone facies can be divided into three units. The lower unit consists of medium crystalline, dark grey and brownish grey dolostone with minor amounts of dolomitic limestone. The middle unit consists of very fine grained, dark grey and light grey weathering limstones with subordinate dolomitic limestone

and calcareous dolostone. The proportion of dolostone increases in the upper unit and the unit consists of dolostone, mottled limestone-dolostone, calcereous dolostone, dolomitic limestone and some limestone. Dark grey chert lenses occur locally. The dolostone facies of the Cairn Formation consists mainly of medium crystalline, dark grey to brownish grey, crystalline dolostones with local stromatoporoid beds (Ollerenshaw, 1968).

The Southesk Formation (estimated thickness 150 to 270m), which overlies the Cairn Formation, consists of medium to coarsely crystalline, saccharoidal, light grey, massive to thickly bedded dolostone that is commonly porous and vuggy. Stringers and nodules of grey and black chert occur locally (Ollerenshaw, 1968).

The only two working sites in the Fairholme Group are in the Southesk Formation.

The Alexo-Sassenach Formation (estimated thickness 90 to 110m), which overlies the Fairholme Group, consists mainly of bedded and brecciated limestone, some fine sandstone and dolostone. All contain or are interbedded with siltstone (deWit and Mclaren, 1950).

The Palliser Formation (estimated thickness 150 to 410m) overlies the Alex-Sassenach Formation and it is divided into a lower Morro Member and an upper Costigan Member. The Morro Member consists of finely crystalline to dense, dark grey brownish grey, cliff forming and massive limestone, which is in part vaguely bedded and in places

altered to dolostone. The Costigan Member consists of bedded and fossiliferous limestone, which is in places underlain by a variable thickness of thin to medium bedded dolostone and layers of limestone breccia (Beach, 1943).

The stratigraphic sequences in the lower and middile parts of the Mississippian succession are different east and west of the McConnell thrust (Middleton, 1963). These two different stratigraphic sequences were termed as the eastern and western facies by Macqueen and Bamber (1967). The study area is west of the McConnell thrust fault. The stratigraphic units include the Exshaw Formation, the Banff Formation and the Rundle Group which consists of the Livingston Formation, the Mount Head Formation and the Etherington Formation (Middleton,1963).

The Exshaw Formation is found within the lowermost Mississippian and consists of a lower black shale member about 6m thick and an upper siltstone-limestone member ranging from a few metres to over 30m (Macqueen, *et al.*, 1972).

The Banff Formation overlies the Exshaw Formation. In the Rocky Mountain Front Ranges, the Banff Formation consists of a sequence of recessive, medium gray or brownish grey, argillaceous carbonate rocks and/or dolomitic shales. The Banff Formation is about 280m to 430m thick in Front Range sections(Macqueen *et al.*, 1972)

The Livingston Formation (340m) overlies the Banff Formation and comprises medium to coarse grained skeletal

limestone; medium crystalline, porous dolostone; fine grained, argillaceous, dolomitic or cherty limestone; and fine crystalline dolostone (Douglas, 1958, p.39).

The Mount Head Formation overlies the Livingston Formation and consists of approximtely 150m to 300m of limestones and dolostones, with local shales, sandstones, siltstones and solution breccias (Macqueen *et al.*, 1972, p. 27).

The Etherington Formation (60m to 90m) overlies the Mount Head Formation and consists of a lower, varicoloured, recessive unit of green shale, micritic and fine grained limestone and microcrystalline to finely crystalline dolostone; a more resistant middle unit of fine grained, sandy and cherty limestone and medium crystalline dolostone; and an upper unit of microcrystalline to finely crystalline dolostone (Douglas, 1958, p.62).

The Rocky Mountain Group overlies the Rundle Group and is divided into three formations, the Tunnel Mountain Formation, the Kananaskis Formation and the Ishbel Formation from bottom to top.

The Tunnel Mountain Formation (estimated thickness 120 to 210m) consists of brown-weathering cliff-forming dolomitic siltstones and sandstones with some bedded and nodular chert. The Kananaskis Formation (estimated thickness 15 to 45m) consists of silty dolostones with chert breccias and nodular and bedded cherts. The Ishbel Formation (estimated thickness 30 to 75m) consists of a chert member

overlying dark cherty, sometimes phosphatic, quartzitic siltstones with rhythemically inter-bedded shaly siltstones (McGugan and Rapson, 1962).

In the study area the rocks of the Rocky Mountain Group are found to be quartz sandstones. The sandstones belong to the lower part of the Tunnel Mountain Formation. The lower part of the Tunnel Mountain Formation is mainly composed of sandstones (Halladay and Mathewson, 1971).

The Sulphur Mountain Formation(estimated thickness 0 to 90m) consists of platy to thin bedded and locally medium-bedded, light yellowish brown to medium brown, medium reddish brown-weathering, dolomitic siltstones and very fine-grained sandstones. These rocks are commonly finely laminated (Ollerenshaw, 1968).

2.5 Slope types and potential rockslides

Many factors can influence the stability of a rockslope, such as climate, seismicity, human intervention, erosion, intact rock strength and mechanical properties of discontinuities within rock masses. The strength of a rockslope, however, is largely controlled by the orientation of discontinuities in the rock mass (Selby, 1982). Faults, joints and bedding are common discontinuities in rocks. In the study area, bedding is the major discontinuity. It is useful then to classify slopes according to the relationships between the orientations of the slopes and those of the bedding surfaces.

According to the relationship between the attitude of the bedding and the dip direction of the slope, the slopes can be divided into four types. They are the cataclinal slope where the slope dips in the same direction as the bedding, anaclinal slope where the slope dips in the oppsite direction to the bedding, orthoclinal slope where the slope is perpendicular to the dip direction of the bedding and plagioclinal slope where the slope is oblique to the dip direction of the bedding (Cruden, 1987). Cataclinal slopes can be divided into overdip slopes, dip slopes and underdip slopes.

An overdip slope is steeper than the dip of the bedding in the rock forming the slope and the two dip directions are the same or the angle between these two dip directions is not larger than 20°. Because bedding surfaces daylight or are exposed on the surfaces of overdip slopes, any bedding surface can be a potential sliding surface if the strength along the surface can become smaller than the sliding force caused by gravity, seismicity and other factors. Two examples of the changes of the frictional properties of discontinuities due to environment changes are that water pressure can reduce the shear strength and cohesion can be worn out with time. In this thesis, an overdip slope is considered to be a potential rockslide if the basic friction angle along the potential sliding surface is less than the dip angle of the bedding. The potential sliding surface is assumed to pass through or around the foot of the overdip

slope because the difference between the resistant force to sliding and the sliding force along the bedding surface through the toe of the slope is larger than those along other bedding surfaces across the slope if the other bedding surfaces are not weaker than the bedding surface through the toe with respect to sliding. This is obvious from the following expression that is derived from Cruden (1975):

$$(R-T)/A=c+H\gamma\cos\beta\tan\phi-H\gamma\sin\beta=c-H\gamma(\sin\beta-\cos\beta\tan\phi) \qquad (2.1)$$

If the pore pressure is taken into account, a similar result can be reached.

In the field investigation, an overdip slope was no longer considered as the potential rock slide if the bedding dip was less than the lower bound of the basic friction angles for the specific rock type from Eaton (1986). In other situations, the overdip slopes were considered as potential rockslides and rock samples were taken to determine basic friction angles later.

A dip slope is parallel to the bedding surfaces. Dip slopes may be considered as the equilibrium phase of an overdip slope from which the rock mass above a certain bedding surface has slid. The common movement of dip slopes is bedding buckling if the bedding is steep enough. Simmons (1977) commented that dip slopes over 50° may fail by rupture across discontinuities. Cavers (1981) analyzed failure of steeply dipping rock masses by buckling and

described a case history from a coal mine in the Rocky Mountains.

Underdip slopes are those slopes whose slope angles are smaller than the dip angles of the major discontinuities. The slopes and the major discontinuities dip in the same direction or the angle between the dip direction of the slope and that of the major discontinuity is less than 20°. Tang (1986) reported two large topples on steep underdip slopes in the Canadian Rockies.

Anaclinal slopes are those which dip in the opposite direction to the major discontinuities in rocks and the angle between the dip direction of the slope and the strike of the major discontinuity is from 70° to 110°. Topplings and rockfalls are common movements for this kind of slope.

When the angle between the dip direction of a slope and the strike of the major discontinuity is within ±20°, the slope is an orthoclinal slope. When the angle between the dip direction of a slope and the strike of the major discontinuity is from 20° to 70°, the slope is a plagioclinal slope. The common movements of these two kinds of slopes are rockfalls.

Based on the measurement of the area of overdip slopes on the 1:50000 topographic maps and the results of Eaton (1986, p.63), the area of overdip slopes was found to be 2.5% of all slopes and glaciers in the study area.

3. Site feature descriptions

3.1 Introduction

3.1.1 Previous work

Locat and Cruden (1977) discussed several rockslides in the Rockies. One of them, the slide at Mt. Indefatigable is along the north shore of Upper Kananaskis Lake. Simmons (1977) observed translational rockslides south of 52° north latitude and cited at least 80 rock slope failures. Bayrock and Reimchen (1980) noted over 900 slides while mapping surficial geology in the Rocky Mountains and Foothills of Alberta and several of the rockslides are in the present study area. Gardner (1980,1982,1983) discussed frequency, magnitude and spatial distribution of rockfalls, rockslides and other forms of alpine mass-wasting in the Highwood Pass area of Peter Lougheed Provincial Park. Eaton (1986) did detailed hazard mapping of rock slope movements in Kananaskis Country, west of Calgary, Alberta.

3.1.2 Objectives and observations made in the field investigations

The objectives of the field investigations were:

1. To confirm and correct the results of the preliminary air photo interpretations. These results include volumes of the potential rock slides identified in the preliminary work, attitudes of the potential sliding

surfaces, geological formations and groups and geological structure at these sites. During the preliminary office work, all the overdip slopes were considered as the potential rock slides. In the field investigation, the overdip slopes where the bedding dips are less than the lower bounds of the basic friction angles from Eaton (1986) are no longer considered as the potential rockslides. The basic friction angles were to be examined later for further evaluations of cohesion along bedding surfaces and stabilities of the potential rockslides. Observe rock types and geological structure in detail.

2. To study the factors which influence rock mass strength ratings, calculate the rock mass strength rating at each site in order to correlate the results with the slope angles of the natural rock slopes.
3. To investigate all the working sites and measure the slope profiles if needed.
4. To take rock samples for determining basic friction angles.

The observations made in the field investigations include:

1. Stratigraphy, geological structure and surficial geology at the working sites. These include descriptions of rock type, attitudes of bedding surfaces and joint planes, folds, faults, colluvium deposits, talus and possible origins of overdip slopes.

At all the working sites, the carbonate rocks are recrystallised. Depositional textures can not be discerned in the carbonate rocks at most of the sites though a few skeletal remains can be seen. So the grains of carbonate rocks include mainly crystals of calcite and dolomite, microsparites and also skeletal grains and maybe lime-mud. In the thesis, if not specified, the carbonate rocks are always considered as crystalline rocks.

The grain sizes of carbonate rocks at the sites follow the grain size classification of Leighton and Pendexter (1962). Fine grains are from 0.12 to 0.25 mm, medium grains are from 0.25 to 0.5 mm, and coarse grains are from 0.5 to 1 mm. In the field, grains less than 0.12 mm were also described as fine grains and grains larger than 1 mm also described as coarse grains. The thickness of the bedding layers are defined as follows: thinly bedded 1 to 10 cm, medium bedded 10 to 30 cm, thickly bedded 30 to 100 cm and massive bedded larger than 100 cm (Ingram, 1954). The attitudes of the bedding surfaces and the joint surfaces are represented by their dip directions and their dip angles unless they are indicated specifically. For example, 235°/30° indicates that the dip direction and the dip angle of the discontinuity are 235° and 30° respectively. But 235° (strike)/90° indicates that the strike of the discontinuity is 235° and it is vertical.

2. Strength of intact rock

One generally accepted measure of strength of intact rock is uniaxial compressive strength. Measurement of this parameter is simple in the laboratory but it requires precisely cut specimens. So it is not possible to use this measure for field investigations at a reconnaissance level. Two field tests of rock strength which may be correlated with uniaxial compressive strength are the point-load strength test and the Schmidt Hammer test.

The point-load test was developed in Russia to provide a rapid strength test of irregularly shaped rock specimens (Protodyakonov, 1960). The International Society for Rock Mechanics (1973) subsequently incorporated the PROTODYAKONOV test as a standard technique. The point-load strength test may be carried out rapidly on irregularly shaped samples and the correlation between the point-load strength index and the uniaxial compressive strength is good for hard rocks.

The Schmidt Hammer test was devised in 1948 by E. Schmidt for carrying out in situ non-destructive tests on concrete. The test measures the distance of rebound of a controlled, spring-load mass impacting on a concrete or rock surface. Because elastic recovery of the rock surface depends upon the hardness of the surface and the hardness is related to uniaxial

compressive strength of the rock, the distance of rebound is a relative measure of surface hardness and the strength of rock. There are three types of Schmidt Hammer. The 'N' type hammer is perhaps the most commonly used for testing rocks. The Schmidt Hammer is light, weighing only 2-3 kg, easy to carry, easy to use and relatively cheap. Large numbers of tests may be done in a short time on a variety of rock surfaces. But the results of Schmidt Hammer test are extremely sensitive to discontinuities within rocks. Even hair-line fractures may lower readings by 10 points. Also the results of the Schmidt Hammer test are sensitive to the weathering of rock surfaces and to moisture on rock surfaces. Due to the long distances from the highway to most of the working sites, only Schmidt Hammer tests were conducted at the working sites.

Of the 10 Schmidt Hammer tests from each rock type at all the sites, the five lowest readings were ignored. Then the mean and the standard deviation were calculated and the mean used as the estimate of the intact rock strength (International Society for Rock Mechanics, 1978). It was found that the difference of the Schmidt Hammer readings among different carbonate rocks is small in the study area. There are generally more than one rock type and textures change for the same rock type within several metres at many of the working sites. So only one Schmidt Hammer reading is used to estimate the

rock mass strength rating at a site because the small variations of the rock strength make no difference for the rock mass strength rating based on the classification used. The results of the Schmidt Hammer reading are represented as mean±standard deviation in this thesis. The Schmidt Hammer readings from intact rocks and from fresh rocks are compared in this thesis where needed. Intact rocks mean that the rocks do not contain cracks or fissures that can be distinguished with a 10X magnifying lens. Fresh rocks mean that the surfaces of the rocks are sawn. The strength classification of intact rock of Selby (1980) is used in this thesis.

3. Weathering conditions

The state of weathering of rocks has an important influence upon its strength. But it is difficult to quantify weathering because zones of weathering may be irregular. Several schemes have been devised for the description of weathering conditions (Moye 1955, Ruxton and berry 1957, Dearman 1974 and 1976). Most schemes divided weathering conditions into six grades ranging from fresh unweathered rock to residual soil. All these classifications are based on changes in color,texture and structure. It is not easy to apply these classifications to carbonate rocks because changes of color, texture and structure of the carbonate rocks due to weathering are not distinct.

The weathering process of carbonates is mainly the dissolution of limstones and dolomites by carbonic acid. The principal reactions are shown by the following simplified equations (Carroll, 1970):

$H_2O+CO_2 \rightarrow H_2CO_3+(HCO_3)^-$ .....production of carbonic acid

$CaCO_3+H^++(HCO_3)^- \rightarrow Ca^{++}+2(HCO_3)^-$ .....limestone reaction in solution

$CaMg(CO_3)_2+2CO_2+2H_2O \rightarrow Ca(HCO_3)_2+Mg(HCO_3)_2$ .....dolomite reaction

The weathering of carbonates produces karren and wide gaps from joints. But unfortunately these processes have not been quantified. Selby (1980) gave a classification modified from the classification of Dearman (1974, 1976). In this thesis the classification of Selby (1980) is used.

It was found that the rock strengths are not noticeably weaker than those of the fresh rocks by Schmidt Hammer tests at all the sites and colour changes of the carbonates are not distinct even around the discontinuities. So it is reasonable to think that the weathering of carbonates does not reduce the strength of the rocks considerably. The rocks at all the sites are considered as slightly weathered.

4. Spacing of discontinuities

The spacing of discontinuities largely controls the size of individual blocks of intact rock. Also the spacing of discontinuities can influence the mechanical properties of rock mass. In the work area, there are at least 3 sets of discontinuities, i.e. bedding surfaces and two sets of joint surfaces. Selby (1980) used the classification of spacing of discontinuities of Deere (1968) to calculate the rock mass strength ratings. This classification is also used in the thesis. If the range of spacings of discontinuities at a site overlies two or more categories of spacings from the classification, an average value is estimated from all the categories involved. This average value is used to calculate the rock mass strength rating.

5. Orientation of discontinuities

The stability of a slope formed in stratified rocks depends primarily on the orientation of the major discontinuity with respect to the hillslope if the uniaxial compressive strength of the rock is greater than 30 MPa (Selby, 1980). Strength classification for orientation of discontinuities of Selby (1980) is used in the thesis.

6. Width of discontinuities

Width of discontinuities largely controls the frictional strength along the discontinuities as well as the flow of groundwater and the rate of weathering of the wall rock. The resistance to shear for widely open

discontinuities depends on the properties of the fill in the discontinuities. But the resistence to shear for tightly closed discontinuities depends on the mechanical properties of the wall rocks and the roughness angle. In the field investigations, the widths of the discontinuities at all the sites are from 0.1 mm to 1 mm except around the slope surfaces where the discontinuities have been opened by the weathering process and the widths here can be larger than 1 mm. Because the stability of the rock masses of a slope is controlled by the strengths of the whole unfavorable penetrative discontinuity and the large part of the discontinuity is within the slope, 0.1 mm to 1 mm of the widths of discontinuities are used to calculate the rock mass strength ratings at all the sites.

7. Size and fill of discontinuities

If a set of discontinuities is not continuous, more cohesion along the discontinuities exists than in the case where the discontinuities are continuous. Filling materials in discontinuities may be composed of clays. So the mechanical properties of the discontinuities can be changed due to different clay mineral contents of the filling material within the discontinuities.

8. Groundwater conditions

Groundwater can promote instability of slopes in the following ways:

a. Water pressure along discontinuities reduces

effective normal stress between rock walls.

b. Water in the pores of rocks and filling materials in discontinuities speeds weathering, solution and disintegration of the rock and alters the cohesion and frictional properties of the infilling materials and rocks.

9. Roughness angle if any exists. Roughness angles are represented as the measured angles between the average dips at the sites and the dips measured on the scale of the measuring lengths. In most of the situations, the measuring lengths are 0.91 m. But 3 m and 5 m are also used as measuring lengths sometimes in order to find the roughness angle on larger measuring base lengths than 0.91 m for the stability analysis. In the field investigation, when the measuring base length was larger than 0.91 m, the roughness angle was estimated by visal estimations. Visal estimations were made by tracing the surface of a rock layer with the help of the geological compass. The measuring lengths are also reported in the thesis. For example, 5°/0.91 m indicates the roughness angle is 5° when the measuring base length is 0.91 m.
10. Thickness and volume of the potential sliding mass.
11. Evidence of movements and failures of the slopes.
12. Profile of slopes_

The shape of the slopes at most of the sites can be described as either planar or convex. The slope angle of a planar overdip slope does not noticeably change from

the toe of the slope to the top of it. The convex overdip slope consists of two parts. The lower part is an overdip slope, on which the bedding dip is less than the slope angle. The upper part is actually a dip slope. At some sites the upper parts are still overdip slopes but the slope angles are less than those of the lower parts.

Based on the results of strengths of intact rocks, weathering conditions, spacings of discontinuities, orientations of discontinuities, widths of discontinuities, sizes and the fill of discontinuities and groundwater conditions, the rock mass strength ratings for the rock masses on slopes can be calculated. The classification of Selby (1980) for rock mass strength ratings is used to calculate rock mass strength ratings in this thesis.

In the individual field description, the names of parking lots, hiking trails, and places are from the maps of Ribbon Creek/Spray Recreation Areas Summer Trails and Kananaskis Provincial Park Summer Trails produced by Alberta Recreation and Parks, Design and Implementation Division, Graphics, Design Branch in 1985.

A series of air photographs of 1:15840 taken in 1958 (Fig. 3.1) are used for the preliminary office work. In this thesis, all the working sites are shown on the overlays of air photographs. The locations of the centre of the sites are represented with the coordinates using the principal point of the photograph as the origin of the coordinates

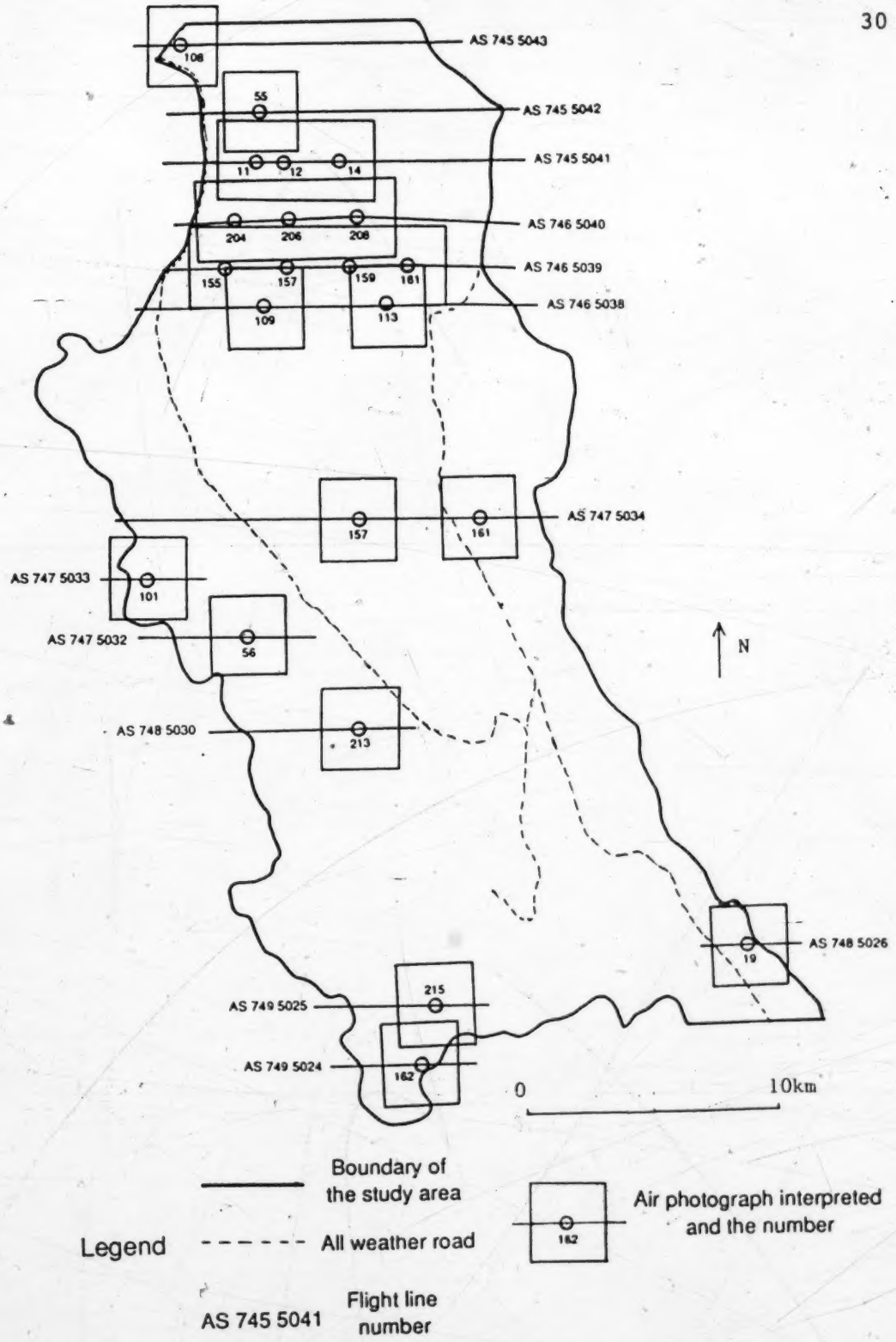

Figure 3.1 Interpreted air photographs in the study area

(Norris,1972). An example is in Figure 3.2. In this example, the coordinates of the point #1 are (10 mm, 20 mm) and those of the point #2 are (-50 mm, 40 mm) with respect to the origin. The stratigraphy and geological structure on the overlays were determined based on the geological map of Seebe-Kananaskis Area (Bielenstein *et al.*, 1971) during the preliminary office work and confirmed in the field investigations.

Cross-sections and geological coulomns are also used in the field descriptions. The scales of the cross-sections in the thesis are same both in the horizontal and vertical directions. So only one scale is given in each cross-section. The descriptions of rock types in the geologic coulomns to show the lithology around the estimated potential sliding surfaces include only colour, grain size and rock type because it seems that only grain size and rock type influence changes of basic friction angles of crystalline carbonate rocks and sandstones.

All the working sites in the study area are grouped by the areas and described in this chapter. Cruden and Eaton (1985a, 1985b) investigated the rockslide hazards in Kananaskis Country and described several sites. Some areas in the thesis fall into the sites of Cruden and Eaton (1985b) and these areas are going to be mentioned in this chapter.

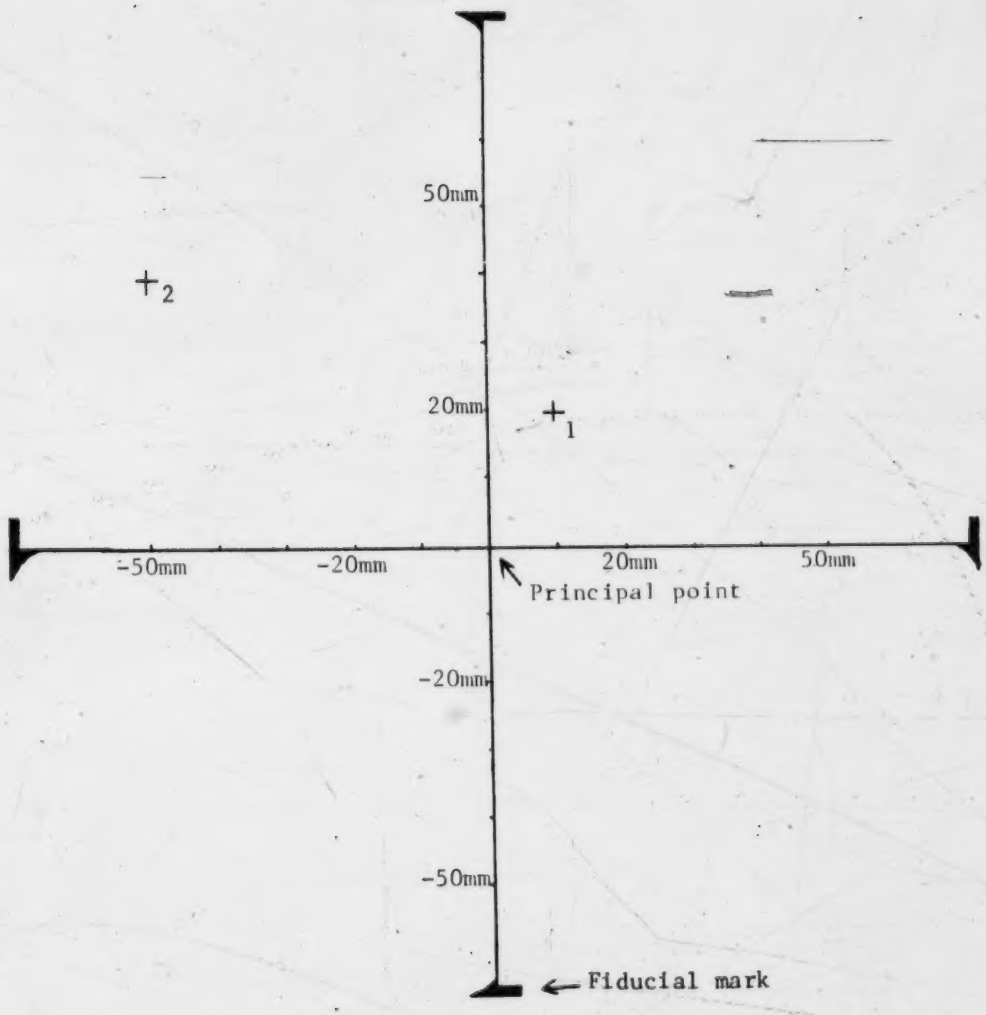

Figure 3.2 Schematic drawing of examples of the locations of the centres of the working sites by an overlay on an air photograph

3.2 Area north of Mt. Lougheed

Three sites (Fig. 3.3) were investigated in the area during the summer of 1986. The sites are 500 m to 1500 m east of the Driftwood Picnicking point on the east shore of the Spray Lakes Reservoir. The access is from the Smith-Dorrien-Spray Trail. Park about 1 km southeast of the Driftwood Picnicking point then hike east to reach the sites. Fairholme Group, Palliser Formation, Banff Formatiom and Rundle Group outcrop in the area. All the strata around the three sites are dipping southwest.

3.2.1 Site 1

The center of the site is at (-10mm, -45mm) on the air photograph AS 745 5043 108 and the site is 500 m east of the road. The rocks around the base of the overdip slope are interlayers of gray, fine to coarse grained limestone, gray, fine to medium grained limestone and light gray, coarse grained limestone of the Rundle Group (Fig. 3.4). The rocks are thinly to medium bedded. The Schmidt Hammer readings do not vary with rock types and are 45±2. The potential sliding surface is within 10 to 20 metres from the base of the Rundle Group. The attitudes of the bedding surfaces are 235°/36°. There are two joint sets and the attitudes of them are 55° /54° to 80° and 235° (strike)/around 90° respectively. The spacings of the bedding surfaces and the joints are about 50 mm to 200 mm and 50 mm to 100 mm respectively. The bedding surfaces are continuous and

Figure 3.3 Geology and Working Sites North of Mt. Lougheed, Based on the Air Photograph AS 746 5043 108

82-J-14 50° - 59' 1:15840 24-8-58
58-1 IR
A. 746 5043 108

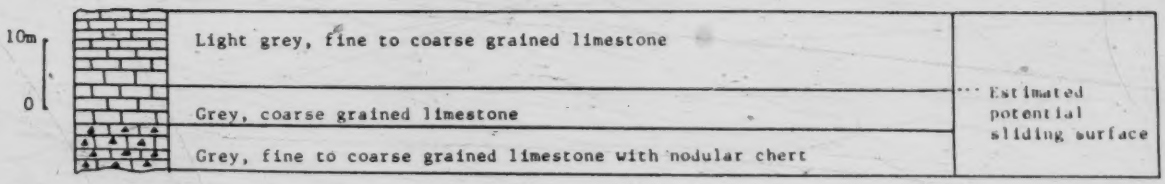
10m
0
Light grey, fine to coarse grained limestone
Grey, coarse grained limestone
Grey, fine to coarse grained limestone with nodular chert
Estimated potential sliding surface

Figure 3.4 Lithology around the potential sliding surface at Site 1

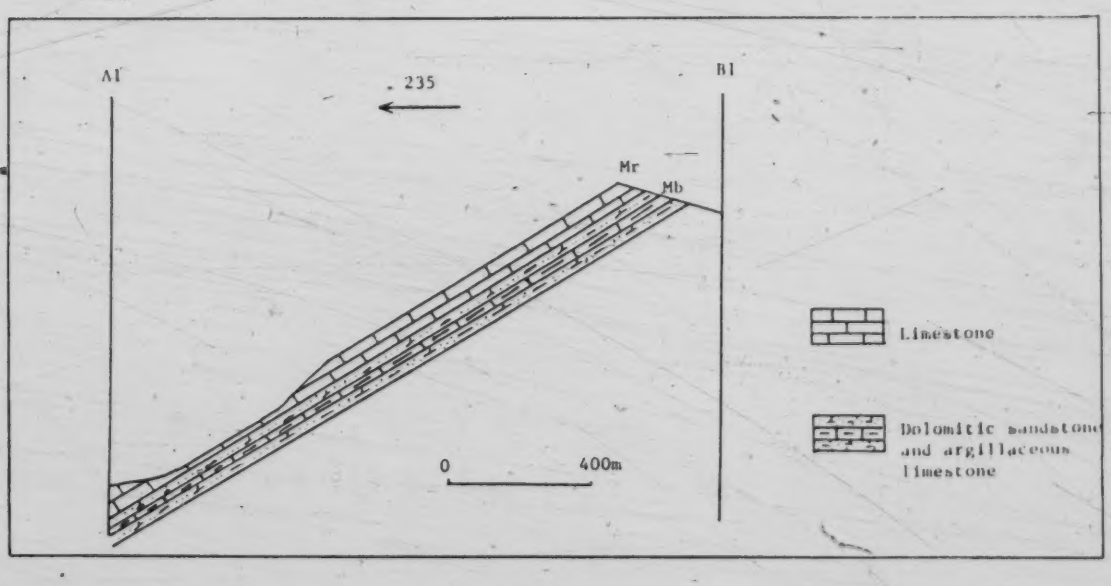

Figure 3.5 Cross section of the slope at Site 1

without fill materials. No groundwater seeps out of the slope. The slope is convex and consists of an overdip slope part and a dip slope part (Fig. 3.5). The slope angle of the overdip slope is 45°. A U-shaped valley is in front of the slope so the overdip slope was formed by glacial processes.

The roughness angle of the bedding surfaces is 0°/0.91m.

The thickness and the volume of the potential sliding mass are 60 m and 26×10^4 m^3 respectively.

Since the bedding surfaces are quite steep and there is no lateral restraint for sliding, there might be some cohesion between the bedding surfaces to prevent the slope from sliding.

3.2.2 Site 2

The site is about 1500 m east of Driftwood Picnicking point on the east shore of the Spray Lakes Reservoir and the center of the site is at the point (60mm, -5mm) with respect to the principal point of the air photograph AS 745 5043 108. The rocks outcropped on the slope are dark grey, medium bedded, fine to coarse grained limestones of the Palliser Formation. The Schmidt Hammer reading is 46±3. The attitude of the bedding surfaces is 220°/25°. Two joint sets exist here and the attitudes of them are 40° to 50°/65° to 80° and 220° (strike)/around 90° respectively. The spacings of the bedding surfaces and the joints are about 200 mm and 120 mm to 450 mm respectively. The bedding surfaces are continuous

and without fill materials. No groundwater seeps out of the slope. The bedding surfaces daylight on the slope formed by a small gully. The slope angle is only 27°, therefore the slope is close to a dip slope. An overdip scarp with the thickness of the strata of less than 2 m can be seen. Most of the slope is covered by the loose rock debris. The slope is planar.

The main types of rock mass movements are rock falling and rolling down the slope and the rock blocks are mainly produced by the joint sets.

3.2.3 site 3

This site is about 200 m southeast of Site 2 and the center of the site is at (80mm, -15mm) with respect to the principal point of the air photograph AS 745 5043 108. The rocks outcropped on the slope are dark grey, thinly to medium bedded, fine to coarse grained limestones of the Palliser Formation. The Schmidt Hammer reading is 47±2. The attitude of the bedding surfaces is 220°/25°. Two joint sets exist here and the attitudes of them are 40°/65° to 80° and 220° (strike)/around 90° respectively. The spacings of the bedding surfaces and the joints are about 50 mm to 200 mm and 120 mm to 450 mm respectively. The bedding surfaces are continuous and without fill materials. No groundwater seeps out of the slope. The slope is similar to that at Site 2. The bedding surfaces daylight on the slope formed by a small gully. The slope angle is only 27° and the thickness of the

thin layers forming the overdip scarp is less than 3 m, therefore the slope is close to a dip slope. Most of the slope is covered by the loose rock debris. The slope is planar.

The main types of rock mass movements are rock falling and rolling down the slope and the rock blocks are mainly produced by the joint sets.

3.3 Area of Mt. Lougheed

Three sites (Fig. 3.6) in the area were visited in the summer of 1986. Access is from the Smith-Dorrien-Spray Trail. Park at the point where the easting is 618300m and the northing is 5645600m on the 1:50000 topographic map. A creek flows west into the Spray Lakes Reservior here. Hike east along the creek for 2500 m to reach Site 4 and hike another 2 km to reach Site 5. Park at the point where the easting is 618150m and the norhting is 5647600m on the 1:50000 topographic map. Hike east along the creek here for 3500 m to reach Site 6. The Rundle Group, the Banff Formation and the Palliser Formation outcrop in the area. A syncline and an anticline go through the area.

3.3.1 Site 4

The center of the site is at the point (-15mm, -30mm) with respect to the principal point of the air photograph AS 745 5042 55. The rocks here are dark grey, fine grained, cherty limestone and bedded, black chert of the Banff

Figure 3.6 Geology and Working Sites in the Area of Mt. Lougheed, Based on the Air Photograph AS 745 5042 55

82 J 14
50° - 58'
24 8 58
58 - 1
IR

Formation. The Schmidt Hammer reading is about 44±2. This overdip slope is on the west limb of an anticline but it is close to the hinge of the anticline. The dip direction of the bedding surfaces is 240° and the dip is from 0° around the hinge of the anticline to 20° around the scarp of the overdip slope. There are two joint sets and both of them are perpendicular to the bedding surfaces. The strike of one joint set is perpendicular to that of the bedding surfaces and the strike of the other joint set is parallel to that of the bedding surfaces. The spacings of the bedding surfaces are between 50 mm and 250 mm and the spacings of the joints are also between 50 mm and 250 mm. The bedding surfaces are continuous and without fill materials. No groundwater seeps out of the slope. The slope is planar and the slope angle is 37°. Because the dip angles of the bedding surfaces are less than 20° which is less than the lower bound of basic friction angles of any rock type (Eaton, 1986), the site is no longer considered as a potential rockslide.

3.3.2 Site 5 and Site 6

The centers of Site 5 and Site 6 are at the points (85mm, -10mm) and (35mm, 65mm) with respect to the principal point of the air photograph AS 747 5042 55. Both the sites are within the Rundle Group and also both of them are around the hinge of the syncline here. It is difficult to climb up the two sites. So no detailed investigations were conducted at the sites. But it can be seen at a distance that the

bedding surfaces dip at less than 15°. The site is no longer considered as a potential rockslide.

3.4 Area of Mt. Sparrowhawk

Four sites (Figs. 3.7 and 3.8) were investigated during the summer of 1986 in the area. The area is within the area immediately east of the Smith-Dorrien-Spray Trail in Cruden and Eaton (1985b). The access to the sites is from the Smith-Dorrien-Spray Trail. Park 750 m north of the Sparrowhawk parking lot and hike up eastward for about 1000 m to reach site 7. The other sites are southeast of this site and on the northeast side of the same valley. All the sites are in the Rundle Group and the bedrock dips to the southwest. One large rockslide occurred in the area. So this area is active with respect to rocksliding.

3.4.1 site 7

The center of this site is at the point (-75mm, -25mm) with respect to the principal point of the air photograph AS 745 5041 11. The bedrock at the site is composed of limestone and dolostone and black chert nodules also exist locally (Fig. 3.9). The grain sizes of the limestones varies from fine to coarse. The Schmidt Hammer reading for the rocks here is 51±2. The attitude of the bedding surfaces is 235° to 240°/27° to 32°. There are two joint sets and the attitudes of them are 55° to 60°/55° to 60° and 240° (strike)/about 90° respectively. The spacings for the

Figure 3.7 Geology and Working Sites in the Area of Mt. Sparrowhawk, Northern Part, Based on the Air Photograph AS 745 5041 11

4854A
6041
BLJ4
50°
58-1 IR
AS 745

Figure 3.8 Geology and Working Sites in the Area of Mt. Sparrowhawk, Southern Part, Based on the Air Photograph AS 746 5040 206

AREA A 3040
9
OD
Mr
RO
OD
CRO
OD
13
OD
D

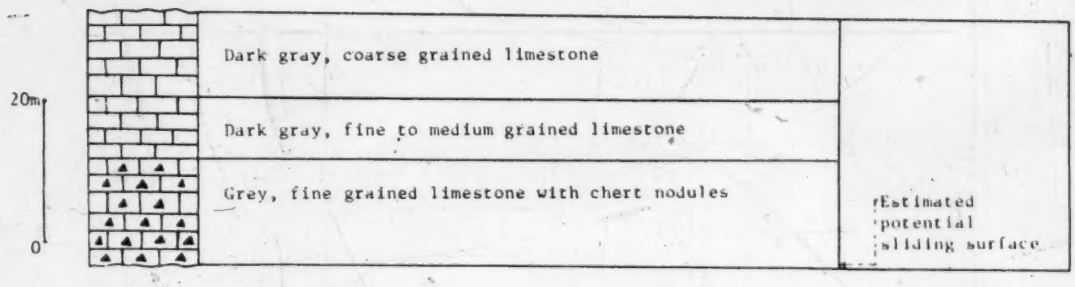
20m
0
Dark gray, coarse grained limestone
Dark gray, fine to medium grained limestone
Grey, fine grained limestone with chert nodules
Estimated potential sliding surface

Figure 3.9 Lithology around the potential sliding surface at Site 7

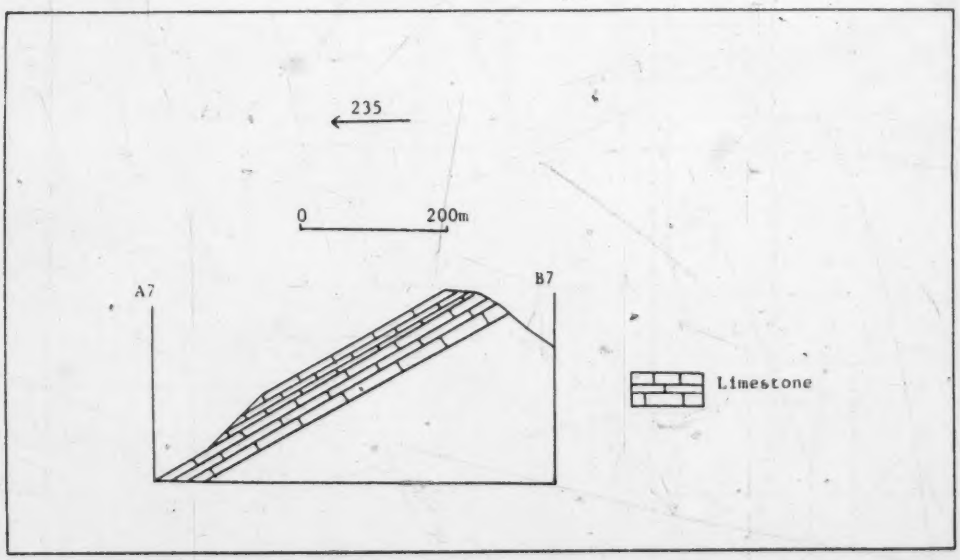

Figure 3.10 Cross-section of the slope at Site 7

bedding surfaces are between 250 mm and 500 mm and the spacings for the two joint sets are about 250 mm and 25 mm to 2 m. The bedding surfaces are continuous and without fill material. Very little groundwater can be seen seeping out of the bedding planes the base of the overdip slope. The roughness angle is 0°/0.91m. The slope is convex and consists of an overdip part and a dip part (Fig. 3.10). The slope angle for the overdip slope is 45°.

The thickness and the volume of the potential sliding mass are 28 m and 30×10^3 m^3 respectively. There are no significant lateral restraints.

3.4.2 Site 8

The site is 250 m southeast of Site 7 and the center of the site is at the point (-35mm, -50mm) with respect to the principal point of the air photograph AS 745 5041 11. Coarse grained limestones and fine grained limestones outcrop on the slope. The rocks around the base of the overdip slope are mainly coarse grained limestones. But 60cm layer of yellowish fine grained limestone also exists around the base (Fig. 3.11). The Schmidt Hammer reading is 52±1. The attitude of the bedding surfaces is 235°/28° to 34°. There are two joint sets and the attitudes for them are 65°/55° to 60° and 235° (strike)/around 90°. The spacing for the bedding surfaces is 25 mm to 600 mm and the spacings for the two joint sets are 250 mm to 500 mm and about 5 m. Fine grained limestones have smaller discontinuity spacings than

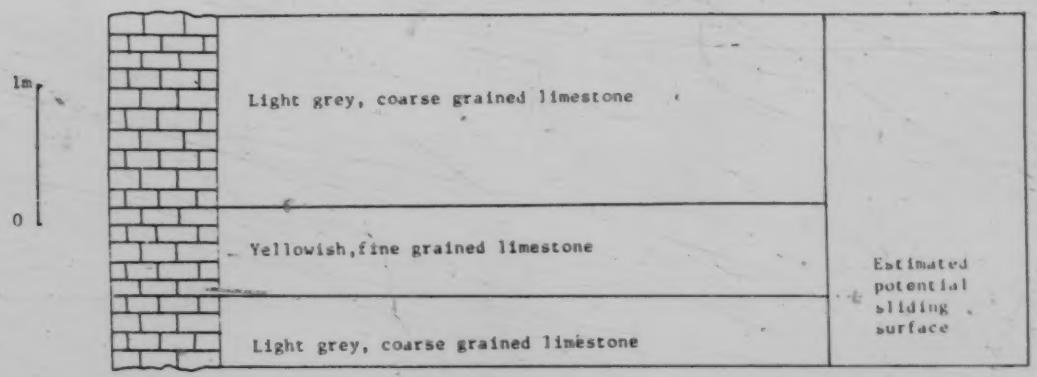

Figure 3.11 Lithology around the potential sliding surface at Site 8

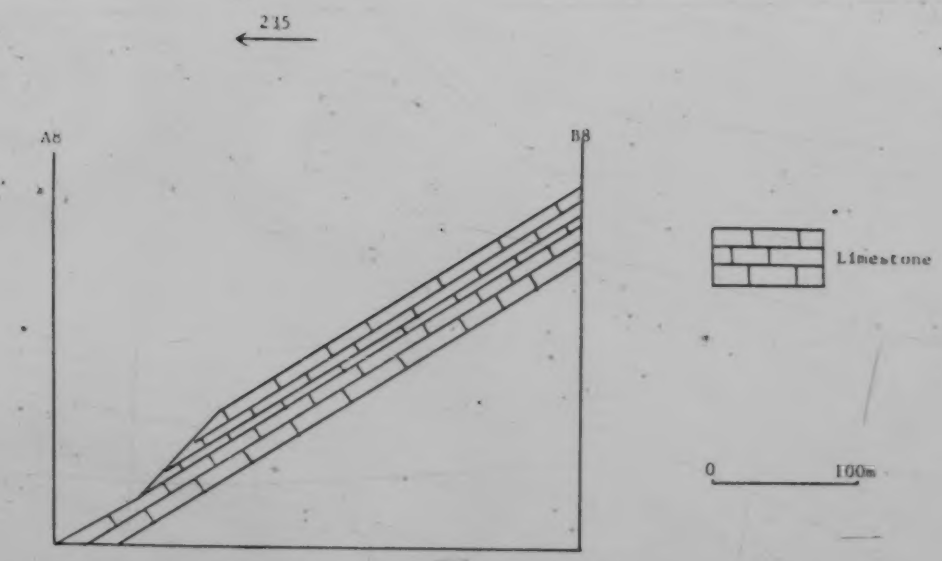

Figure 3.12 Cross-section of the slope at Site 8

coarse grained limestones. The bedding surfaces are continuous and without fill materials. Very little groundwater seeps out of the slope from the bedding planes around the base of overdip slope. The roughness angle is 0°/0.91m.

The thickness and the volume of the potential sliding mass are 24 m and 10×10^4 m^3 respectively. The slope is convex and consists of an overdip part and a dip part (Fig. 3.12).

The slope angle of the overdip slope is 49°. There are no significant lateral restraints on the potential sliding mass.

3.4.3 Site 9

The site is about 1000 m southeast of the site 8 on the east slope of the same valley. The center of the site is at the point (20mm, -80mm) with respect to the principal point of the air photograph AS 745 5041 11. The rocks outcropping on the overdip slope are light grey, coarse grained, medium bedded limestone. Only around the base of the overdip slope can fine grained limestone be seen. The Schmidt Hammer reading here is 42±1. The attitude of the bedding surfaces is 230° to 240°/29°. There are two joint sets and the attitudes of them are 240° (strike)/about 90° and 60°/55° to 65°. The spacing for the bedding sufaces is 100 mm to 250 mm and the spacings for the two joint sets are 100 mm to 1500 mm and 50 mm to 450 mm. The bedding surfaces are continuous

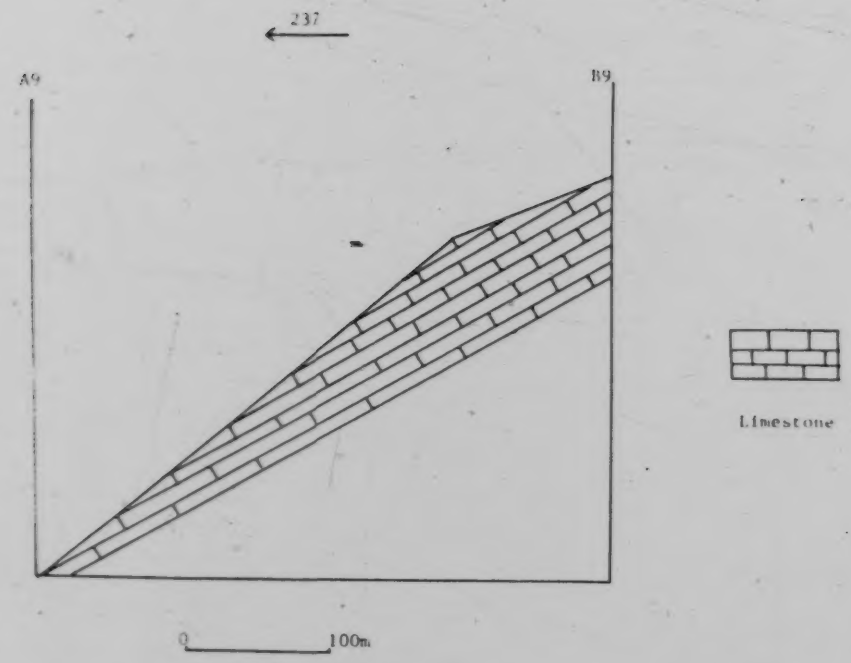

Figure 3.13 Cross-section of the slope at Site 9

and without fill materials. No groundwater seeps out of the slope. The roughness angle is 5°/0.91m and 0°/3m by estimation. The slope is planar (Fig. 3.13) but the slope angle becomes smaller around the top of the slope. The slope angle is 40° here. Below the base of the overdip slope the slope type is dip slope. The dip angle of the bedding planes here is around 35°, which indicates that the rock masses will slide if the bedding dips over 35° along the bedding surfaces around the toe of the overdip slope. The thickness and the volume of the potential sliding mass are 28 m and 18×10^3 m^3 respectively.

3.4.4 Site 10

This site is 1000 m southeast of Site 9 on the east slope of the valley. The center of the site is at the point (40mm, 15mm) with respect to the principal point of the air photograph AS 746 5040 206. There is a large rockslide between Site 9 and Site 10. The rocks on the overdip slope are light grey, coarse grained, thinly to massively bedded limestone. Around the potential sliding surface there is a layer of fine grained limestone about 1m thick. The Schmidt Hammer reading is 42±1. The attitude of the bedding surfaces is 205°/30°. There are four joint sets here and the attitudes for three of them are 205° (strike)/ around 90°, 100°/65° and 75°/65°. Another joint set is subparallel to the bedding surfaces. The spacing of the bedding surfaces and the spacing of the joint set subparallel to the bedding

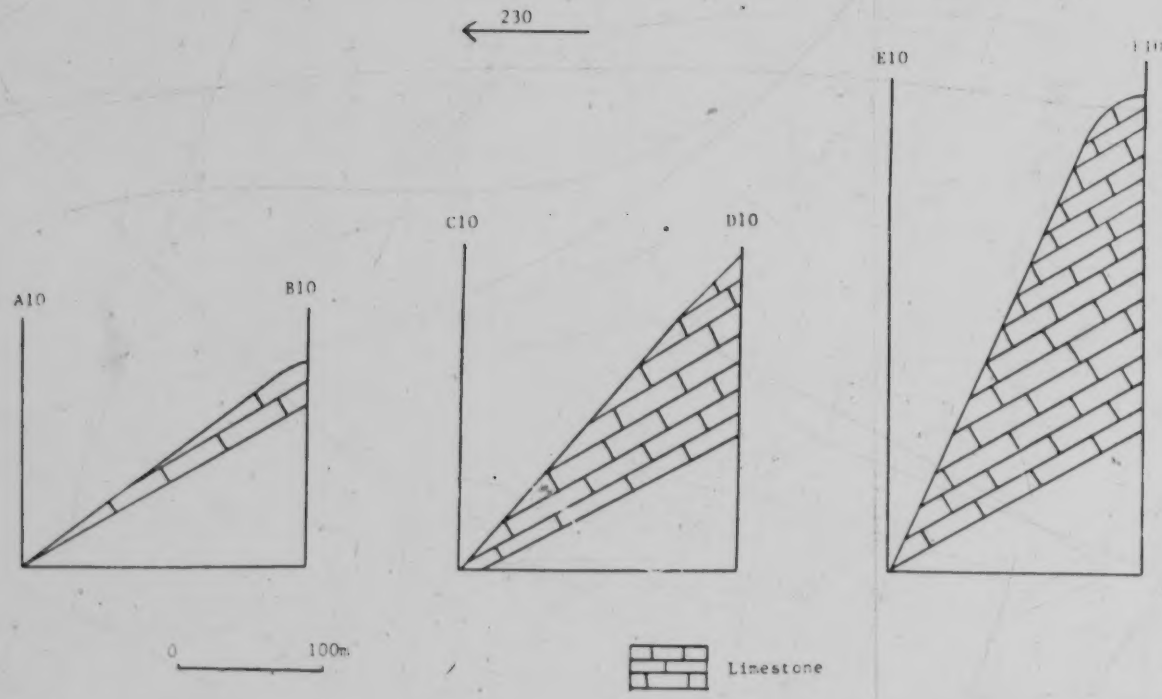

Figure 3.14 Cross-sections of the slope at site 10

planes are difficult to measure due to mutual crossing of the two sets of the discontinuities. They appear to be larger than 50 mm. The spacings for the other three joint sets are 25 mm to 250 mm, 25 mm to 250 mm and 50 mm to 1 m. The bedding surfaces are continuous and without fill materials. No groundwater can be seen seeping out of the slope. The roughness angle is 5°/0.46m and 0°/0.91m. The shape of the potential sliding mass is narrow and long, 1700 m by 240 m measured from the air photograph. It extends in the direction parallel to the strike of the bedding surfaces. The slope is planar but the slope angle becomes smaller around the top of the slope. The slope angles varies from 38° to 65° at different sections (Fig. 3.14). The average thickness of the potential sliding mass in cross-sections parallal to the dip direction of the slope changes from 20 m to 110 m. The part with average thickness larger than 90 m in the cross-section seems to be butressed. The estimated avarage thickness for the site and the volume of the potential sliding mass are 75 m and 48×10^4 m^3.

3.5 Quartzite Ridge Area

The area is east of the Spray Lakes Reservoir and there are three sites, 11, 12 and 13 (Fig. 3.15). Site 11 and Site 12 are within the area immediately east of the Smith-Dorrien-Spray Trail in Cruden and Eaton (1985b). Access is from the Smith-Dorrien-Spray Trail. Park about 200 m north of the Spray Lakes Parking Lot. A small creek flows

from east to west. hike east along the creek for 1000 m to reach Site 11. Sites 12 and 13 are south of Site 11. Rockslides are active in the area and rockslide deposits are distributed around Site 11, Site 12 and in between.

3.5.1 Site 11

The center of the site is at the point (-15mm, 30mm) with respect to the principal point of the air photograph AS 746 5040 204. The rocks are light grey to white, fine grained, thin to medium bedded, planar cross-bedded quartz sandstones of the Rocky Mountain Group. The Schmidt Hammer reading here is 44±1. The attitude of the bedding surfaces is 235°/25°. There are three joint sets at 55°/35°, 55°/65° and 235° (strike)/ about 90°. The spacings of the bedding surfaces are from 25 mm to 200 mm. The spacings of the three joint sets are 25 mm to 500 mm, 25 mm to 500 mm and around 50 mm. The bedding surfaces are continuous and without fill materials. No groundwater seeps out of the slope. The roughness angle is 0°/0.91m . The slope is planar but the slope angle is smaller around the top of the slope and greater around the foot of the slope due to erosion (Fig. 3.16). The slope angle of the overdip slope except the top and the toe is 38° and vegetation is well developed on the slope. The average thickness and the volume of the potential rockslide are 60 m and 14×10^4 m^3 respectively.

Figure 3.15 Geology and Working Sites in the Area of Quartzite Ridge, Based on the Air Photograph AS 746 5040 204

AS 746 - 5040 204

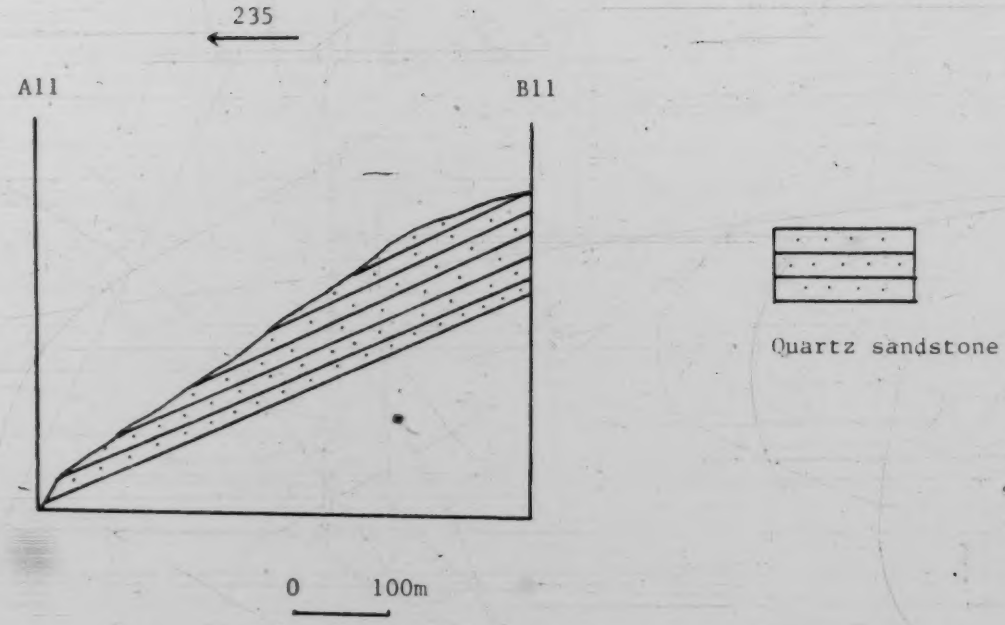

Figure 3.16 Cross-section at Site 11

3.5.2 Site 12

This site is 600 m southeast of Site 11 and the centre of the site is at the point (70mm, -15mm) with respect to the principal point of the air photograph AS 746 5040 204. The rocks here are light brown to white, fine grained, laminar cross-bedded quartz sandstones of the Rocky Mountain Group. The Schmidt Hammer reading is 52±2. The attitude of the bedding surfaces is 237°/25°. There are two joint sets and the attitudes of them are 60°/ 65° to 70° and 237° (strike)/ around 90°. The spacings of the bedding surfaces are 25 mm to 600 mm. The spacings of the two joint sets are 50 mm to 500 mm and 25 mm to 500 mm. The bedding surfaces are continuous and without fill materials. No groundwater seeps out of the slope. The roughness angle is 0°/0.91m. The shape of the potential sliding mass is narrow and long, 1600 m by 300 m measured from the air photograph. A large rockslide occurred at the north end of the site. The slope is planar but the slope angle becomes smaller around the top of the slope (Fig. 3.17). The slope angle is about 37°. The average thickness and the volume of the potential rockslide are 90 m and 62×10^4 m^3.

3.5.3 Site 13

This site is 1000 m south of Site 12 and the center of the site is at the point (50mm, -75mm) with respect to the principal point of the air photograph AS 746 5040 204. The rocks here are dark to light grey, fine grained, dolomitic

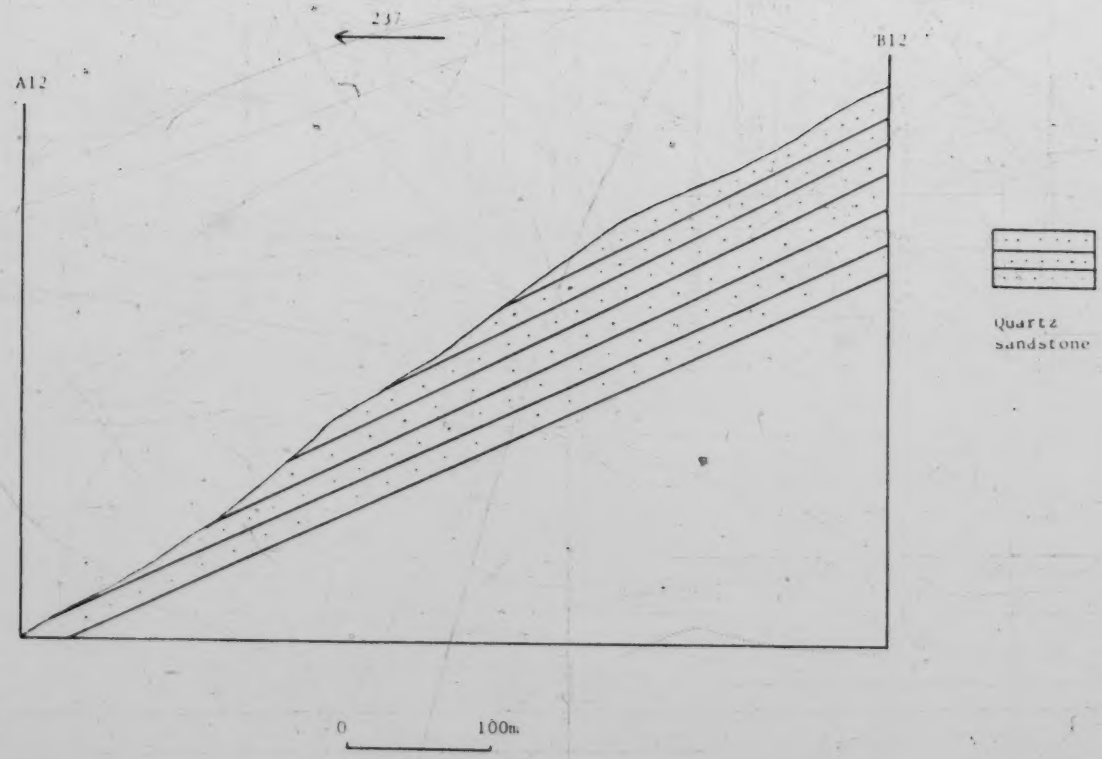

Figure 3.17 Cross-section of the slope at site 12

sandstones of the Sulphur Mountain Formation. The Schmidt Hammer reading here is 52±2. The attitude of the bedding surfaces is 240°/20°. There are two joint sets and the attitudes of them are 60°/75° and 240° (strike)/ about 90°. The spacings of the bedding surfaces are around 50 mm. The spacings of the two joint sets are 25 mm to 1000 mm and larger than 50 mm. The bedding surfaces are continuous and without fill materials. No groundwater seeps out of the slope. The roughness angle is 0°/3m by estimation. The slope is planar and the slope angle is 40°. But local slope angles can reach 45°. All the slope is covered by rock debris. From the observations at the site the main movement type for the rock mass here is that rocks disintegrated and then moved down the slope slowly, as a rock glacier.

3.6 Area of Mt. Buller and Mt. Engadine

There are three sites in the area (Fig. 3.18 and Fig. 3.19) and all of them are on the hanging wall of the Sulphur Mountain Thrust. Sites 14 and 15 are in the Fairholme Group and Site 16 is in the Palliser Formation. Access to these sites are from the Smith-Dorrien-Spray Trail.

3.6.1 Site 14

The center of the site is at the point (-50mm, -5mm) with respect to the principal point of the air photograph AS 746 5039 155. Park around 4000 m north of the Buller Mountain Parking lot and hike southeast for 1000 m to reach

Figure 3.18 Geology and Working Sites around Mt. Buller,
Based on the Air Photograph AS 746 5039 155

82-3-17
13
14
10
15
Op

Figure 3.19 Geology and Working Sites east of Mt. Engadine, Based on the Air Photograph AS 746 5038 109

Alberta
15
S

the site. The rocks at the site are light grey, coarse grained, medium bedded dolostones of the Fairholme Group. The Schmidt Hammer reading here is 51±2. The attitude of the bedding surfaces is 245°/34°. But around the top of the slope the dip of the bedding surfaces decreases to 31°. There are three joint sets at 60°/55° to 60°, 240° (strike)/ around 90° and 200°/65° to 70°. The spacings of the bedding surfaces are 100 mm to 250 mm. The spacings of the three joint sets are 100 mm to 1 m, 250 mm to 500 mm and larger than 100 mm. The bedding surfaces are continuous and without fill materials. Very little groundwater seeps out of the slope. The roughness angle is 0°/0.91m. The slope is planar (Fig. 3.20). The slope angle of the overdip slope is 37°. The average thickness of the potential sliding mass is 10 m. The volume of the potential rockslide is 2.3×10^5 m^3.

3.6.2 Site 15

The center of the site is at the point (55mm, -90mm) with respect to the principal point of the air photograph AS 746 5039 155. Park at the Buller Mountain parking lot and hike along the hiking trail to the east for 4000m to reach the site. The rocks around the base of the overdip slope are dark grey, fine grained, medium bedded dolostones of the Fairholme Group. There are also some thin layers of chert. The Schmidt Hammer reading here is around 46±2. The attitude of the bedding surfaces is 235°/20°. There are three joint sets. One joint set is subparallel to the bedding surfaces.

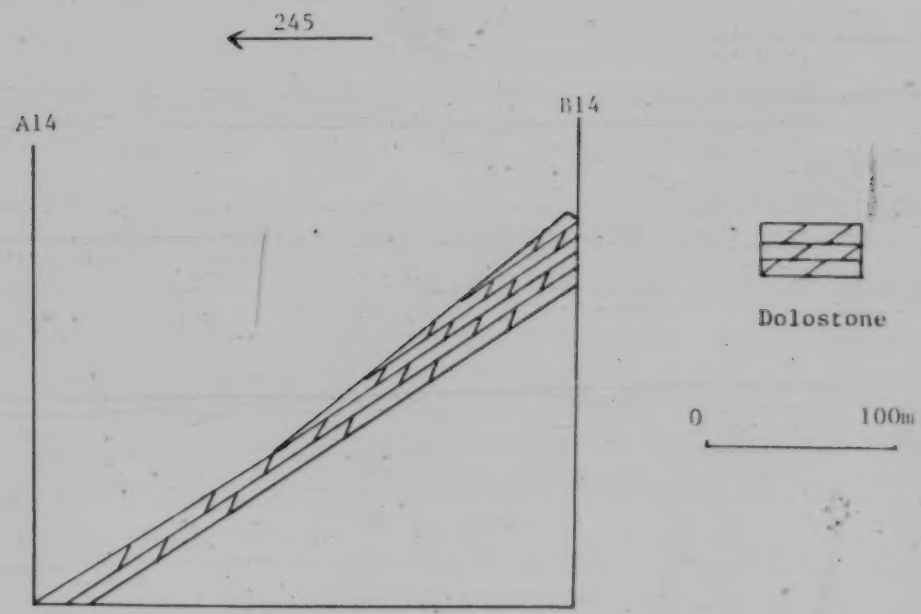

Figure 3.28 Cross section of the slope at Site 14

The attitudes of the other two joint sets are 60°/70° and 235° (strike)/around 90°. The spacings of the bedding surfaces are 100 mm to 400 mm. The spacings of the two joint sets which are not subparallel to the bedding surfaces are 50 mm to 400 mm and around 400 mm. The bedding surfaces are continuous and without fill materials. Very little groundwater seeps out of the slope. The slope is planar and the slope angle for the overdip slope is 37°. Because the bedding dip is only 20°, the site is no longer considered as a potential rockslide.

3.6.3 Site 16

The site is east of Mt. Engadine and the center of the site is at the point (-20mm, -70mm) with respect to the principal point of the air photograph AS 746 5038 109. Park at the Buller Mountain parking lot and hike east for 3000 m along the Buller Creek hiking trail. Then turn right into the valley and hike another 2500 m to reach the site. The site is in the Palliser Formation and the rocks are dark grey, fine to coarse grained, thickly to thinly bedded limestones. The Schmidt Hammer reading is 52±3. The attitude of the bedding surfaces is 235°/30°. There are two joint sets at 60°/70° and 235° (strike)/90°. The spacings of the bedding surfaces are 25 mm to 800 mm. The spacings of the joints are from 50 mm to 400 mm. The bedding surfaces are continuous and without fill materials. A little groundwater seeps out of the base of the overdip slope. The overdip

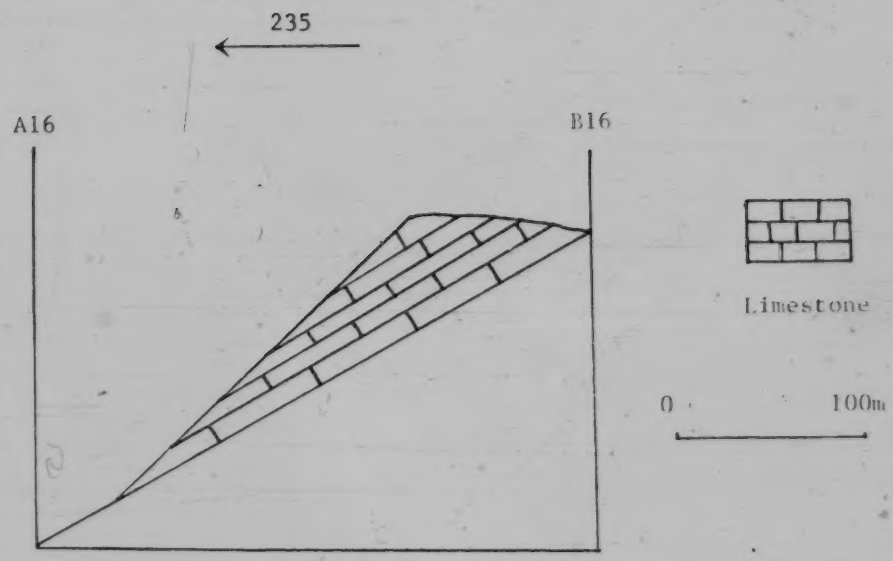

Figure 3.11 Cross-section of the slope at Site 16

slope is just above an old cirque. The slope is planar and the slope angle is 44° (Fig. 3.21). The average thickness and the volume of the potential rockslide are 25 m and 1.5×10^4 m^3.

3.7 Area of North Ribbon Creek

There are four sites, 17, 18, 19 and 20 in this area (Figs. 3.22, 3.23 and 3.24). The access is from No. 40 highway. Park at the parking lot of Ribbon Creek. Walk about 3 km along the Ribbon Creek hiking trail and then turn right to enter North Ribbon Creek valley. Walk another 4 km to reach the area.

3.7.1 Site 17 (Mt. Bogart)

The center of this site is at the point (-35mm, 15mm) with respect to the principal point of the air photograph AS 746 5040 208 and the site is on the left side of the North Ribbon Creek (looking up the creek). Because it is too difficult to climb up the slope, only the base of the slope has been investigated. The site is within the Rundle Group. The rocks here are light grey,thickly bedded, medium to coarse grained limestones. The Schimidt Hammer reading here are 52±3. The hinge of a syncline is through the foot of the slope. The bedding surfaces near the base of the slope are nearly horizontal. The dip angles increase from the toe to the top of the slope. There is a dip slope part on the upper

Figure 3.22 Geology and Working Sites in the Area of North Ribbon Creek, 1, Based on the Air Photograph AS 746 5040 208

RD
17
D
OD

Figure 3.23 Geology and Working Sites in the Area of North Ribbon Creek, 2, Based on the Air Photograph AS 745 5041 12

82 J 14
50° 56'
24-8-58
Mr
Mr
Mb
S
19
OD
Mr
D
Mb
18
OD
OD

Figure 3.24 Geology and Working Sites in the Area of North Ribbon Creek, 3, Based on the Air Photograph AS 745 5041 14

OD
Jk
D
RD
58-1

is subparallel to the bedding surfaces and the attitues of the other two joint sets are 70° (strike)/ 90° and 260°/75° around the base of the slope. The spacings of the bedding surfaces are about 500 mm. The spacings of the two joint sets which are not subparallel to the bedding surfaces are 75 mm to 250 mm and 75 mm to 500 mm. The bedding surfaces are continuous and without fill materials. No groundwater seeps out of the slope. The slope angle of the lower part of the slope is 57°.

3.7.2 Site 18

This site is just 400 m east of the peak of Mt. Sparrowhowk. The center of the site is at (20mm, -15mm) with respect to the principal point of the air photograph AS 745 5041 12. Since the hinge of an anticline is through the site, The bedding dips less than 15° by estimation. So the site is no longer considered as a potential rockslide. No further invistigations have been made.

3.7.3 Site 19

The center of the site is at the point (90mm, 50mm) with respect to the principal point of the air photograph AS 745 5041 12. The rocks here are dark grey, thinly to thickly bedded, medium to coarse grained limestones with abundant nodular chert. The site is around the base of the Rundle Group. The Schmidt Hammer reading here is 42±2. The attitude of the bedding surfaces is 250°/20°. There are two joint

sets and the attitudes of them are 70°/ 65° to 80° and 250° (strike)/ around 90°. The spacings of the bedding surfaces are 75 mm to 500 mm. The spacings of the two joint sets are 75 mm to 1000 mm and 75 mm to 400 mm. The bedding surfaces are continuous and without fill materials. No groundwater seeps out of the slope. The slope is planar and the slope angle is 40°. Because the dip angle of the bedding surfaces is only 20° and this value is smaller than the basic frictional angles of the limestones (Eaton,1986), the site is no longer considered as a potential rockslide.

3.7.4 Site 20

The center of the site is at the point (-7mm, 30mm) with respect to the principal point of the air photograph AS 745 5041 14. The rocks here are dark grey, fine to coarse grained, thinly to medium bedded limestones of the Palliser Formation. The Schmidt Hammer reading is 45±1. The attitude of the bedding surfaces is 235°/44°. There are three joint sets at 120°/80°, 20°/65° and 70°/50°. The spacing of the bedding surfaces are 25 mm to 250 mm. The joint spacings are between 50 mm and 500 mm. The bedding surfaces are continuous and without fill materials. No groundwater seeps out of the slope. The roughness angle is 3°/0.46m and 0°/0.91m. Some rock layers sit on the bedding surfaces to form the overdip scarp and the slope angle of the overdip slope is 45° (Fig. 3.25). The thickness of the sliding mass is 10 m. The volume of the potential sliding mass is 2.8x10⁴

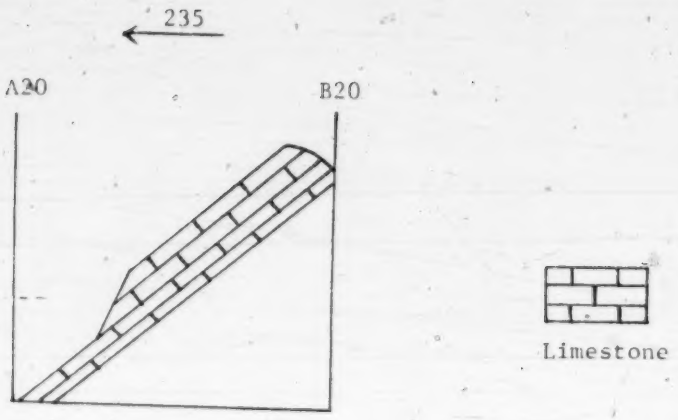

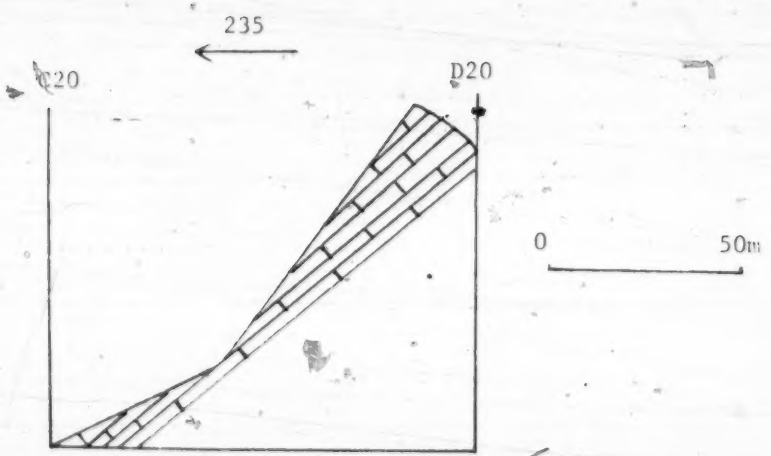

Figure 3.25 Cross-sections of the slope at Site 20

m^3.

3.8 Area of Ribbon Creek

There are three sites, 21, 22 and 23 (Figs. 3.26 and 3.27) in the area. Access is from No. 40 Highway. Park at the Ribbon Creek parking lot and hike west about 13 km along the Ribbon Creek hiking trail to reach the Ribbon Lake just above the Ribbon waterfalls. All the sites are around here.

3.8.1 Site 21

The center of the site is at the point (30mm, -5mm) with respect to the principal point of the air photograph AS 746 5039 157. The rocks here are medium grey, fine to medium grained, thinly to thickly bedded quartz sandstones of the Rocky Mountain Group. The Schmidt Hammer reading here is 53±3. The attitude of the bedding surfaces is 250°/24°. There are three joint sets here. One joint set is subparallel to the bedding planes. The attitudes of the other two joint sets are 70°/70° and 250° (strike)/ around 90°. The spacings of the bedding surfaces are 75 mm to 1 m. The spacings of the joint sets which are not subparallel to the bedding planes are 75 mm to 1 m and less than 120 mm. The bedding surfaces are continuous and without fill materials. A little groundwater seeps out of the slope. The roughness angle is 0°/0.91m. The slope is planar and the slope angle is 40°. The main movement type of the slope is falling and rolling down of rock blocks produced by joints.

Figure 3.26 Geology and Working Sites in the Area of Ribbon Creek, West Part, Based on the Air Photograph AS 746 5039

157

82-3-14
50°-54'
1:15840
9-9-58
RD
D
Prm
Mr
UD
UD
UD
Mr
RD
UD
5039
157

Figure 3.27 Geology and Working Sites in the Area of Ribbon Creek, East Part, Based on the Air Photograph AS 746 5039 159

Alberta
23
00
21
58-1-1R

Some rock fall debris is just at the foot of the slope. The maximum dimension of the blocks can reach 10 m. Also toppling exists here. The average thickness and the volume of the potential sliding mass are 35 m and 9.6×10^4 m^3.

3.8.2 Site 22

The center of the site is at the point (70mm, 80mm) with respect to the principal point of the air photograph AS 746 5039 157. The rocks around the base of the overdip slope are dark grey to black, coarse grained to fine grained, thinly to medium bedded limestones. The nodulars of chert exist in some layers. The site is in the Rundle Group. The Schmidt Hammer reading is 42±1. The attitude of the bedding surfaces is 245°/20°. There are four joint sets at 360°/72°, 240° (strike)/ around 90°, 30°/86° and 65°/70°. The spacings of the bedding surfaces are less than 150 mm. The spacings of the joint sets are 50 mm to 1 m. The bedding surfaces are continuous and without fill materials. No groundwater seeps out of the slope. The slope is planar and the slope angle is 37°. From observations at the site, the rock blocks detach from each other along the joint planes then fall into the small gullies on the slope. Finally, water flow or snow avalanches carry these rock blocks down. So there is more rock debris around the outlets of the small gullies on the slope than at other places. The overdip slope is covered by the rock debris. Because the beddings dip only 20°, the site is no longer considered a potential rockslide.

3.8.3 Site 23

The site is about 400 m southeast of the Site 22 and the center of the site is at the point (-55mm, 55mm) with respect to the principal point of the air photograph AS 746 5039 159. This site is 500 m north of the Ribbon waterfalls. Because the slope is too steep, only the base of the overdip slope has been investigated. The rocks here are light grey, coarse grained, medium to thickly bedded limestones of the Rundle Group. The Schmidt Hammer reading is 45±2. The attitude of the bedding surfaces is 265°/15°. There are two joint sets at 85°/75° to 80° and 265° (strike)/ around 90°. The spacings of the bedding surfaces are 100 mm to 1 m. The spacings for the two joint sets are 75 mm to 500 mm and around 250 mm. The bedding surfaces are continuous and without fill materials. No groundwater seeps out of the slope. The rock layers daylight on the overdip slope formed by a small gully here. The overall slope angle for the entire overdip slope is 37° from the topographic map. The slope angle where the investigation was conducted is from 50° to 60° due to erosions. The site is no longer considered a potential rockslide because the bedding dips only 15°.

3.9 Area of Mt. Kidd

There are two sites in this area (Fig. 3.28) and both the sites are west of the Kananaskis River. This area is within the area of east slopes of Mt. Bogart and Mt. Kidd in Cruden and Eaton (1985b). Site 24 is south of the peak of

Mt. Kidd and Site 25 is west of the peak of Mt. Kidd. An anticline and a syncline extend through this area and both the sites are around the hinges of the fold structures.

3.9.1 Site 24

This site is just below and south of the main peak of Mt. Kidd. The center of the site is at the point (-30mm, -35mm) with respect to the principal point of the air photograph AS 746 5039 161. Access to the site is from Highway 40. Park at the parking lot of Galatea Creek. Walk north for about 2000 m along the hiking trail just west of the Kananaskis River, then turn left and hike for about 2000 m along the creek below Mt. Kidd, turn right and hike up to the site. The rocks on the lower part of the slope are buff to light grey, coarse grained and crinoidal, medium to thinly bedded limestones. The Schmidt Hammer reading is 50±2. The site is around the hinge of an anticline. The attitude of the bedding surfaces around the base of the slope is 215° to 250°/15° to 17°. The dip angle of the bedding surfaces increases to 20° up the slope. There are three joint sets. One joint set is subparallel to the bedding surfaces. The other two joint sets are perpendicular to the bedding surfaces. The strike of one joint set is parallel to that of the bedding surfaces and the strike of the other joint set is perpendicular to that of the bedding surfaces. The slope angle of the lower part of the slope is about 50° due to undercutting and the slope angle of the

Figure 3.28 Geology and Working Sites in Mt. Kidd Area,
Based on the Air Photograph AS 746 5039 161

Dp
Mb.1
Mr

upper part of the slope is only 30°. The dip direction of the slope here is 200° to 210°. The angle between the dip direction of the bedding and the dip direction of the slope is larger than 20°. The bedding surfaces are continuous and without fill materials. No groundwater seeps out of the slope. The site is no longer considered a potential rockslide.

3.9.2 Site 25

This site is just 1000 m west of Site 24 and the center of the site is at the point (-85mm, -15mm) with respect to the principal point of the air photograph AS 746 5039 161. Access to this site is from Highway 40. Park at the parking lot of the Ribbon Creek and walk west for about 10km along the hiking trail of the Ribbon Creek. Then turn left to hike up for about 1300 m along the gully below the site. Turn left again to to hike up the slope to reach the site. The lower part of the site is dip slope and the upper part of the slope is overdip slope (Fig. 3.29). The rocks around the base of the overdip slope are light to medium grey, coarse grained, thinly to thickly bedded limestones. But a thin layer of yellowish, very fine grained limestone outcrops on the dip slope as at Site 8. The Schmidt Hammer reading is 43±2. The attitude of the bedding surfaces around the base of the overdip slope is 230°/15° to 35°. The variation of the dip angle of the bedding surfaces is due to the fold structure here. On the dip slope the dip angle of the

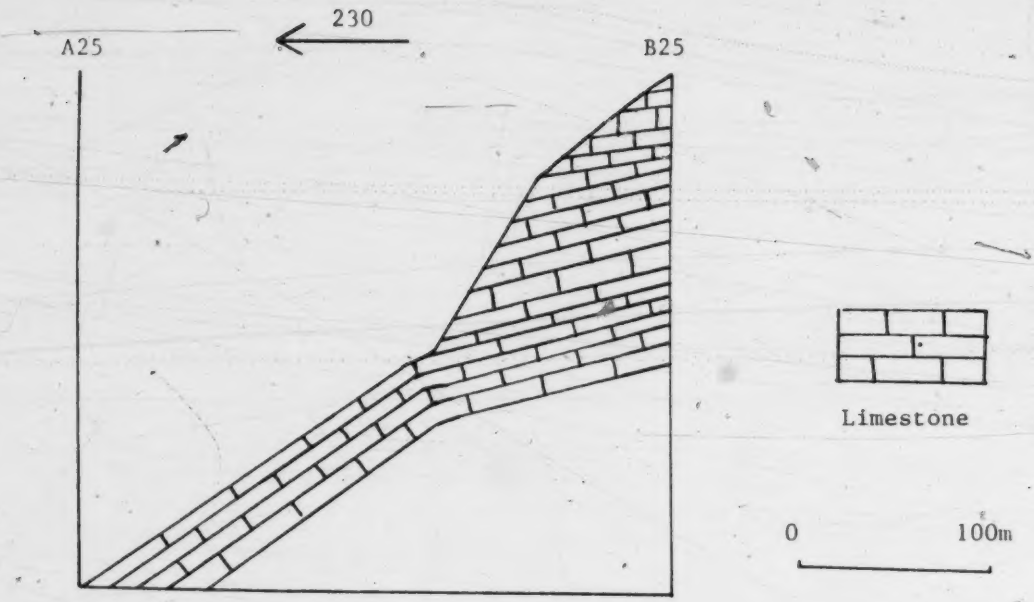

Figure 3.29 Cross-section of the slope at Site 25

bedding surfaces is 35°. The dip of the bedding planes decreases from dip slope part to overdip slope part. On the overdip slope the bedding dips less than 15°. There are three joint sets. One joint set is subparallel to the bedding planes. Both the other two joint sets are perpendicular to the bedding planes. The strike of one joint set is parallel to that of the bedding surfaces and the strike of the other joint set is perpendicular to that of the bedding surfaces. The spacings of the bedding surfaces are 50 mm to 500 mm. The spacings of the two join sets which are not subparallel to the bedding surfaces are 50 mm to 750 mm and around 150 mm. The bedding surfaces are continuous and without fill materials. A little groundwater seeps out of the slope. The slope angle for the dip slope is 35° and that for the overdip slope is about 60°. Because the bedding dip of the overdip slope part is only around 15°, the site is no longer considered a potential rockslide.

3.10 Area of Galatea Creek

There are two sites, 26 and 27, in this area (Fig. 3.30) and both sites are on the northern slope of the Galatea Creek. Access is from Highway 40. Park at the Galatea Creek parking lot. Walk along the hiking trail westward to reach the two sites.

Figure 3.30 Geology and Working Sites in the Galatea Creek Area, Based on the Air Photograph AS 746 5038 113

4867 5038 64
Alberta
58-1 IR
AS 746

3.10.1 Site 26

The centre of the site is at the point (10mm, -35mm) with respect to the principal point of the air photograph AS 746 5038 113. Start from the Galatea Creek parking lot and walk for 2 km along the official hiking trail and then turn right to climb up about 500 m to reach the site. Because the slope is too steep, only the base of the overdip slope was investigated.

The overdip slope here was formed by a small gully in the northwest-southeast direction.

The site is within the Rundle Group and the rocks around the base of the overdip slope are mainly light gray, coarse grained, crinoidal limestones. Schmidt Hammer readings around the toe of the overdip slope is 42±2. The attitude of the bedding surfaces around the toe of the overdip slope is 235°/30 to 32°. The spacings of the bedding surfaces are 50 mm to 500 mm. There are three joint sets. One joint set is subparallel to the bedding. The attitudes of the other two joint sets are 235° (strike)/about 90° and 55°/60° to 65°. The spacings of the joint sets are between 50 mm to 500 mm. The bedding surfaces are continuous and without fill materials. No groundwater seeps out of the slope. The slope angle around the foot of the slope is between 40° and 60° due to erosion. The overall slope angle from the toe to the top of the mountain are less than 40°. Because the basic friction angle of coarse grained limestones are around or larger than 35° (Eaton, 1986), the

overdip slope is not subject to sliding along bedding surfaces.

3.10.2 Site 27

The centre of the site is at (-82mm, 0mm) with respect to the principal point of the air photograph AS 746 5038 113. Start from the Galatea Creek parking lot and walk west for 4 km along the Galatea Creek hiking trail. Then turn right to climb up for 2000 m to reach the site. The site is around the top of the Rundle Group and the bottom of the Rocky Mountain Group. The rocks of the lower part of the slope are yellow, medium grey, weathering, fine grained, thickly to thinly bedded dolostones and medium grey, light weathering, coarse grained limestones with local interbedded chert of the Rundle Group. The rocks of the middle part and the upper part of the slope are quartz sandstones of the Rocky Mountain Group. The slope is planar and the slope angle is 31°. The Schmidt Hammer reading of the carbonate rocks is 46±2. The Schmidt Hammer reading of the quartz sandstones is 50±3. The attitude of the bedding surfaces is 240°/30°. The spacings of the bedding surfaces are 75 mm to 600 mm. There are three joint sets. One joint set is subparallel to the bedding and the attitudes of the other two joint sets are 150° (strike)/about 90° and 60°/60 to 70°. The spacings of the joint sets are 75 mm to 500 mm. Little groundwater seeps out of the slope. The slope here is an overall dip slope because the difference between the

slope angle and the bedding dip is only one degree.

3.11 Area of Opal Range

There is only one site (Site 28) in this area (Fig. 3.31). This area is within the area of Opal Range, West Ridge, North of Grizzly Creeek in Cruden and Eaton (1985b). The centre of the site is at the point (25mm, -30mm) with respect to the principal point of the air photograph AS 747 5034 161. Access is from Highway 40. Park 1 km south of Fortess Junction Service Centre and climb up the slope on the east side of the Highway for about 1500 m (horizontal distance) to reach the site. The site is within the Rundle Group and the Lewis thrust fault is east of the site. The potential sliding surface is circular in cross section (Fig. 3.32). The rocks around the potential sliding surface are dark grey, thickly to thinly bedded, fine grained limestone, yellow, medium bedded, fine grained dolostones and medium grey, thinly bedded, coarse grained limestones (Fig. 3.33). The Schmidt Hammer readings are 52±2. The attitude of the bedding surfaces changes from 30° in the lower part of the site to larger than 50° at the top of the range. The spacings of the bedding surfaces are from 120 mm to 500 mm. There are two joint sets and both of them are perpendicular to the bedding surfaces. The strike of one joint set is parallel to that of the bedding surfaces and the strike of the other joint set is perpendicular to that of the bedding surfaces. The spacings of the joint sets are 50 mm to 500

mm. The bedding surfaces are continuous and without infill materials. A little groundwater seeps out of the slope. The slope angle is 70°. A small rockslide occurred here before (Eaton, 1986). The average thickness and the volume are 35 m and 3500 m^3/m measured from the cross section in the dip direction of the slope.

3.12 Area of Mt. Inflexible

There is only one site (Site 29) in this area (Fig. 3.34). The centre of the site is at the point (50mm, -25mm) with respect to the principal point of the air photograph AS 747 5034 157. The access is from Smith-Dorrien-Spray Trail. Park at the Sawmill parking lot. Walk along the old logging trail northward for 2 km and then turn right to enter a valley there leading to the site. Walk along the valley for 2500 m to reach the the foot of Mt. Inflexible and then climb up for 500 m to reach the site. The site is around the top of the Rundle Group. The rocks around the potential sliding surface are dark grey, medium to thickly bedded, fine to medium grained limestone with locally interbedded black chert. The Schmidt Hammer readings are 52±3. The attitude of the bedding surfaces is 215°/25°. The spacings of the bedding surfaces are from 125 mm to 1 m. There are two joint sets at 20°/70° and 210° (strike)/90°. The spacings of the joint sets are 75 mm to 500 mm. The bedding surfaces are continuous and without fill materials. Little groundwater seeps out of the slope. The slope is convex and

Figure 3.31 Geology and the Working Site in the Area of Opal Range, Based on the Air Photograph AS 747 5034 161

4865A
5034
82 J 14
115.840
30
28
AS 147 5034

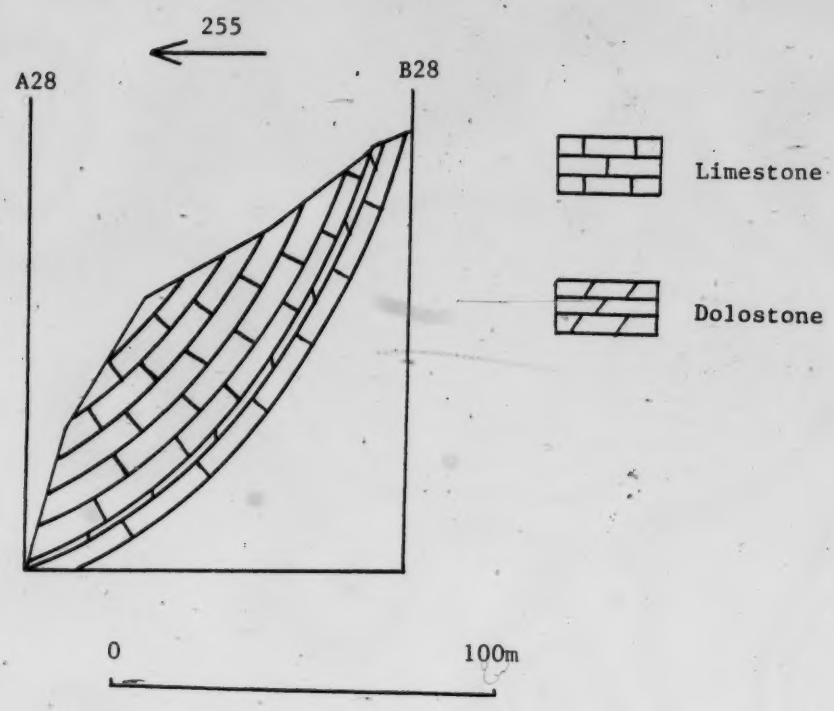

Figure 3.32 Cross-section of the slope at Site 28

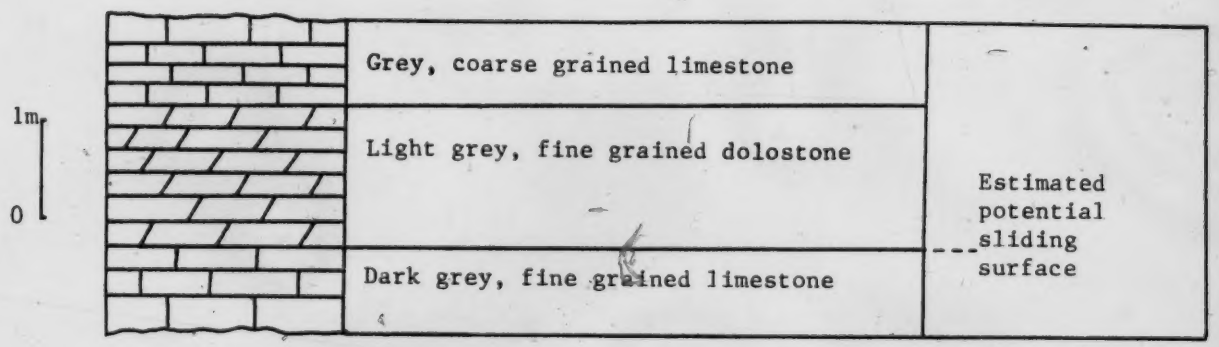

Figure 3.33 Lithology around the potential sliding surface at Site 28

the slope angle of overdip slope is 37° (Fig. 3.35). There is a dip slope part. The roughness angle is 0°/0.91m. The average thickness and the volume are 60 m and 7.6×10^4 m^3.

3.13 Area of Burstall Pass

There are three sites in the area (Fig. 3.36) Access to the area is from the Smith-Dorrien-Spay Trail. Park at the parking lot south of the Mud Lake. Walk following the Burstall Creek hiking trail for 7.5 km to get the area.

All the sites are in the Palliser Formation. There are two anticlines and one syncline in the area.

3.13.1 Site 30

The centre of the site is at the point (60mm, -100mm) with respect to the principal point of the air photograph AS 747 5033 101. The rocks at the site are dark grey to black, thinly to medium bedded, fine grained limestone, with local small nodules of black chert. The Schmidt Hammer readings are 52±2. The attitude of the bedding surfaces is 270°/39°. The spacings of the bedding surfaces are from 50 mm to 200 mm. There are two joint sets at 90 to 105°/55 to 60° and 270° (strike)/85 to 90°. The spacings of the joint sets are 50 mm to 250 mm. The bedding surfaces are continuous and without fill materials. Little groundwater seeps out of the slope. The roughness angle is 0°/0.91m. The slope is steplike and several rock layers on the slope form the overdip slope (Fig. 3.37). The slope angle is 43°. The

Figure 3.34 Geology and Working Site in the Area of Mt. Inflexible, Based on the Air Photograph AS 747 5034 157

Mr
29
OD
A29
RD
D
D
D

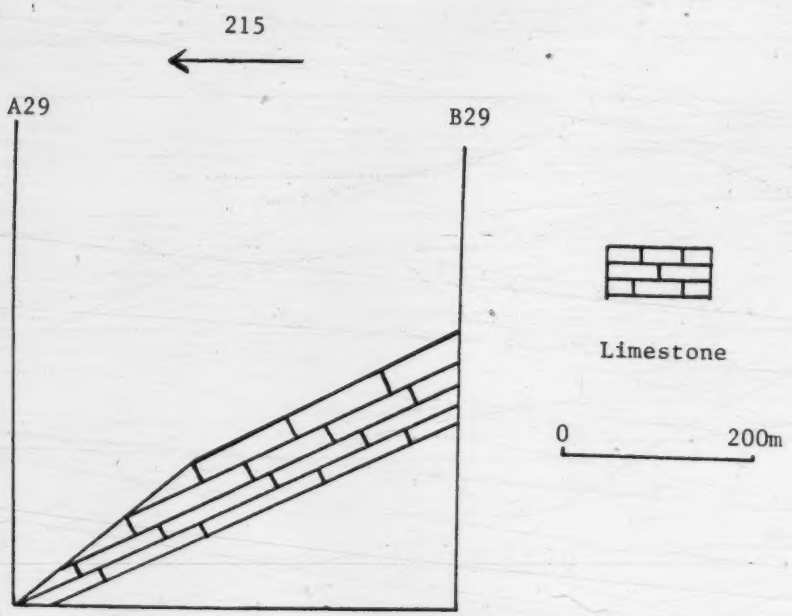

Figure 3.35 Cross-section of the slope at Site 29

Figure 3.36 Geology and Working Sites in the Burstall Pass Area, Based on the Air Photograph AS 747 5033 101

4863
933
BZ-J-14
50° - 45'
115,840
25-B-58
58-1
IR
AS 741
5033
101

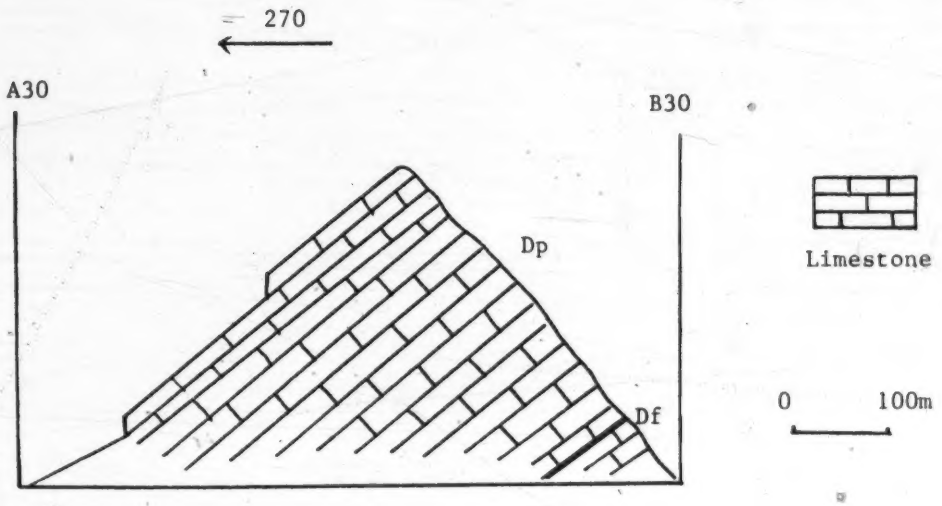

Figure 3.37 Cross-section of the slope at Site 30

thickness of the potential rockslide is 7 m and the volume of the potential sliding mass is 8.5×10^5 m^3.

3.13.2 Site 31

The site is north of Site 30 and the centre of the site is at the point (50mm, -75mm) with respect to the principal point of the air photograph AS 747 5033 101. The rocks at the site are dark grey to black, thinly to medium bedded, fine grained limestone, The Schmidt Hammer readings are 52±3. The attitude of the bedding surfaces is 275°/39°. The spacings of the bedding surfaces are from 50 mm to 200 mm. There are two joint sets at 95°/55 to 60° and 270° (strike)/85 to 90°. The spacings of the joint sets are 50 mm to 300 mm. The bedding surfaces are continuous and without fill materials. Little groundwater seeps out of the slope. The roughness angle is 0°/0.91m. It was found that the shape of the slope changes (Fig. 3.38) and although the thickness estimated from north part of the site might be about 20 m, there seems to be lateral restraints there. So the thickness of the potential slide is estimated as 8 m from the south part of the working site. The volume of the potential sliding mass is 8.3×10^5 m^3.

3.13.3 Site 32

This site is 300 m north of Site 31 and the centre of the site is at the point (5mm, 0mm) with respect to the principal point of the air photograph AS 747 5033 101. The

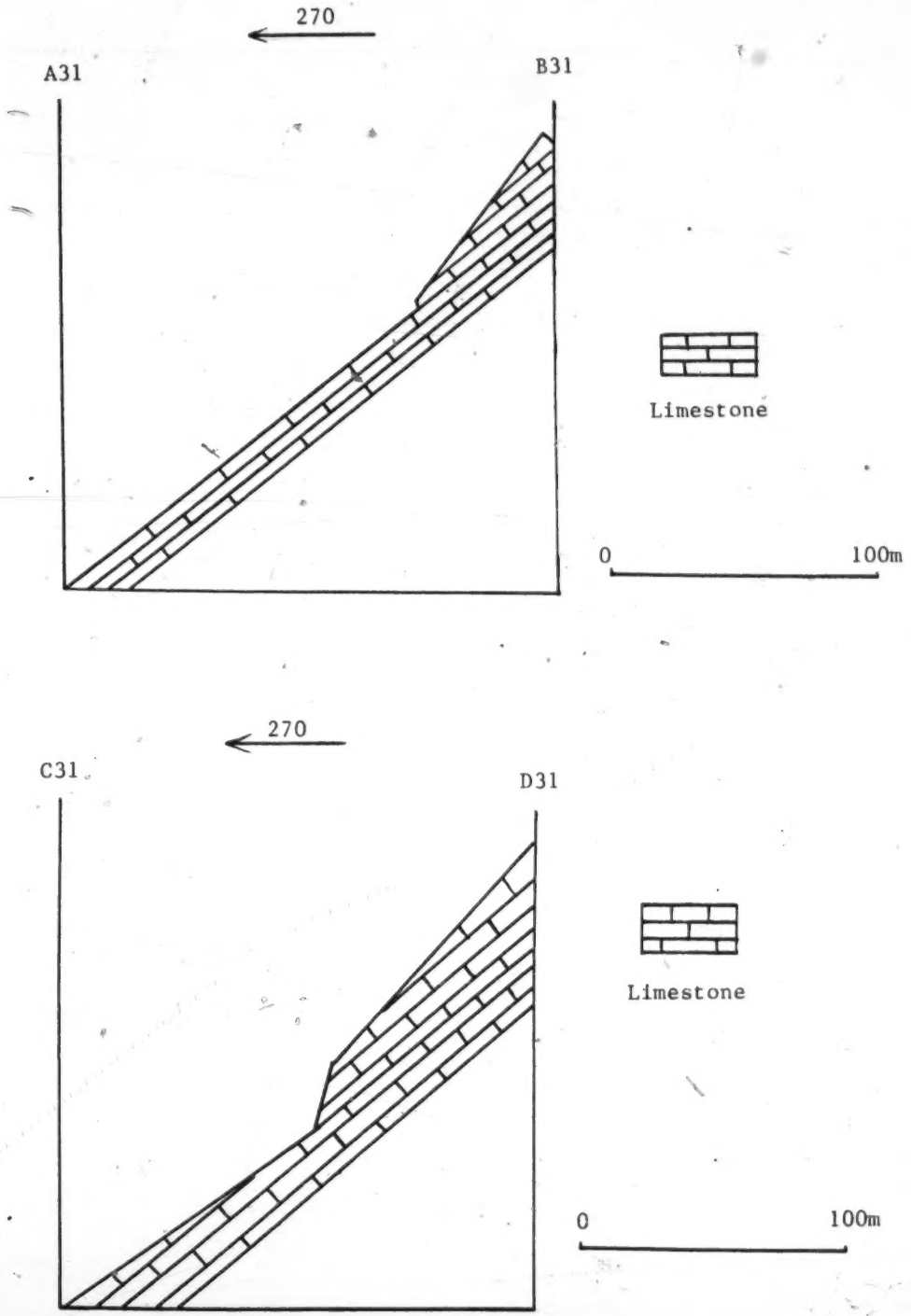

Figure 3.38 Cross-sections of the slope at Site 31

site is a rockslide site (Eaton, 1986). The rocks here are dark grey, medium to thinly bedded, fine grained limestones of the Palliser Formation. The dip angles of the bedding surfaces change from 35° to 44° or more around the top of the slope. The dip angle around the rupture surface is 44°. From the rockslide deposited material, the thickness of the slide was estimated as 5 m.

3.14 Area of Mt. Murray

There are two sites in this area (Fig. 3.39). Site 34 is 500 m north of Mt. Murray and Site 33 is 200 m south of Mt. Murray. Access is from the Smith-Dorrien-Spray Trail. Both the sites are in the Banff Formation.

The centre of Site 33 is at the point (35mm, 40mm) with respect to the principal point of the air photograph AS 747 5032 56. Park at the Sawmill parking lot and walk westward. Cross the Smith-Dorrien Creek and hike southwest along the valley south of Mt. Murray for 2500 m to reach the site. Several small anticlines and synclines penetrate the site. The slope here was reclassified as a plagioclinal slope. No further investigations were conducted.

The centre of Site 34 is at the point (13mm, 105mm) with respect to the principal point of the air photograph AS 747 5032 56. Park at the parking lot just south of the Mud Lake and hike along the hiking trail of French Creek for 3500 m. Turn left and climb up for 1500 m to reach the site. The hinge of a syncline is through the slope surface. The

lower two thirds is an anaclinal dip slope and the upper third is an overdip slope. Because the access to the overdip slope is difficult, no further investigations were conducted. From the orthoclinal slope on the west side of the slope, it can be estimated that the dip angles of the bedding surfaces are less than 15°.

3.15 Area east of Mt. Black Prince

There is only one site (Site 35) in this area (Fig. 3.40). The site is 1500 m east of Mt. Black Prince and the centre of the site is at the point (20mm, -35mm) with respect to the principal point of the air photograph AS 748 5030 213. The access is from Smith-Dorrien-Spray Trail. Park at the Black Prince parking lot. Walk along the hiking trail westward for 3200 m to reach a small lake. Continue to hike southwest for 750 m and turn left to climb up into another valley striking southeast-northwest. Hike for another 500 m to reach the site. The site is around the top of the Pallier Formation. The rocks around the potential sliding surface are dark grey to black, medium to thinly bedded, coarse grained limestone. The Schmidt Hammer reading is 43±1. The attitude of the bedding surfaces is 240°/54°. The spacings of the bedding surfaces are from 50 mm to 250 mm. There are two joint sets at 60°/30 to 35° and 240° (strike)/90°. The spacings of the joint sets are 75 mm to 1000 mm. The bedding surfaces are continuous and without fill materials. No groundwater seeps out of the slope. The slope angle is 55°.

Figure 3.39 Geology and Working Sites in the Area of Mt. Murray, Based on the Air Photograph AS 747 5032 56

4865A
5032
33
RD
Mr
D
IR
5032

The slope is convex and there is a dip slope part. The roughness angle is 2.5°/0.9 m. The thickness and the volume of the potential rockslide is 5 m and 4.4×10^5 m^3.

3.16 Area of Aster Lake

There are six sites in the area (Figs. 3.41 or 3.42). The access to the area is from Kananaskis Lakes Trail. Park at the North Interlakes parking lot. Walk west along the north shore and then the west shore of the Upper Kananaskis Lake following the official hiking trail for 6500 m to reach the area between the Upper Kananaskis Lake and the Hidden Lake. Walk south to reach the north shore of Hidden Lake and then walk along the east shore of the Lake to get the south end of the Lake. Hike up south for 1500 m and Climb up the Fossil Falls. Hike another 1500 m southwestward to reach the area.

3.16.1 Site 36

The centre of the site is at the point (70mm, 45mm) with respect to the principal point of the air photograph AS 749 5024 162. The site is within the Rundle Group and on the east limb of a syncline. The rocks are mainly dark grey to black, thickly to thinly bedded, coarse grained limestones with the fine grained matrix. The Schmidt Hammer reading is 43±2. The attitude of the bedding surfaces is 220°/25°. The spacings of the bedding surfaces are from 30 mm to 550 mm. There are three joint sets. One joint set is subparallel to

Figure 3.40 Geology and Working Site East of Mt. Black Prince, Based on the Air Photograph AS 748 5030 213

82 J 11
50° - 41'
1:15,840
4842
5030
563
5641 IR

Figure 3.41 Geology and Working Sites in the Aster Lake Area, Southern Part, Based on the Air Photograph AS 749 5024

82-J-11 50°-33' 1:15,840 10-8-58
AS 749 5624 162

Figure 3.42 Geology and Working Sites in the Aster Lake Area, Northern Part, Based on the Air Photograph AS 749 5025 215

82-I-11
50°- 35'
1:15,840
25-8-58
RD
AS 749
5025

the beddings and the other two are at 40°/65° and 220° (strike)/90°. The spacings of the joint sets are 50 mm to 1000 mm. The bedding surfaces are continuous and without fill materials. No groundwater seeps out of the slope. The roughness angle is 2.5°/0.91m. Because the bedding dip is less than the basic friction angles for the coarse grained limestones from Eaton (1986), the site is no longer considered a potential rockslide. There are a small syncline and a small anticline extending through the slope surface. The slope is covered by a thin layer of rock debris. The slope is planar and the slope angle is 40°.

3.16.2 Site 37

The centre of the site is at the point (-30mm, 45mm) with respect to the principal point of the air photograph AS 749 5024 162. The site is within the Rundle Group and is on the west limb of a syncline. The rocks are dark grey to black, thinly to thickly bedded, coarse grained limestones and dark grey thinly to thickly bedded, fine to medium bedded dolostones. The Schmidt Hammer reading is 51±3. The attitude of the bedding surfaces is 70°/54 to 58°. The spacings of the bedding surfaces are from 50 mm to 1000 mm. There are three joint sets. One joint set is subparallel to the beddings and the other two are at 250°/30° and 70° (strike)/90°. The spacings of the joint sets are 50 mm to 1000 mm. The bedding surfaces are continuous and without fill materials. No groundwater seeps out of the slope. This

slope is an overall dip slope but some rock layers on the slope form overdip scarps. The thicknesses of the rock layers are less than 5m by estimation. Lateral restraints as well as the friction and cohesion prevent these thin rock layers from sliding.

3.16.3 Site 38

The centre of the site is at the point (70mm, -40mm) with respect to the principal point of the air photograph AS 749 5025 215. The site is within the Rundle Group. The rocks are interlayers of medium to dark grey, thinly to thickly bedded, coarse grained and fine grained limestones. The Schmidt Hammer reading is 44±2. The attitude of the bedding surfaces is 240°/40°. The spacings of the bedding surfaces are from 50 mm to 500 mm. There are two joint sets at 60°/45 to 50° and 240° (strike)/90°. The spacings of the joint sets are 50 mm to 1 m. The bedding surfaces are continuous and without fill materials. No groundwater seeps out of the slope. The slope angle is 40°. So this slope is an overall dip slope and there are some layers on the slope to form overdip scarps. The thicknesses of the layers are less than 3m. Lateral restraints as well as the friction and cohesion prevent these thin rock layers from sliding.

3.16.4 Site 39

The centre of the site is at the point (0mm, 40mm) with respect to the principal point of the air photograph AS 749

5025 215. The site is within the Rundle Group. The rocks are dark grey, thinly to thickly bedded, fine grained limestones with interbedded black chert nodulars (Fig. 3.43). The Schmidt Hammer reading is 54±3. The attitude of the bedding surfaces is 235°/30°. The spacings of the bedding surfaces are from 50 mm to 250 mm. There are three joint sets. One joint set is subparallel to the bedding surfaces. The other two are at 235° (strike)/90° and 55°/60°. The spacings of the joint sets are 100 mm to 600 mm. The bedding surfaces are continuous and without fill materials. No groundwater seeps out of the slope. The roughness angle is 0°/0.91m. The slope is convex (Fig. 3.44) and there is a dip slope part in the east part. The largest slope angle is 60° at the overdip slope, where the investigation was conducted. The west part of the slope is covered by rock debris and the slope angle here is only 31°. The rockslide deposits are below the slope of the west part. The thickness and the volume of the potential sliding mass are 22 m and 8.0×10^5 m^3 calculated from the east part.

3.16.5 Site 40

The center of the site is at the point (-10mm, 80mm) with respect to the principal point of the air photograph AS 749 5025 215. The Slope is in the Rundle Group. The dip direction of the slope is due west and the dip direction of the beddeing surfaces is 230 to 240°. So it is reclassified as a plagioclinal slope.

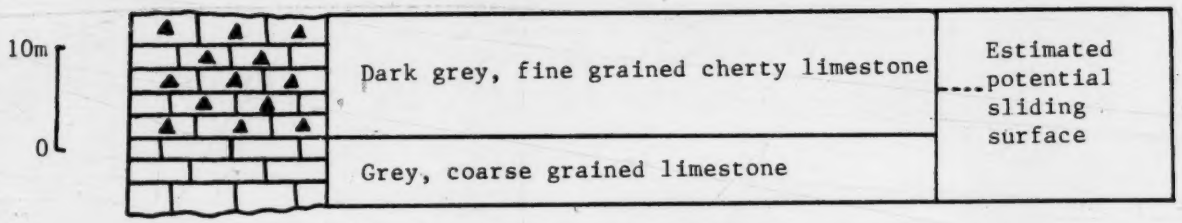

Figure 3.43 Lithology around the Potential Sliding Surface at Site 39

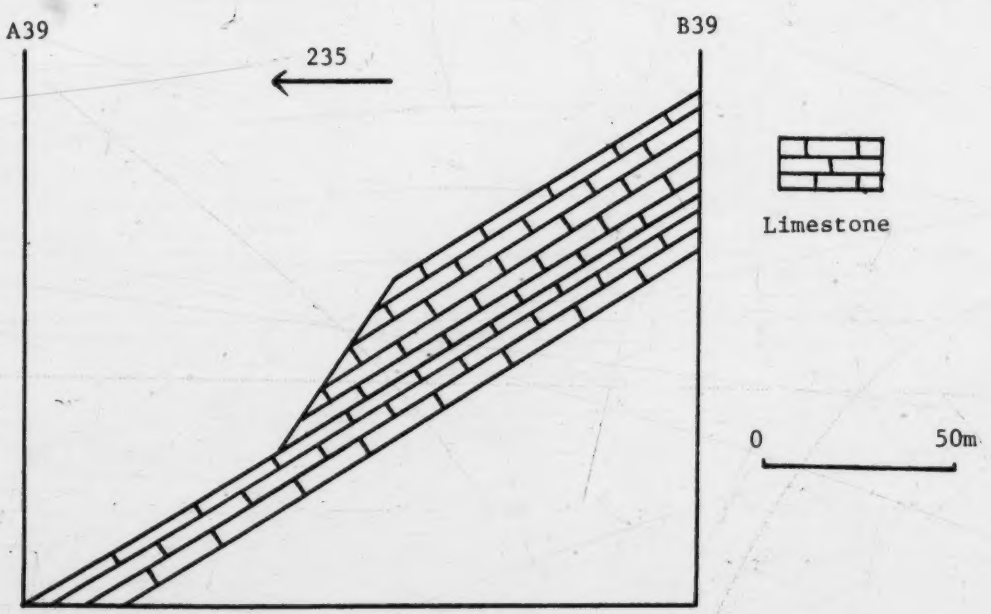

Figure 3.44 Cross-section of the slope at Site 39

3.16.6 Site 41

The centre of the site is at the point (0mm, 40mm) with respect to the principal point of the air photograph AS 749 5025 215. The site is within the Rundle Group. The rocks are dark grey, medium to thickly bedded, coarse grained limestones, chert-rich, dark grey, fine grained limestones and dark grey, fine grained dolomstones (Fig. 3.45). The Schmidt Hammer reading is 42±2. The attitude of the bedding surfaces is 250°/31°. The spacings of the bedding surfaces are from 100 mm to 1 m. There are five joint sets. One joint set is subparallel to the bedding surfaces. The other four are at 250° (strike)/90°, 70°/60 to 65°, 140°/55° and 320°/55°. The spacings of the joint sets are 50 mm to 2 m. The bedding surfaces are continuous and without fill materials. No groundwater seeps out of the slope. The roughness angle is 0°/0.91m. The slope is convex and there is a dip slope part (Fig. 3.46). The slope angle of the overdip slope is 80°. The thickness and the volume of the potential sliding mass are 30 m and 9.6×10^4 m^3.

3.17 Area of Highwood Pass

There are two sites, 42 and 43, in this area (Fig. 3.47). The access is from Highway 40. Park at the Highwood Pass parking lot. Walk 900 m north, turn right to enter the valley there and hike up about 2 km to reach Site 42. Walk about 1 km south from the parking lot, turn left to enter the valley there and hike up about 1500 m to reach Site 43.

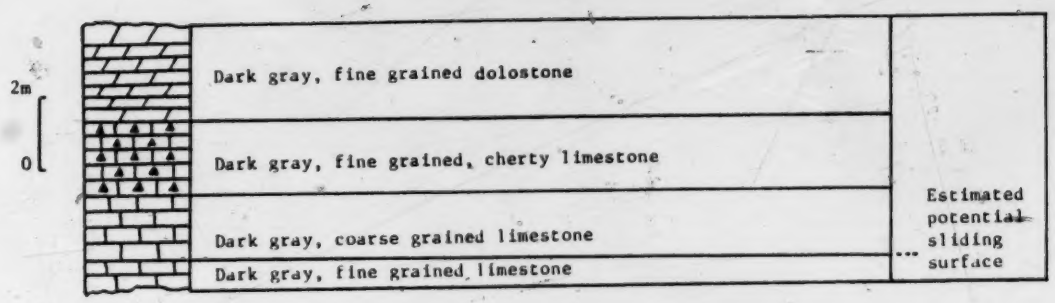

Figure 3.45 Lithology around the Potential Sliding Surface at Site 41

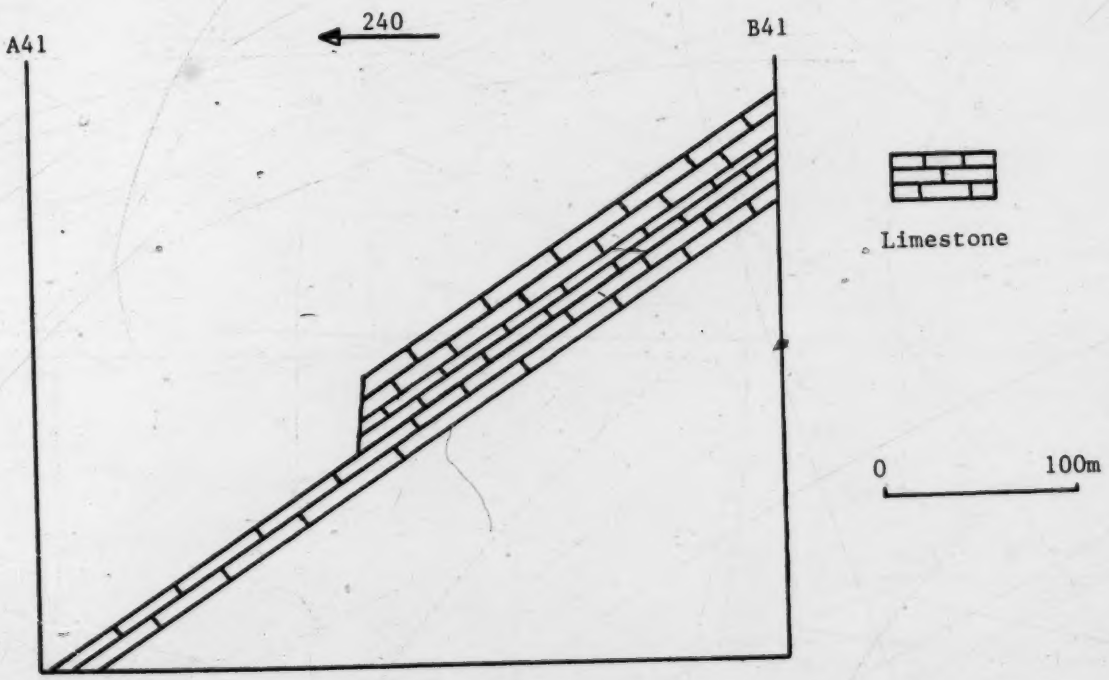

Figure 3.46 Cross-section of the slope at Site 41

Figure 3.47 Geology and the Working Sites in the Area of Highwood Pass, Based on the Air Photograph AS 748 5026 19

4633-5026
81-J-10
50°-36
115.840
AS 748

3.17.1 Site 42

The centre of the site is at the point (-20mm, 100mm) with respect to the principal point of the air photograph AS 748 5026 19. The site is within the Rundle Group. The rocks are dark grey, thinly to thickly bedded, crinoidal limestones and dark grey, fine grained dolomitic limstones. The Schmidt Hammer reading is 43±2. The attitude of the bedding surfaces is not constant at the site. The dip direction is 235° but the dip angles are 30° to 50°. The overall dip angle over the slope is 45°. The spacings of the bedding surfaces are from 75 mm to 500 mm. There are three joint sets. One joint set is subparallel to the bedding surfaces. The other two are perpendicular to the bedding surfaces and the strikes of two joint sets are parallel to and perpendicular to the bedding surfaces respectively. The spacings of the joint sets are 25 mm to 500 mm. The bedding surfaces are continuous and without fill materials. No groundwater seeps out of the slope. The slope angle is 60° for the overdip slope. The roughness angle is 10°/0.91m and it was estimated that the roughness angle on a 10m scale is still not less than 10°. Because the bedding dip changes up to 20°, more detailed work is needed to evaluate the effective friction angle and the stability of the slope.

3.17.2 Site 43

The centre of the site is at the point (30mm, 5mm) with respect to the principal point of the air photograph AS 748

5026 19. The site is within the Rundle Group. The rocks are medium to dark grey, thinly to medium bedded, coarse grained limestones. Fine to medium grained limestones exist locally. The Schmidt Hammer reading is 41±1. The attitude of the bedding surfaces is not constant at the site. The dip direction is 245° but the dip angles are 10 to 55°. The overall dip angle over the slope is 38°. The spacings of the bedding surfaces are from 50 mm to 250 mm. There are two joint sets. Both the two are perpendicular to the bedding surfaces and the strikes of two joint sets are parallel to and perpendicular to the bedding surfaces repectively. The spacings of the joint sets are 25 mm to 500 mm. The bedding surfaces are continuous and without fill materials. No groundwater seeps out of the slope. The slope angle is 38° so the slope is an overall dip slope. Only at the top of the slope a small part of the slope is overdip because the dip angle of the bedding surfaces becomes small and it is estimated to be less than 15°.

4. Basic friction angles and the factors influencing variation of basic friction angles

4.1 Tilting table tests and the results

4.1.1 Introducion to the tilting table tests

The tilting table is designed to estimate the friction angles between two smooth rock surfaces. The basic friction angle is one of the most important measures of the frictional properties of rock. It is defined as the friction angle between sawn surfaces lapped with #80 grit (Coulson, 1972).

Hoek and Bray (1974) suggested that the friction angle could be obtained by a simple tilt test when a clearly defined failure surface existed. They commented on the possible toppling of the upper block from the lower block due to the interlocking of asperities. In 1981, they suggested that the tilting tests for the basic friction angle were unreliable due to the influence of surface roughness at a very small scale. Cawsey and Farrar (1976) used a tilting table to measure the friction angle of naturally rough surfaces of soft Upper chalk. Barton and Choubey (1977) used a tilting table to estimate the residual friction angle on flat sawn surfaces. Bruce (1978) used a tilting table to evaluate the mineralogic and basic friction angles of a quartzite and a dolomite. Eaton (1986) used a tilting table to determine the basic friction angles of

limestones, dolostones and quartzites.

Hencher (1976) summarized some advantages and disadvantages of the tilting table. The advantages are: Observations of the mode of failure is easier than in an enclosed shearbox, failure is due to gravity as it is in the field, sliding tests can be repeated to give much greater displacments than using a direct shear test, the effect of block geometry and distribution of load may be analyzed, tests may be designed associated with field problems and testing procedure is simple. The disadvantages are: the applied loads are from the weight of the upper block which limits the range of loads possible, the test involves sudden sliding of the upper block so displacements cannot be controlled with the apparatus in its present form and the stress distribution along the contact between the two blocks is uneven.

The tilting table the author used was constructed by Eaton (1986) in the Department of Civil Engineering of University of Alberta. A rigid frame supports a hinged table and electric motor drive assembly. The drive assembly rotates a drum which has a wire cable attached to the hinged table. So the hinged table can be tilted when the drive assembly is on. Also the hinged table is equipped with brackets to hold samples from 5 by 5 cm to 15 by 15 cm. The plate sample is mounted in the brackets and the slider sample is placed on top of it. A linear voltage displacement transducer (LVDT) and a rotary voltage displacement

transducer (RVDT) are used and connected to a X-Y plotter to record the movement of the slider and the rotated angle of the table. A protractor is mounted on the end of the hinge of the tilting table to provide a quick visual reference. The table rotates from 0° to 52° with the present mounting of the drive and drum assembly.

4.1.2 Sample preparation and testing procedure

Rock samples were collected in Kananaskis Country during the summer of 1986 at the working sites of potential rockslides as well as at other working sites of overdip slopes. At most of the potential rockslides, samples were taken from beds around the potential sliding surfaces which are around the toes of the overdip slopes. But at a few sites the samples were taken from other locations because it was not possible to take rock samples which were big enough. All the carbonate samples are crystalline rocks although skeletal remains can be seen from a few samples.

A 60 cm diameter, self-advancing, diamond-tipped, water-lubricated rock saw was used to make the first cuts of the samples. A smaller hand-controlled saw was used to make delicate final cuts. All the rock samples were cut to 5 cm in length, 5 cm in width and 1.5 to 2.5 cm in thickness. Eaton (1986) noted that examination of fresh cut surfaces showed no distinction between cuts parallel to bedding and cuts orthogonal or oblique to it for most of the limestone and dolostone samples. So this is not considered further.

Samples then were lapped using a lapping table. #80 grit was used and all the samples were lapped with water. Lapping time for the limestone and dolostone samples were over 90 minutes and that for the quartz sandstone samples were over 2 hours.

After lapping the surfaces of the samples were cleaned with an air hose at a pressure of 965KPa. The sliding direction of the samples were indicated for all the plates and sliders. The plate was mounted on the tilting table by either clamping with the side brackets or resting the edge against the bottom bracket. The sliding surface was levelled with a level before tilting the sample.

Tilting table tests were conducted at the rate of 8° per minute. Each sample was tested 5 to 8 times and the results of the tests were recorded with the X-Y plotter.

The LVDT and the RVDT were calibrated before testing. The X-Y plotter was used to record the test results. Both the relationships between the displacement in X direction of the plotter and the angle rotated and between the displacement in Y direction of the plotter and that of the slider were linear. The LVDT's calibration is 8mm per volt and the RVDT's calibration is 5.26° per volt. The conversions in the X-Y plotter are 0.5 volt per centimeter in both X and Y direction.

The tests involved tilting the samples until the slider slid off the plate and recording the sliding angle by the X-Y plotter.

4.1.3 Test results

57 pairs of sliders and plates which were cut from 32 rock samples (Table 4.1) were tested. Of these samples, 30 are carbonate rocks and 2 are sandstones. The carbonate rocks include crystalline limestones, which vary in lithology from very coarse grained to finely micro-grained limestones based on the texture classification by Leighton and Pendexter (1962), and dolostones, which also vary from fine grained to coarse grained dolostones. All the rock samples were identified and described with the help of a hand lens, a penknife and 10% HCl.

From the X-Y plotter the initial sliding angles at which the sliders start to slide and the final sliding angles at which the sliders have slid more than 2 cm were determined. The mean initial and final sliding angles from 5 to 8 repeated tests for each pair of sliding samples were calculated (Table 4.2) and the mean final sliding angles are used to estimate the basic friction angles.

The basic friction angles attained from tilting tests vary from 24.4° to 26.5° for the quartz sandstone samples, from 21.1° to 31.5° for the dolostone samples and from 22.8° to 41.4° for the limestone samples. From Table 4.2, the basic friction angles of the dolostones are smaller than 32° and the fine grained limestone samples have smaller basic friction angles than the coarse grained limestone samples. The basic friction angles of the quartz sandstones are less than those of most of the carbonate rocks. The variability

Table 4.1 Rock samples and the sliding samples

Working Sites	Rock Samples	Sliding Samples
1	1-1	1-1-1
		1-1-2
		1-1-3
	1-2	1-2-1
		1-2-2
2	2-1	2-1-1
		2-1-1
4	4-1	4-1-1
7	7-1	7-1-1
	7-2	7-2-1
		7-2-2
	7-3	7-3-1
		7-3-2
8	8-1	8-1-1
		8-2-1
	8-2	8-2-2
9	9-1	9-1-1
		9-1-2
	9-2	9-2-1
		9-2-2
10	10-1	10-1-1
		10-1-2
	10-2	10-2-1
		10-2-2
11	11-1	11-1-1
		11-1-2
12	12-1	12-1-1
13	13-1	13-1-1
		13-1-2
14	14-1	14-1-1
15	15-1	15-1-1
		15-1-2
16	16-1	16-1-1
		16-1-2
20	20-1	20-1-1
		20-1-2
25	25-1	25-1-1

Continued on the next page...

Table. 4.1. Continued from previous page...

Working Sites	Rock Samples	Sliding Samples
26	26-1	26-1-1
27	27-1	27-1-1
		27-1-2
	27-2	27-2-1
		27-2-2
28	28-1	28-1-1
		28-1-2
	28-2	28-2-1
29	29-1	29-1-1
		29-1-2
30	30-1	30-1-1
		30-1-2
31	31-1	31-1-1
		31-1-2
35	35-1	35-1-1
		35-1-2
42	42-1	42-1-1
		42-1-2
43	43-1	43-1-1
		43-1-2

Rock Samples: The samples taken from the working sites in the study area.

Sliding Samples: The samples cut from the rock samples for tilting table tests. 1-1-1, 1-1-2 and 1-1-3 were cut from 1-1. and so on.

Table 4.2 Mean Initial and Final Sliding Angles of the Samples

Sliding Samples	Final Sliding Angles (Degree)	Initial Sliding Angles (Degree)	Lithology Determined in the Field
1-1-1	35.1±2.2	30.0±3.4	fine to coarse grained limestone
1-1-2	36.1±1.6	30.0±2.9	
1-1-3	35.1±2.6	27.3±2.8	
1-2-1	32.1±2.1	29.4±3.5	fine to coarse grained limestone
1-2-2	34.8±1.3	31.5±1.6	
2-1-1	23.4±1.2	19.6±1.1	fine grained limestone
2-1-2	25.6±2.7	23.4±2.1	
4-1-1	24.0±1.4	20.9±1.6	fine grained limestone
7-1-1	26.8±1.9	23.8±1.1	fine grained limestone
7-2-1	30.6±0.6	28.4±0.6	fine grained dolostone
7-2-2	29.6±1.3	27.5±2.5	
7-3-1	38.4±0.4	34.6±2.6	coarse grained limestone
7-3-2	37.6±1.6	34.9±1.6	
8-1-1	22.8±2.8	22.2±3.1	fine grained limestone
8-2-1	36.7±4.8	33.0±5.4	coarse grained limestone
8-2-2	39.4±2.7	39.0±3.0	
9-1-1	32.1±2.5	29.4±2.2	fine to coarse grained limestone
9-1-2	32.7±0.5	30.2±1.5	
9-2-1	41.4±3.3	39.9±2.4	coarse grained limestone
9-2-2	41.1±1.2	38.6±1.0	
10-1-1	33.0±1.2	29.9±2.4	fine to coarse grained limestone
10-1-2	28.3±2.0	26.7±1.2	
10-2-1	31.3±2.5	31.3±2.5	fine to coarse grained limestone
10-2-2	26.8±1.5	26.8±1.5	
11-1-1	23.1±1.4	20.8±1.0	quartz sandstone
11-1-2	25.7±1.5	23.2±1.9	
12-1-1	26.5±2.7	23.2±1.9	quartz sandstone
13-1-1	23.9±4.7	23.9±4.7	fine grained dolostone
13-1-2	24.4±2.1	22.6±3.6	
14-1-1	23.9±1.0	15.1±4.0	coarse grained dolostone
15-1-1	21.1±1.5	17.0±1.6	fine grained dolostone
15-1-2	22.0±1.1	20.8±1.4	
16-1-1	35.6±1.1	35.3±1.4	fine grained limestone
16-1-2	31.2±1.1	29.4±2.2	
20-1-1	34.3±2.0	33.5±2.7	fine to coarse grained limestone
20-1-2	37.1±3.5	37.1±3.5	
25-1-1	39.4±1.3	35.5±2.1	coarse grained limestone

Continued on the next page...

Table 4.2. Continued from previous page...

Sliding Samples	Final Sliding Angles (degree)	Initial Sliding Angles (degree)	Lithology Determined in the Field
26-1-1	34.7±2.9	34.7±2.9	coarse grained limestone
27-1-1	30.1±1.6	30.1±1.6	fine to coarse
27-1-2	31.6±1.6	31.6±1.6	grained limestone
27-2-1	29.3±1.4	27.6±1.7	fine grained
27-2-2	27.2±2.5	26.3±2.1	dolostone
28-1-1	29.6±3.7	27.4±5.0	fine grained
28-1-2	28.7±3.8	26.1±3.4	limestone
28-2-1	31.5±1.8	31.5±1.8	fine grained dolostone
29-1-1	31.5±2.6	31.2±3.1	fine to coarse
29-1-2	31.5±5.6	31.1±5.9	grained limestone
30-1-1	30.2±1.8	28.5±1.5	fine grained
30-1-2	30.3±2.5	29.6±2.6	limestone
31-1-1	36.7±0.7	35.7±1.7	fine grained
31-1-2	32.9±4.8	32.9±4.8	limestone
35-1-1	37.3±3.8	33.4±4.4	coarse grained
35-1-2	40.6±0.6	37.8±2.1	limestone
42-1-1	32.6±2.5	28.5±4.7	fine grained
42-1-2	36.7±1.3	36.7±1.3	dolostone
43-1-1	35.3±1.9	32.3±2.9	fine to coarse
43-1-2	33.3±0.9	29.7±1.6	grained limestone

The final and initial sliding angles in this table are represented as the mean ± standard deviation.

of the basic friction angles of limestones is larger than those of dolostones. All this might be due to variations of frictional properties of carbonate minerals and the mineral aggregates of carbonates. The mineral compositions based on the chemical analysis and the microscopic work are going to be determined later in this chapter. The rock textures are also going to be examined.

Coulson (1972) did direct shear tests for many kinds of rocks and gave four types of curves, which showed the relationships between the shear strengths and the displacements. The type 1 curve showed no change in shear strength with displacement. The type 2 curve showed shear strength decreases with displacement. The type 3 curve showed shear strength decreases with displacment at the beginning and then increases with displacement. The type 4 curve showed shear strength increases with displacement. Rock types, normal stresses and sliding surface conditions influence this type of behaviour.

For the six oven-dry limestone samples of Coulson's lapped with #600 grit or #80 grit or sandblasted, one gave a type 1 curve, one gave a type 2 curve and all the others gave type 3 or 4 curves when the normal stresses were low. All six samples gave type 3 or 4 curves when the normal stresses were high. The three oven-dry dolostone samples lapped with #600 grit or #80 grit or sandblasted gave type 2 curves when the normal stresses were low and they gave type 3 or 4 curves when the normal stresses were high. The

sandstones gave type 2 or type 3 or type 4 curves.

Bishop (1973) introduced the brittleness index I_B:

$$I_B=(\tau_f-\tau_r)/\tau_f \qquad (4.1)$$

τ_f is the peak shear strength and τ_r is the residual shear strength attained from the triaxial tests or direct shear tests.

For the tilting table tests conducted by the author, each sample was slid several times under very low normal stress caused only by the weight of the slider. Some factors, such as possibly different interlocking conditions for each sliding of one pair of samples and minor vibrations from the surroundings, can influence the results to some degree. Several different sliding angles were attained for each pair of the sliding samples. The sliding angles often increase and decrease several times. So it is difficult to compare the relationship between the displacement and the friction angle from tilting tests with the relationship of Coulson (1972) directly. In order to evaluate the major trend of the shear strength change with displacement, the expression for the brittleness index is modified and the every reading for each test is taken into account. The modified brittleness index(I_{MB}) is represented as:

$$I_{MB}=\Sigma[(\phi_{bi}-\phi_{bi+1})/\phi_{max}] \qquad (4.2)$$

ϕ_{bi} is the final sliding angle of ith sliding and the ϕ_{bi+1} is the final sliding angle of (i+1)th sliding. ϕ_{max} is

the largest final sliding angle for this sliding test. Σ means the summation of all the terms. The modified brittleness index for all the sliding samples was calculated (Table 4.3).

From Table 4.3, almost all the dolostone and sandstone samples have positive values, which means the shear strength decreases with displacement. The results are similar to those of Coulson (1972). The modified brittleness indexes for some of the limestone samples are negative and for some positive. That indicates the shear strength of limestones can either increase or decrease with displacement. The wear properties of the limestones might relate to their mineral compositions and textures. The results are also similar to those of Coulson (1972).

4.2 Chemical Analysis of the carbonate rocks

Little work has been done about the relationship between the mineral compositions and the frictional properties of the carbonate rocks. The chemical analyses were conducted to determine major mineral compositions of carbonates in the isotope laborotary of Department of Geology of the Unversity of Alberta. The chemical components which could be dissolved with hydrochloric acid were determined with the method of the atomic absorption spectromitry (Perkin-Elmer, 1976) and the insoluble components were examined under the binocular mocroscope.

Table 4.3 Modified brittleness indexes for the sliding samples

Sliding Samples	Modified Brittleness Indexes	Lithology	Sliding Samples	Modified Brittleness Indexes	Lithology
1-1-1	0.055	f-c ls	15-1-1	0.039	f dl
1-1-2	-0.043	f-c ls	15-1-2	0.090	f dl
1-1-2	-0.110	f-c ls	16-1-1	0.090	f ls
1-2-1	-0.080	f-c ls	16-1-2	0.072	f ls
1-2-2	0.027	f-c ls	20-1-1	0.144	f-c ls
2-1-1	-0.049	f ls	20-1-2	0.124	f-c ls
2-1-2	-0.063	f ls	25-1-1	0.077	c ls
4-1-1	-0.081	f ls	26-1-1	-0.051	c ls
7-1-1	-0.103	f ls	27-1-1	0.064	f-c ls
7-2-1	0.054	f dl	27-1-2	0.113	f-c ls
7-2-2	0.064	f dl	27-2-1	0.111	f dl
7-3-1	0.018	c ls	27-2-2	0.234	f dl
7-3-2	0.035	c ls	28-1-1	0.281	f ls
8-1-1	-0.079	f ls	28-1-2	0.301	f ls
8-2-1	-0.097	c ls	28-2-1	0.127	f dl
8-2-2	-0.056	c ls	29-1-1	0.194	f-c ls
9-1-1	-0.144	f-c ls	29-1-2	0.252	f-c ls
9-1-2	0.006	f-c ls	30-1-1	0.142	f ls
9-2-1	-0.046	c ls	30-1-2	0.170	f ls
9-2-2	0.026	c ls	31-1-1	0.021	f ls
10-1-1	0.061	f-c ls	31-1-2	0.143	f ls
10-1-2	0.035	f-c ls	35-1-1	0.146	c ls
10-2-1	0.153	f-c ls	35-1-2	0.012	c ls
10-2-2	0.063	f-c ls	42-1-1	0.165	f dl
11-1-1	0.112	q ss	42-1-2	0.039	f dl
11-1-2	0.080	q ss	43-1-1	0.133	f-c ls
12-1-1	0.221	q ss	43-1-2	0.063	f-c ls
13-1-1	0.380	f dl			
13-1-2	-0.123	f dl			
14-1-1	0.085	c dl			

f-c ls: fine to coarse grained limestone.

f ls: fine grained limestone.

c ls: coarse grained limestone.

f dl: fine grained dolostone

c dl: coarse grained dolostone

q ss: quartz sandstone.

4.2.1 Test procedure

All the carbonate samples were first decomposed with hydrochloric acid. The procedure to decompose the samples followed the method of Hillebrand *et al.* (1953, pp.964-965) but only 0.5 gram rock was used instead of 1 gram in Hillebrand *et al.* (1953) in order to get the solution within the range of specified concentrations for the chemical components to be determined. Then the insoluble materials were examined under the binocular microscope and the $CaCO_3$ contents and $CaMg(CO_3)_2$ contents were determined with the solutions using the Perkin-Elmer#503 Atomic Absorption Instrument. The method of conducting atomic absorption analyses followed Perkin-Elmer (1976).

30 carbonate rock samples of 5 to 10 grams were crushed to fine powder with a steel ball mill. About 0.5 gram powder from each sample was weighed and dissolved with 50% HCl. The samples were left to react with hydrochloric acid for over 24 hours. The solutions with the insoluble materials were leached with the filter papers of known weight.

Then the filter papers with the insoluble materials were dried with an oven and the temperature of the oven were adjusted to 90° to 95°. After the filter papers were completely dried, they were weighed and the weight of the insoluble materials and the insoluble material contents of the samples were calculated. The insoluble material contents of some samples were too low for precise determination so the insoluble materials are reported here only from the

samples with the insoluble materials over 5% by weight. The insoluble materials then were examined under a binocular microscope. Because there were only a few samples with insoluble contents larger than 10%, the possibility of finding a quantitative relationship between the basic friction angle and the insoluble mineral compositions was small and no precise examinations, such as X-ray analysis, of insoluble materials were made. Quartz was identified and distinguished from other materials which are almost all clay minerals and probably contain some organic materials in some samples.

The solution without the insoluble materials after leaching for each sample was transferred to a volumetric flask of 250 ml. Distilled water was added to the flask to reach the fill mark. Then 5 ml of the solution from the flask was taken out and put into another volumetric flask of 250 ml. 4 ml of $La(NO_3) \cdot 6H_2O$ solution which has 0.4 gram La per milliliter was added to the flask. La was used to remove the interferences caused by other elements, such as silicon and alumium, for both Ca and Mg and the slight ionization interference for Ca in the air-acetylence flame. Also 12.5 ml of concentrated HCl was added to the flask to make the concentration of HCl to be 5% because the concentrations of HCl of the standard solutions were 5%. Then the flask was filled with distilled water to 250 ml.

Several standard solutions of Mg and Ca were used to get the standard relationships between the readings from the

instrument and the concentrations of the solutions (Fig. 4.1 and Fig. 4.2). The concentrations of Mg and Ca in the prepared solutions were then determined.

4.2.2 Test results

The concentrations of Mg and Ca for all samples were calculated from the readings of the machine using the standard curves. Then the weights (mg) and the numbers of atomic milligrams for both Mg and Ca of all the samples were calculated. Next the numbers of molecular milligrams for the dolomite and calcite were calculated assuming that the molecular formulas of them are $CaMg(CO_3)_2$ and $CaCO_3$ respectively, i.e. no ionic substitution. Finally the weights and percentages of dolomites, calcites and insoluable materials for all the samples were attained (Table 4.4).

All the carbonate samples were reclassified (Table 4.5) according to the composition classification of Leighton and Pendexter (1962).

From the chemical compositions of the samples and the determined basic friction angles, we can see that the dolomites have basic friction angles less than 32°, all the impure carbonate samples with the insoluable materials larger than 10% except one have basic friction angles less than 31.5° and the limestones have basic friction angles from 22.8° to 41.4°.

Table 4.4 Weights and Percentages of $CaMg(CO_3)_2$, $CaCO_3$ and Impurities of the Carbonate Samples

Rock Samples	Weights(mg)			Percentages(%)		
	CM	CA	IMP	CM	CA	IMP
1-1	244.62	263.67	0	48.1	51.9	0
1-2	265.48	227.37	0	53.9	46.1	0
2-1	14.22	513.58	7.20	2.6	96.0	1.4
4-1	12.32	274.26	199.40	2.5	56.4	41.1
7-1	224.70	268.88	0	45.6	54.4	0
7-2	184.89	86.95	222.40	37.4	17.6	45.0
7-3	70.17	405.17	27.50	14.0	80.6	5.4
8-1	52.63	456.83	0	10.3	89.7	0
8-2	32.23	478.83	0	6.3	93.7	0
9-1	82.49	386.01	21.50	16.8	78.8	4.4
9-2	22.28	476.68	6.50	4.4	94.3	1.3
10-1	346.06	136.81	15.80	69.4	27.4	3.2
10-2	9.48	491.18	0	1.9	98.1	0
13-1	384.00	10.09	92.60	78.9	2.1	19.0
14-1	464.58	13.17	6.8	95.9	2.7	1.4
15-1	470.28	10.08	0	97.9	2.1	0
16-1	114.72	368.51	18.2	22.9	73.5	3.6
20-1	38.09	481.90	0	7.3	92.7	0
25-1	11.38	480.79	9.0	2.3	95.9	1.8
26-1	351.21	160.62	16.0	64.8	32.0	3.2
27-1	14.22	460.51	22.6	2.9	92.6	4.5
27-2	137.48	0	371.90	27.0	0	73.0
28-1	11.38	340.31	144.80	2.3	68.5	29.2
28-2	336.58	34.26	138.35	66.1	6.7	27.2
29-1	57.83	361.92	70.60	11.8	73.8	14.4
30-1	21.82	456.39	19.30	4.4	91.7	3.9
31-1	79.65	400.03	10.50	16.2	81.6	2.1
35-1	10.44	475.06	20.50	2.1	93.9	4.0
42-1	215.22	195.35	101.20	42.0	38.2	19.8
43-1	65.43	395.26	27.60	13.4	80.9	5.7

CM: $CaMg(CO_3)_2$ Dolomite

CA: $CaCO_3$ Calcite

IMP: Impurity.

Table 4.5 Rock types of the carbonate samples after the reclassification based on mineral compositions

Rock Samples	Rock Types
1-1	Dolomitic Limestone
1-2	Calcareous Dolostone
2-1	Limestone
4-1	Quartz limestone
7-1	Dolomitic Limestone
7-2	Clay Dolomitic Limestone
7-3	Dolomitic Limestone
8-1	Dolomitic Limestone
8-2	Limestone
9-1	Dolomitic Limestone
9-2	Limestone
10-1	Calcareous Dolostone
10-2	Limestone
13-1	Clay Dolostone
14-1	Dolostone
15-1	Dolostone
16-1	Dolomitic Limestone
20-1	Limestone
25-1	Limestone
26-1	Calcareous Dolostone
27-1	Limestone
27-2	Dolomitic Quartz Sandstone
28-1	Quartz Limestone
28-2	Clay Calcareous Dolostone
29-1	Quartz Dolomitic Limestone
30-1	Limestone
31-1	Dolomitic Limestone
35-1	Limestone
42-1	Clay Calcareous Dolostone
43-1	Dolomitic Limestone

Figure 4.1 Calibrated standard relationship between the reading from the Perkin-Elmer#503 Atomic Absorption Instrument and the concentration for magnesium ion

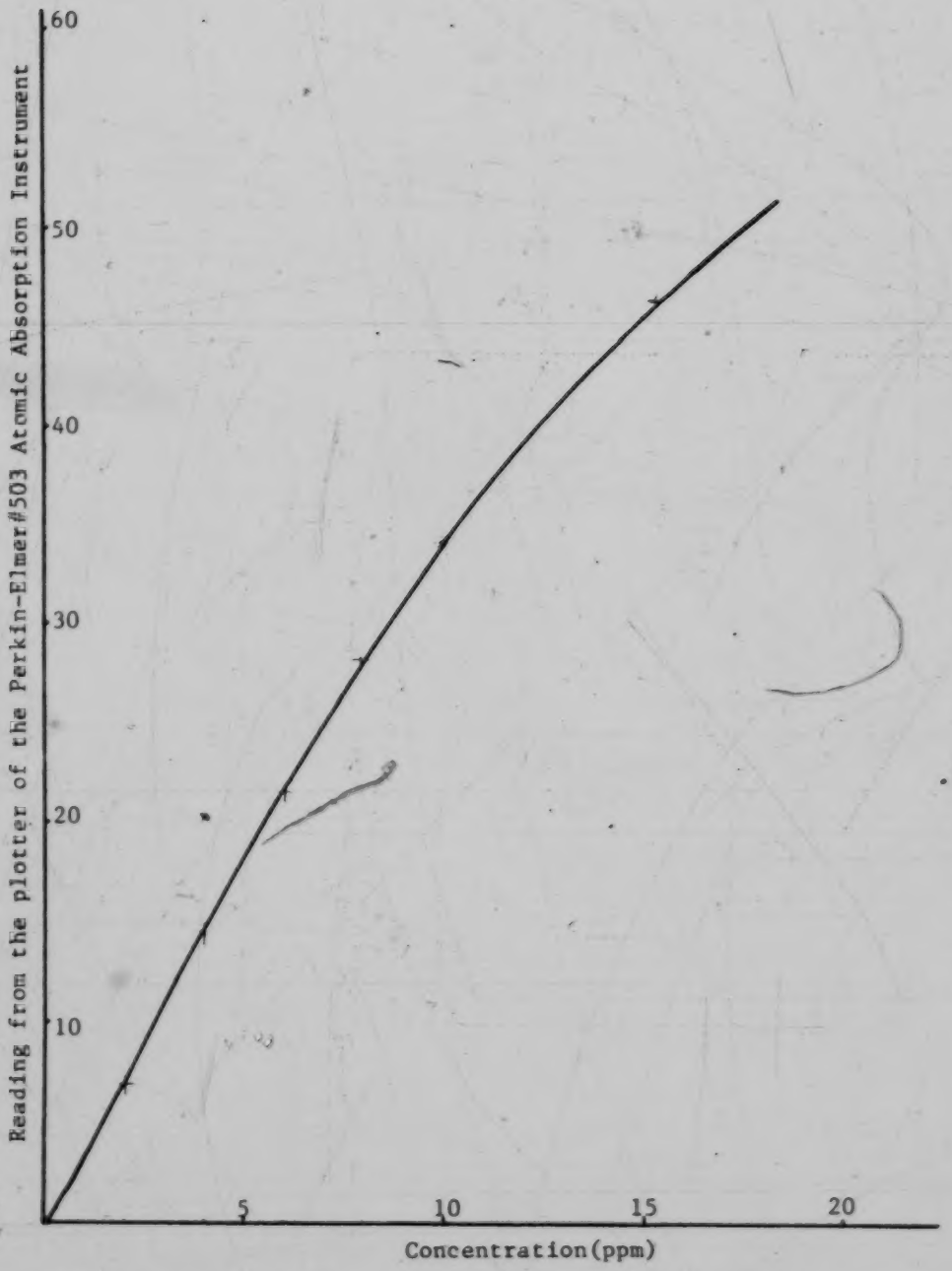

Figure 4.2 Calibrated standard relationship between the reading from the Perkin-Elmer#503 Atomic Absorption Instrument and the concentration for calcium ion

4.3 Grain sizes of the samples

Besides mineral composition, grain size is also one of the important factors influencing the frictional properties of the crystalline carbonate rocks. From the results of Eaton (1986) and the basic friction angles attained from tilting table tests and the visal examinations of the grain sizes in the field by the author, the basic friction angle decreases as the grain size decreases for most of the carbonate rock samples, especially for limestone samples.

Fookes and Higginbottom (1975) devised a classification of limestones for engineering purposes. In this classification, 0.002 mm, 0.06 mm and 2 mm were used to specify the boundaries between carbonate mud and silt, between carbonate silt and sand (or between fine grained limestone and detrital limestone) and between carbonate sand, calcarenite or detrital limestone and carbonate graval,calcirudite or conglomerate limestone respectively.

It is not possible to determine the mean grain size and the sorting of crystallised carbonate rocks at present. In order to evaluate the relationship between the grain sizes and the frictional properties of the carbonate rocks, the percentages of the grains whose sizes are larger than 0.06 mm were estimated (Table 4.6) using a binocular microscope with the help of the comparison chart for visal percentage estimation of grains (Terry and Chilingar, 1955). Because the percentages of the grains were estimated from flat surfaces, the percentages of larger grains have been

underestimated due to the cut effect.

4.4 Relationship between basic friction angle, mineral composition and grain size

From the discussion above, the basic friction angles of the crystalline carbonate rocks relate to their chemical compositions and grain sizes. From the results of the chemical analyses, 22 out of the 30 carbonate samples have less than 10% impurities (pure carbonate rocks) and the other 8 have more than 10% impuruties (impure carbonate rocks). It is found that the basic friction angles for all of impure carbonate samples except one are not larger than 31.5° but those for pure carbonates range from 22.8° to 41.4°. So it is reasonable to study the pure and impure carbonate samples separately.

4.4.1 Basic friction angles of the pure carbonate rocks

Because the basic friction angles of carbonate rocks depend on at least two factors, dolomite content and grain size, multiple linear regression analysis might be helpful to study the relationship between the basic friction angle, dolomite content and grain size. Before the multiple regression, the distribution of the data points was reviewed and the relationships between the basic friction angle and dolomite content and between the basic friction angle and percentage of grains larger than 0.06 mm were examined by simple regression analyses to explore the above

Table 4.6 Percentages of the Grain Sizes Larger Than 0.06mm for the Carbonate Samples

Samples	Percent	Samples	Percent
1-1	35	15-1	10
1-2	50	16-1	50
2-1	15	20-1	20
4-1	10	25-1	80
7-1	20	26-1	80
7-2	5	27-1	80
7-3	5	27-2	5
8-1	5	28-1	0
8-2	45	28-2	0
9-1	10	29-1	10
9-2	50	30-1	0
10-1	50	31-1	0
10-2	0	35-1	70
13-1	0	42-1	5
14-1	95	43-1	10

Percent: The percentages of grains larger than 0.06mm.

relationships.

From the scattergram of the basic friction angles and dolomite contents (Fig. 4.3), most of the samples have low dolomite contents and only a few samples have high dolomite contents. Without the samples with high dolomite contents, the results of simple regression would change significantly if the regresion is conducted. Considering that the basic friction angles of the two dolostone samples with 96% dolomite content and 95% coarse grains and 97% dolomite content and 10% coarse grains are 24° and 21.5° respectively (Table 4.7) and the basic friction angle of dolostones in the same study area determined by Eaton (1986) is about 26°, it is reasonable to think that the carbonates with high dolomite contents have low basic friction angles.

The results of simple regression between the basic friction angle and dolomite content assuming the basic friction angle is the dependent variable (Table 4.8 and Fig. 4.3) were attained from the data (Table 4.7). The R-square is only 0.205 and the correlation coefficient is -0.45. So the simple linear relationship is not significant. From Fig. 4.3, the basic friction angles of the samples those have very low dolomite contents range from 22.8° to 41.3°. The low basic friction angles for some samples with low dolomite contents may be caused mainly by small grain sizes. If all the samples, 2-1, 10-2, 8-1 and 30-1 which have basic friction angles below 31°, dolomite contents below 10% and less than 15% large grain sizes are deleted and the

Table 4.7 Dolomite Contents, Percentages of Grains Larger than 0.06mm and Basic Friction Angles of the Pure Carbonate Samples

Samples	CM	SIZE	FRIC
1-1	48.1	35	35.4
1-2	53.9	50	33.5
2-1	2.6	15	24.5
7-1	45.6	20	26.8
7-3	14.0	5	38.0
8-1	10.3	5	22.8
8-2	6.3	45	38.1
9-1	16.8	10	32.4
9-2	4.4	50	41.3
10-1	69.4	50	30.6
10-2	1.9	0	28.6
14-1	95.9	95	23.9
15-1	97.9	10	21.5
16-1	22.9	50	33.4
20-1	7.3	20	35.7
25-1	2.3	80	39.4
26-1	64.8	80	34.7
27-1	2.9	80	30.8
30-1	4.4	0	30.3
31-1	16.2	0	34.8
35-1	2.1	70	39.0
43-1	13.4	10	34.3

CM: Dolomite contents in percentage.

SIZE: The percentages of the grains larger than 0.06mm.

FRIC: Basic friction angles in degree.

The basic friction angles in the table are the means of the basic friction angles of the sliding samples from the same rock sample.

Table 4.8 Results of the simple regression of the basic friction angle on the dolomite content

Simple Regression X_1: CM Y_1: FRIC

DF:	R:	R-squared:	Adj. R-squared:	Std. Error:
21	.453	.205	.165	5.174

Analysis of Variance Table

Source	DF:	Sum Squares:	Mean Square:	F-test:
REGRESSION	1	138.241	138.241	5.164
RESIDUAL	20	535.37	26.768	p = .0342
TOTAL	21	673.611		

No Residual Statistics Computed

Simple Regression X_1: CM Y_1: FRIC

Beta Coefficient Table

Parameter:	Value:	Std. Err.:	Std. Value:	t-Value:	Probability:
INTERCEPT	34.529				
SLOPE	-8.261	3.635	-.453	2.273	.0342

Confidence Intervals Table

Parameter:	95% Lower:	95% Upper:	90% Lower:	90% Upper:
MEAN (X,Y)	29.962	34.565	30.361	34.166
SLOPE	-15.845	-.677	-14.532	-1.991

CM: Dolomite content.

FRIC: Basic friction angle.

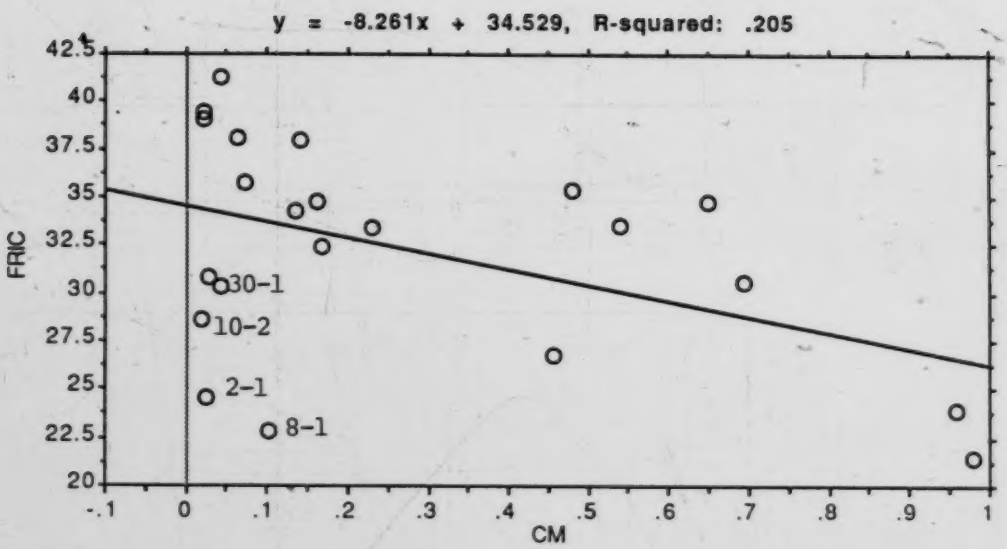

CM: Dolomite content.

FRIC: Basic friction angle.

Figure 4.3 Results of linear Regression between the Basic Friction Angle and the Dolomite Content

regression done again (Fig. 4.4 and Table 4.9). The linear relationship is better. The intercept is 37.7 and the slope is -12.9. The R-square is 0.616 and the correlation coefficient is -0.78. The relationship is significant at the level of 0.0001.

Looking at the scattergram and the results of the simple regression between the basic friction angles and the percentages of the grain sizes assuming that the basic friction angle is the dependent variable (Fig. 4.5 and Table 4.10). The points spread widely. The visal estimations of percentages of grains may introduce some error because the percentages of coarse grains were underestimated due to the cut effect. The relationship being studied is only that between the basic friction angles and underestimated percentages. The R-square is only 0.063 and the correlation coefficient is 0.25. The significance level from F-test is 0.2597. The simple linear relationship is not significant. The relationship is influenced by the dolomite contents because the basic friction angles increase as the dolomite contents decrease. The high basic friction angles for some samples with small grain sizes may be caused by low dolomite contents and the low basic friction angles for some samples with large grain sizes may be caused by high dolomite contents. If we delete all the four samples from 22 samples, 7-3, 14-1, 31-1 and 43-1 which have either high basic friction angles over 34° with less than 10% large grain size and less than 15% dolomite contents or basic friction angles

Table 4.9 Results of the regression of the basic friction angle on the dolomite content after deletion .

Simple Regression X_1: CM Y_1: FRIC

DF:	R:	R-squared:	Adj. R-squared:	Std. Error:
17	.785	.616	.592	3.386

Analysis of Variance Table

Source	DF:	Sum Squares:	Mean Square:	F-test:
REGRESSION	1	294.025	294.025	25.643
RESIDUAL	16	183.455	11.466	p = 1.0000E-4
TOTAL	17	477.48		

No Residual Statistics Computed

Simple Regression X_1: CM Y_1: FRIC

Beta Coefficient Table

Parameter:	Value:	Std. Err.:	Std. Value:	t-Value:	Probability:
INTERCEPT	37.715				
SLOPE	-12.885	2.545	-.785	5.064	1.0000E-4

Confidence Intervals Table

Parameter:	95% Lower:	95% Upper:	90% Lower:	90% Upper:
MEAN (X,Y)	31.841	35.225	32.14	34.927
SLOPE	-18.28	-7.49	-17.328	-8.442

CM: Dolomite content.

FRIC: Basic friction angle

Table 4.10 Results of the simple regression of the basic friction angle on the percentage of grains larger than 0.06mm

Simple Regression X_2: SIZE Y_1: FRIC

DF:	R:	R-squared:	Adj. R-squared:	Std. Error:
21	.251	.063	.016	5.618

Analysis of Variance Table

Source	DF:	Sum Squares:	Mean Square:	F-test:
REGRESSION	1	42.473	42.473	1.346
RESIDUAL	20	631.137	31.557	p = .2597
TOTAL	21	673.611		

No Residual Statistics Computed

Simple Regression X_2: SIZE Y_1: FRIC

Beta Coefficient Table

Parameter:	Value:	Std. Err.:	Std. Value:	t-Value:	Probability:
INTERCEPT	30.634				
SLOPE	4.597	3.963	.251	1.16	.2597

Confidence Intervals Table

Parameter:	95% Lower:	95% Upper:	90% Lower:	90% Upper:
MEAN (X,Y)	29.765	34.762	30.198	34.329
SLOPE	-3.67	12.864	-2.238	11.433

SIZE: Percentage of grains larger than 0.06mm.

FRIC: Basic friction angle.

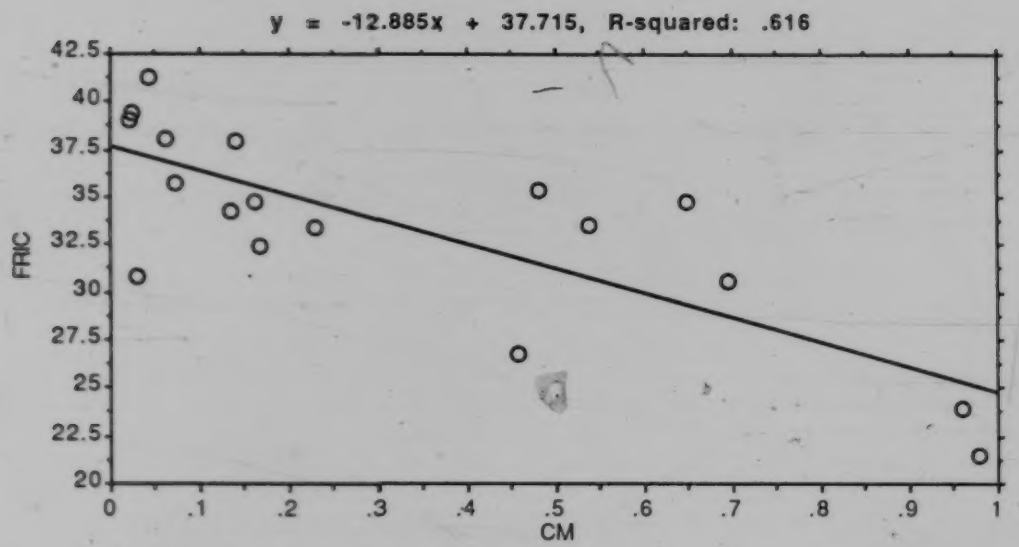

CM: Dolomite content.

FRIC: Basic friction angle.

Figure 4.4 Results of Linear Regression between the Basic

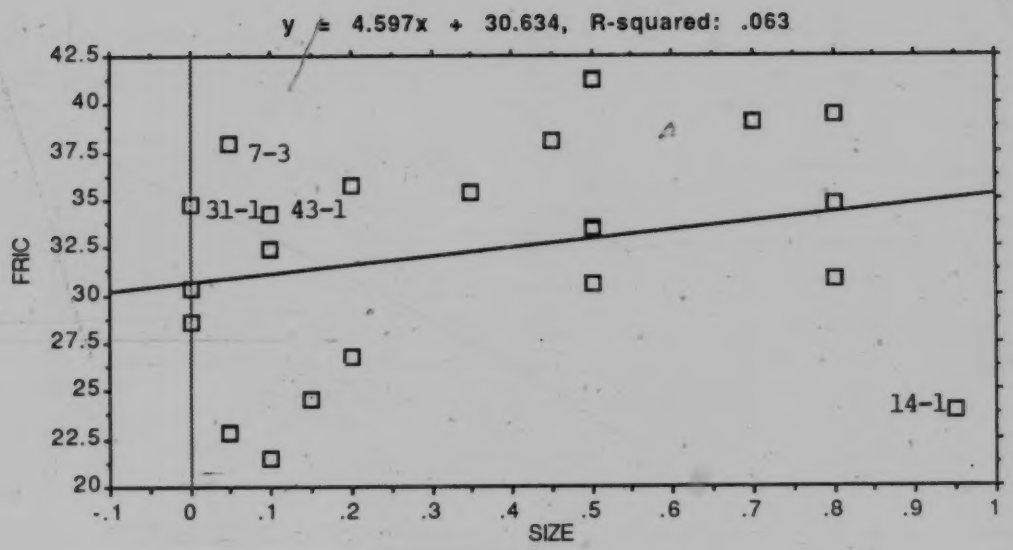

SIZE: Percentage of grains larger than 0.06 mm.

FRIC: Basic friction angle.

Figure 4.8 Results of Linear Regression between the Basic

less than 24° with more than 95% large grains and dolomite contents over 95%, run the regression again and the relationship is better (Fig. 4.6 and Table 4.11). R-square is 0.397 now and the correlation coefficient is 0.63. the relationship is significant at 0.0051. The intercept is 27.3 and the slope is 13.1.

This informal manipulation of the data indicates that a formal multiple regression analysis is necessary.

The results of the multiple regression of the basic friction angles on the dolomite contents and the percentages of the grain sizes (Table 4.12) indicates that the significance level of analysis of variance for the regression is 0.0153. The intercept is 32.4. The slope for the dolomite contents is -10.2 and that for the percentage of the grain sizes is 7.4. Both the slopes are significant at the significance level of 0.05.

$$\phi_b = 32.4 - 10.2(\text{dolomite content}) + 7.4(\%\text{coarse grains}) \qquad (4.3)$$

From the linear multiple regression equation, 18 samples out of 22 have the residuals of basic friction angles (Table 4.13) less than 6°. So the predicted value is a useful estimate of the basic friction angle of the pure carbonate rocks to within 6° and the results give an indication of the form of the above relationships.

Table 4.11 Results of the simple regression of the basic friction angle on the percentage of grains larger than 0.06mm after deletion

Simple Regression X_1: SIZE Y_1: FRIC

DF:	R:	R-squared:	Adj. R-squared:	Std. Error:
17	.63	.397	.359	4.595

Analysis of Variance Table

Source	DF:	Sum Squares:	Mean Square:	F-Test:
REGRESSION	1	222.075	222.075	10.516
RESIDUAL	16	337.89	21.118	p = .0051
TOTAL	17	559.964		

No Residual Statistics Computed

Simple Regression X_1: SIZE Y_1: FRIC

Beta Coefficient Table

Parameter:	Value:	Std. Err.:	Std. Value:	t-Value:	Probability:
INTERCEPT	27.41				
SLOPE	12.75	3.932	.63	3.243	.0051

Confidence Intervals Table

Parameter:	95% Lower:	95% Upper:	90% Lower:	90% Upper:
MEAN (X,Y)	29.859	34.452	30.264	34.047
SLOPE	4.414	21.086	5.885	19.615

SIZE: Percentage of grains larger than 0.06 mm.

FRIC: Basic friction angle.

Table 4.12 Results of the Multiple regression of the Basic Friction Angle, the Dolomite Content and the Percentage of the Grain Size Larger than 0.06mm

Multiple Regression Y_1:FRIC 2 X variables

DF:	R:	R-squared:	Adj. R-squared:	Std. Error:
21	.597	.356	.288	4.779

Analysis of Variance Table

Source	DF:	Sum Squares:	Mean Square:	F-test:
REGRESSION	2	239.758	119.879	5.25
RESIDUAL	19	433.853	22.834	p = .0153
TOTAL	21	673.611		

No Residual Statistics Computed

Multiple Regression Y_1:FRIC 2 X variables

Beta Coefficient Table

Parameter:	Value:	Std. Err.:	Std. Value:	t-Value:	Probability:
INTERCEPT	32.458				
CM	-10.252	3.488	-.562	2.939	.0084
SIZE	7.383	3.502	.403	2.109	.0485

Multiple Regression Y_1:FRIC 2 X variables

Confidence Intervals and Partial F Table

Parameter:	95% Lower:	95% Upper:	90% Lower:	90% Upper:	Partial F:
INTERCEPT					
CM	-17.552	-2.951	-16.283	-4.22	8.64
SIZE	.053	14.713	1.328	13.438	4.446

CM: Dolomite content FRIC: Basic friction angle

SIZE: Percentage of grains larger than 0.06 mm

Table 4.13 Residuals of basic friction angls from the linear multiple regression equation

Samples	FRIC	Residuals
1-1	35.4	5.29
1-2	33.5	2.88
2-1	24.5	-8.80
7-1	26.8	-2.46
7-3	38.0	6.61
8-1	22.8	-8.98
8-2	38.1	2.97
9-1	32.4	0.93
9-2	41.3	5.60
10-1	30.6	1.56
10-2	28.6	-3.66
14-1	23.9	-5.74
15-1	21.5	-1.66
16-1	33.4	-0.40
20-1	35.7	2.51
25-1	39.4	1.27
26-1	34.7	2.98
27-1	30.8	-7.27
30-1	30.3	-1.71
31-1	34.8	4.00
35-1	39.0	1.59
43-1	34.3	2.48

FRIC: Basic friction angle in degree.

Residuals: Differences between measured basic friction angles and those predicted from the regression equation.

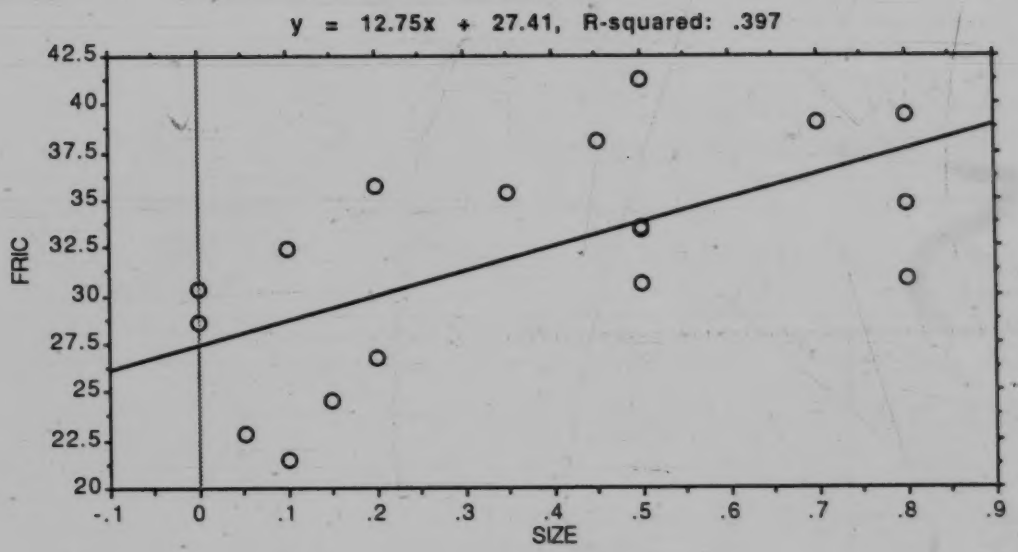

SIZE: Percentage of grains larger than 0.06mm.

FRIC: Basic friction angle.

Figure 4.6 Results of Linear Regression between the Basic Friction Angle and the Percentage of the Grain Size after

4.4.2 The basic friction angles of the impure carbonate rocks

Only 8 out of 30 samples are impure samples with the insoluble contents larger than 10% (Table 4.14). All the samples here are fine grained samples. The range for the basic friction angles of these samples is 24.0 to 34.7°. All the samples except one are not larger than 31.5°. The probable reason is that clay minerals can reduce the friction angles of the samples by lubricating the sliding surfaces. Also quartz can probably reduce the basic friction angles of the samples due to the low friction angle of its mineral surfaces.

Table 4.14 Mineral Compositions of the Impure Carbonate Samples and Their Basic Friction Angles

Samples	CM	CA	Qua	Clay	FRIC
4-1	2.5	56.4	32.8	8.2	24.0
7-2	37.4	17.6	2.2	42.8	30.1
13-1	78.9	2.1	1.0	18.0	24.2
27-2	27.0	0	54.8	18.2	28.3
28-1	2.3	68.5	27.7	1.5	29.2
28-2	66.1	6.7	1.4	25.8	31.5
29-1	11.8	73.8	13.7	0.7	31.5
42-1	42.0	38.2	2.0	17.8	34.7

CM: Dolomite contents in percentage.

CA: Calcite contents in percentage.

Qua: Quartz contents in percentage.

Clay: Clay mineral contents in percentage.

FRIC: Basic friction angles.

The basic friction angles in the table are means of the basic friction angles of the sliding samples from the same rock sample.

5. Stability analyses of the potential rockslides and other overdip slopes

5.1 Evaluation of the cohesion along the potential sliding surfaces

The shear strength between smooth rock surfaces can be estimated using the Mohr-Coulomb law (Goodman, 1980, p. 76).

$$\tau = c + \sigma \tan\phi \qquad (5.1)$$

This equation is valid at low normal stresses (Lama and Vutukuri, 1978, p. 67).

If the friction angle and the cohesion along a potential sliding surface are known, the safety factor of a potential rockslide can be calculated using the formula below.

$$F = \frac{c + [(W\cos\beta)/A - u]\tan\phi}{(W\sin\beta)/A} \qquad (5.2)$$

For impermeable hard rocks, Henkel (1967, p. 455) indicated that "as movement occurs, the tension cracks will open up and the level of water in the tension cracks will fall ..... Catastrophic rapid movements can only occur on these flat slopes if large supplies of surface water are available to maintain the water levels in the cracks as they open up." At all the sites in the study area, the limited water is

of water in discontinuities after the rock mass starts to move. So it is reasonable to ignore the pore pressure in estimating cohesion along bedding surfaces.

The safety factor of any potential rockslide is larger or at least equal to one because, if the safety factor of a potential rockslide were less than one, it would have slid already. So the inequality below can be attained.

$$(W\sin\beta)/A \leq c+(W\cos\beta\tan\phi)/A \qquad (5.3)$$

Based on this inequality, a lower bound (minimum value) of cohesion along the surface can be estimated. if W, A, β and ϕ are known.

In a series of tests on models with regular surface projections and without cohesion, Patton (1966b) demonstrated that if a discontinuity surface with identical asperities at an angle i from the mean discontinuity surface, the friction angle(ϕ) in the above equation is ϕ+i instead of ϕ. The dimensions of the samples of Patton (1966b) are 74.93 mm long by 44.45 mm wide. He also demonstrated the practical significance of this relationship by measurement of the average value of the angle i from photographs of bedding plane traces in unstable limestone slopes.

Fecker and Rengers (1971) measured the roughness angles of roughness surfaces by changing measuring base length and [illegible] that the effective roughness angle(i) decre[illegible]

with increasing measuring base length. Rengers (1970) showed that tan(i) was less than 0.05 when the base length was larger than 100cm by his test. Bruce and Cruden(1980) developed a statistical method to determine the waviness of bedding surfaces at scales up to 30 metres.

At 13 out of 18 sites which seem to be subject to sliding from the field investigation, the roughness angles are zero when the measuring base lengths are 0.91 metre. When the measuring base lengths are over 5 metres, the roughness angles for all these sites are zero by visual estimations.

It is difficult to measure the roughness angle of the bedding surfaces on a scale larger than 10 to 20 meters in the field because large parts of the potential sliding surfaces do not outcrop or access is not possible at most of the sites. But the visual examination of the attitudes of the bedding surfaces indicated that the large scale roughness angles at most of the sites are around 0° and may be ignored in reconnaissance studies.

As the potential sliding mass begins to slide, it will dilate and rest on only a few points along the bedding surface. The sliding rock mass and the rock under the sliding surface are not interlocked any more and sliding debris fills the space along the sliding surface. So the roughness angle at the scale of a few centimetres to 5 m are not important because the dimensions of the potential sliding mass are larger than 10 m at all the above 18 sites.

It is reasonable to ignore the influence of the roughness in estimating the lower bound of cohesion along bedding surfaces and evaluating the stability of a potential rockslide.

Barton (1971) suggested that the effective value of i depends upon the magnitude of the normal stresses. At very low normal stresses, smaller and steeper sided projections control movement. As the normal stress increases, these smaller projections are broken off and the gentle undulations of larger irregularities control the movement.

Cruden (1985) suggested that it was reasonable to take the basic friction angle of hard rocks as an estimate of the friction angle on their bedding surfaces except that when there is a concern that the rock has softened and altered or that the discontinuity has been polished by displacement.

Hoek (1974) described the cohesive strength of gouge-filled discontinuities, cohesive strength of cemented discontinuities, apparent cohesion due to surface roughness and influence of water on cohesive strength.

So if the basic friction angle is used to replace the friction angle in the shear strength equation, the cohesion in the equation is the overall cohesion which contains both the rock bridge cohesive strength and the cohesive strength caused by the surface roughness on local scale.

At many of the working sites, it was seen that there are more than one rock type and grain sizes of the same rock type change around the potential sliding surfaces. Rock

samples were not taken for all rock types due to the difficulty of extracting suitably sized samples and carrying them by backpacking over rough terrain. Rock samples were not taken at some of the sites. So the basic friction angles are estimated based on the field investigations and the results of Chapter 4.

If fine grained limestone exists at the site and no fine grained limestone samples were taken and tested, an estimate of the basic friction angle of 27° is used because all fine grained limestones except two have the basic friction angles not less than 27°. If there exists a rock type with the basic friction angle less than 27°, the actual basic friction angle is used. If there are no fine grained limestones, the basic friction angle is estimated directly from the test results. The basic friction angles for dolostones and quartz sandstones are estimated by the test results.

At some of the working sites, the thickness of the potential sliding mass does not change. At the sites where the thickness changes, the average thickness can be used in calculation. Then W/A which can be represented as the weight per unit area is dependent only on the thickness or average thickness if the density of the rocks is assumed to be constant. The thickness and the dip angle are estimated from the air photographs and topographic maps and confirmed by the field investigation.

Based on all this information, the lower bounds (minimum values) of the cohesion from the sites where the dip angle of the potential sliding surface is larger than the estimated basic friction angle with the thickness larger than 5 m is calculated assuming the unit weight of rocks is 27 KN/m^3 (Table 5.1) and the relationship between the lower bound of the estimated cohesion and the friction angle used to calculate the lower bound of cohesion is plotted (Fig. 5.1).

From the results, it can be seen that the lower bounds of cohesion are from 28KPa to 280KPa and there is no relationship between the apparent cohesion and the basic friction angle. All the calculated cohesion except at 3 sites are between 30 and 50KPa.

The sites that give lower bounds of cohesion larger than 50KPa or less than 30KPa are Site#8, #11 and #28. Site #8 gives a value of 100KPa because the basic friction angle used is only 22.8°. The sample was taken from a layer which was found at only two sites and the thickness is less than 60cm. Site #11 is the only site in quartz sandstones for estimating the cohesion and gives the lower bound of cohesion as 28KPa. The potential sliding surface at Site #28 is circular and it might be the rock mass is buttressed around the toe of the potential slide.

Considering that the rockslide movements are active, especially on overdip slopes, and there are not potential rockslides with big thicknesses, it is reasonable to use the

Table 5.1 Results of the Lower Bounds of Apparent Cohesion along Bedding Surfaces at 18 Working Sites

Sites	T(m)	Dip (degree)	Rock Types With Lowest Basic Friction Angle	Basic Friction Angles (degree)	Apparent Cohesions (KPa)
1	60	36	f-c ls	35.0	34
7	28	30	f ls	26.8	47
8	24	31	f ls	22.8	100
9	28	29	f ls	32.4	XX
10	75	30	f ls	29.0	40
11	90	25	q ss	24.4	28
12	90	25	q ss	26.5	XX
14	10	32	c dl	23.9	42
16	35	30	f ls	33.4	XX
20	8	44	f-c ls	35.7	38
28			f ls	29.1	280
29	60	25	f-c ls	25.0	XX
30	7	39	f ls	30.3	33
31	10	39	f ls	30.3	47
32	5	44	f ls	30.3	37
35	5	54	c ls	39.0	39
39	22	30	f ls	27.0	35
41	30	30	f ls	27.0	48

T: The thickness of the potential sliding mass.
Dip: Bedding dip.
f-c ls: Fine to coarse grained limestone.
f ls: Fine grained limestone.
c ls: Coarse grained limstone.
c dl: Coarse grained dolostone.
q ss: Quartz sandstone.
XX: The apparent cohesion can not be estimated.
The potential sliding surface at Site 28 is circular so the apparent cohesion was calculated by the moments with respect to the centre of the potential sliding surface.

The basic friction angles used at Sites 31 and 32 are same as that of Site 30 because the sample taken from Site 31 was from talus and the three sites are very close.

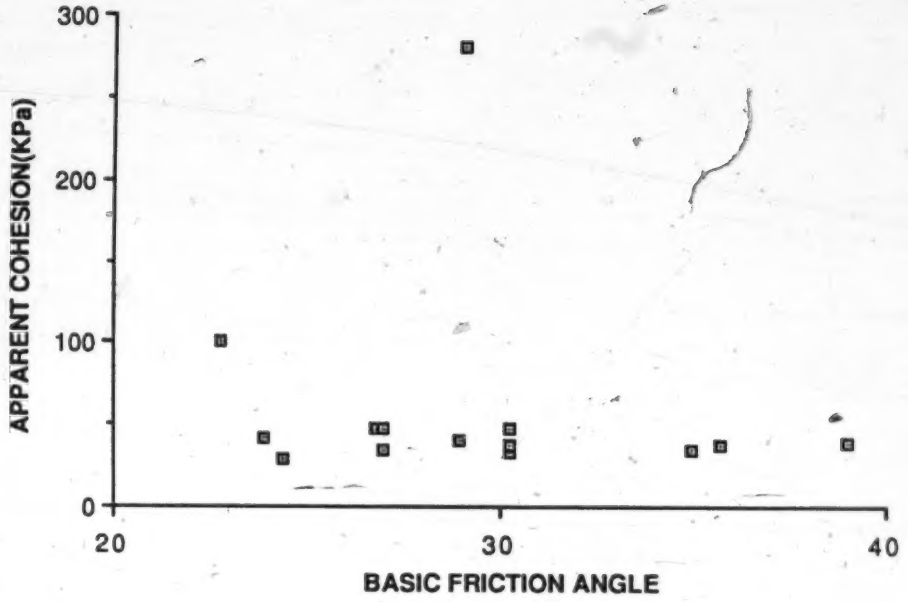

Apparent cohesion here is the lower bound of apparent cohesion along the bedding surface.

Figure 5.1 Relationship between the Apparent Cohesion and the Basic Friction Angle

range of 30 to 50KPa to estimate the cohesion along the bedding in the study area conservatively.

From the Mohr-Coulomb law, the relationship among the cohesion, the friction angle and the uniaxial compressive strength for intact rocks can be represented as follows (Goodman, 1980, p. 77):

$$c=\sigma_c/[2\tan(45°+\phi/2)] \qquad (5.4)$$

ϕ is the friction angle.

σ_c is the uniaxial compressive strength.

Indentation tests were conducted on some of the rock samples and the uniaxial compressive strengths were estimated from this index test(Mining Research and Developement Establishment, 1977). Based on the results of the uniaxial compressive strengths, the percentages of apparent rock bridges are calculated (Table 5.2). The comparison between the cohesion of intact rocks and the lower bound of the cohesion along bedding surfaces indicate that the minimum value of the proportion of rock bridge along bedding surfaces are less than 1% except at Sites 8 and 28 where the calculated apparent lower bounds of cohesion are considerably higher than those at the other sites because the estimated lower bounds of apparent cohesion along the bedding surfaces are higher at the two sites than at any other sites.

Table 5.2 Estimated Percentages of the Lower Bounds of Rock Bridges at 14 Working Sites

Sites	Basic friction angles (degree)	Uniaxial compressive strength (MPa)	COINT (MPa)	COAPP (KPa)	BRIAPP (%)
1	35.0	227	59	34	0.58
7	26.8	198	61	47	0.77
8	22.8	160	53	100	1.89
10	29.0	189	56	40	0.71
11	24.4	364	117	28	0.24
14	23.9	267	87	42	0.48
20	35.7	239	55	38	0.69
28	29.1	233	68	280	4.12
30	30.3	253	72	33	0.46
31	30.3	253	72	47	0.65
32	30.3	253	72	37	0.51
35	39.0	227	54	39	0.72
39	27.0	216	66	35	0.53
41	27.0	216	66	48	0.73

COINT: Cohesion of intact rock.
COAPP: Lower bound of apparent cohesion along bedding surfaces.
BRIAPP: Apparent percentage of lower bounds of rock bridges along bedding surfaces.

The basic friction angles and the uniaxial compressive strengths were estimated from the rock samples in the same way as in estimating basic friction angles for determining the lower bounds of cohesion along bedding surfaces.

Because the sample 31-1 was taken from talus and no sample was taken from Site 32 and the (potential) sliding surfaces at Sites 30, 31 and 32 are very close to each other with the same lithology, the basic friction angle from Site 30 are used for all the three sites, 30, 31 and 32.

5.2 Stability of overdip slopes

From the field investigation and the tests of basic friction angle, it can be found that stabilities of overdip slopes are controlled mainly by the geological structure and the frictional properties of rocks. Overdip slopes can be classified into two classes, potential rockslides and other overdip slopes.

5.2.1 Potential rockslides

If the basic friction angle of the bedding surfaces is less than the dip angle of the bedding surfaces at a site, it is the cohesion along the bedding surfaces that prevents the rock masses above the discontinuities from sliding. Cohesion can be destroyed completely by a small displacement and also cohesion can be worn away with time by weathering processes. All these overdip slopes are considered as potential rockslide slopes.

In the study area there are 13 potential rockslides. The dip angles of the bedding surfaces are from 25° to 54°. The basic friction angles vary from 22.8° to 39°. The lower bounds of the cohesion attained from most of the sites are only between 30KPa and 50KPa. Depending on the relationships among the basic friction angle, the dip angle of bedding surfaces and the cohesion along the potential sliding surfaces, the potential rockslides or rockslides with different volumes can form.

Table 5.3 Potential rock slides in the study area

Working Area	Working Site	Air Photograph number	Geological Formation (Group)
North of Mt. Lougheed	1	AS 745 5043 108	Mr
Mt. Sparrowhawk	7	AS 745 5041 11	Mr
Mt. Sparrowhawk	8	AS 745 5041 11	Mr
Mt. Sparrowhawk	10	AS 746 5040 206	Mr
Quartzite Ridge	11	AS 746 5040 204	Prm
North of Mt. Buller	14	AS 746 5039 155	Df
North Ribbon Creek	20	AS 745 5041 14	Dp
Opal Range	28	AS 747 5034 161	Mr
Burstall Pass	30	AS 747 5033 101	Dp
Burstall Pass	31	AS 747 5033 101	Dp
East of Mt. Black Prince	35	AS 748 5030 213	Dp
Aster Lake	39	AS 749 5025 215	Mr
Aster Lake	41	AS 749 5025 215	Mr

Df: Fairholme Group

Dp: Palliser Formation

Mr: Rundle Group

Prm: Rocky Mountain Group

The potential rockslides in the study area (Table 5.3) are distributed in the Rocky Mountain Group, the Rundle Group, the Palliser Formation and the Fairholme Group.

There is only one potential rockslide in the Fairholme Group. At this site (Site 14), the thickness and volume of the potential sliding mass are small.

The quartz sandstone in the Rocky Mountain Group have low basic friction angles and the rocks are hard. The calculated lower bound of cohesion is only 28KPa. There is a rock slide which is at the north end of Site 12 occurred with the bedding dip of 25°(Eaton, 1986). Although the basic friction angle from the tilting test is larger than the bedding dip at Site 12, it seems that it is still possible for the rock mass to slide because there is a large rockslide near the site.

The Rundle Group and the Palliser Formation are major cliff-forming units in the study area. There are 11 potential rockslides and 9 large rockslides, such as the slides in Mt. Indefatigable and in Mt. Sparrowhawk (Eaton,1986),in these two geological units.

In the Rundle Group, either fine grained limestones or dolostones with low basic friction angles can be found at any site except around the base of the Group where the rocks have higher basic friction angles. The condition that the basic friction angle is only a little less than the bedding dip favors formation of big potential rockslides because less cohesion is necessary in this condition than in the

case that the basic friction angle is much smaller than the bedding dip. Site #1 is an example at which the basic friction angle is only 1° less than the bedding dip. If the bedding dip is too big, a dip slope with some thin rock layers on it forms. Potential rockslides with the thicknesses of 5m to 75m are found through the Group.

In the Palliser Formation, only 8 sites were investigated. There are 4 potential rockslides in the Palliser Formation in the study area. The basic friction angles estimated at these sites are from 30.3 to 39°. The bedding dips are from 39° to 54°. The thicknesses of the potential rockslides are less than 10m due to the steep bedding surfaces. If the bedding surfaces were not as steep as at these sites, it would be possible to form big potential rockslides.

For the potential rockslides, the joint sets perpendicular to bedding surfaces can provide the potential lateral and back rupture surfaces if needed.

The shapes of most of the potential rockslides are convex or steplike. The dip slope parts of these slopes might be caused by earlier sliding.

5.2.2 Other overdip slopes

If the basic friction angle of the rocks at an overdip slope site is larger than the dip angle of the bedding surfaces, it is not likely that the rock mass of the slope will slide along bedding surfaces unless some external

forces act on the slope. These overdip slopes are not considered as potential rockslides. The overdip slopes can have planar surfaces or can have steep slopes caus mainly by the joint sets perpendicular to the bedding surfaces. The overall dip slopes are also included her

According to Selby (1982), if the slope is at the equilibrium state with respect to the rock mass streng rating, not controlled by geological structures and wi undercutting, the slope angle is only dependent on the mass strength rating. This kind of slope evolves paral the slope surface if the rock mass strength rating is constant. The rock mass strength ratings for 36 of the working sites were calculated (Table 5.4). The relatio between the rock mass strength rating and the slope an (Fig. 5.2) are plotted to study the effect of the rock strength ratings on slope angles. If the slope is conv the slope angle of the overdip slope is used. If the s angle changes at different sections, for instance, at 10, or the slope angle from the toe to the top of the changes due to undercutting by erosions, for instance, Sites 23 and 26, an average slope angle is estimated a used in Fig. 5.2. The straight line in the Figure 5.2 from Selby (1980) and is the regression line relating mass strength ratings and slope angles at the equilibr state. Table 5.5 lists all the sites except the potent rock slides. According to Selby (1980), the points wit degrees of the slope angles from the straight line can

Table 5.4 Rock mass strength ratings at 36 sites

Sites	SLAL	RMSR	Sites	SLAL	RMSR
1	45	60	22	37	67
2	27	60	23	50-60	65
3	27	60	24	30	61
4	37	64	25	60	66
7	45	66	26	40-60	61
8	49	63	27	31	60
9	40	63	28	70	64
10	38-65	60	29	37	64
11	38	60	30	43	61
12	37	64	31	43	61
13	40-45	64	35	55	61
14	37	65	36	40	63
15	37	64	37	55	63
16	44	63	38	40	63
17	57	74	39	60	64
19	40	62	41	80	64
20	45	60	42	60	60
21	40	66	43	38	60

SLAL: Slope angles in degree.

RMSR: Rock mass strength rating.

If the slope consists of a overdip slope part and a dip slope part or dip slope parts, the slope angles in the table are those of the overdip slope parts.

Table 5.5 Overdip slope sites except the potential rockslides

Working Area	Working Site	Air Photograph number	Geological Formation (Group)	Remark
North of Mt. Lougheed	2	AS 745 5043 108	Dp	
North of Mt. Lougheed	3	AS 745 5043 108	Dp	
Mt. Lougheed	4	AS 745 5042 55	Mb	
Mt. Lougheed	5	AS 745 5042 55	Mr	*
Mt. Lougheed	6	AS 745 5042 55	Mr	*
Mt. Sparrowhawk	9	AS 745 5042 11	Mr	
Quartzite Ridge	12	AS 746 5040 204	Prm	
Quartzite Ridge	13	AS 746 5040 204	Trs	**
Mt. Buller and Mt. Engadine	15	AS 746 5039 155	Df	
Mt. Buller and Mt. Engadine	16	AS 746 5038 109	Dp	
North Ribbon Creek	17	AS 746 5040 208	Mr	
North Ribbon Creek	18	AS 745 5041 12	Mr	*
North Ribbon Creek	19	AS 745 5041 12	Mr	
Ribbon Creek	21	AS 746 5039 157	Prm	
Ribbon Creek	22	AS 746 5039 157	Mr	
Ribbon Creek	23	AS 746 5039 159	Mr	
Mt. Kidd	24	AS 746 5039 161	Mr	*
Mt. Kidd	25	AS 746 5039 161	Mr	
Galatea Creek	26	AS 746 5038 113	Mr	
Galatea Creek	27	AS 746 5038 113	Mr	
Mt. Inflexible	29	AS 747 5034 157	Mr	
Burstall Pass	32	AS 747 5033 101	Dp	Rockslide
Mt. Murray	34	AS 747 5032 56	Mb	*
Aster Lake	36	AS 749 5024 162	Mr	
Aster Lake	37	AS 749 5024 162	Mr	
Aster Lake	38	AS 749 5025 215	Mr	
Headwood Pass	42	AS 748 5026 19	Mr	
Headwood Pass	43	AS 748 5026 19	Mr	

Df: Fairholme Group
Dp: Palliser Formation
Mb: Banff Formation
Mr: Rundle Group
Prm: Rocky Mountain Group
Trs: Sulphur Mountain Formation

*: The site is around the hinge of an anticline or a syncline.

**: Rock glacier

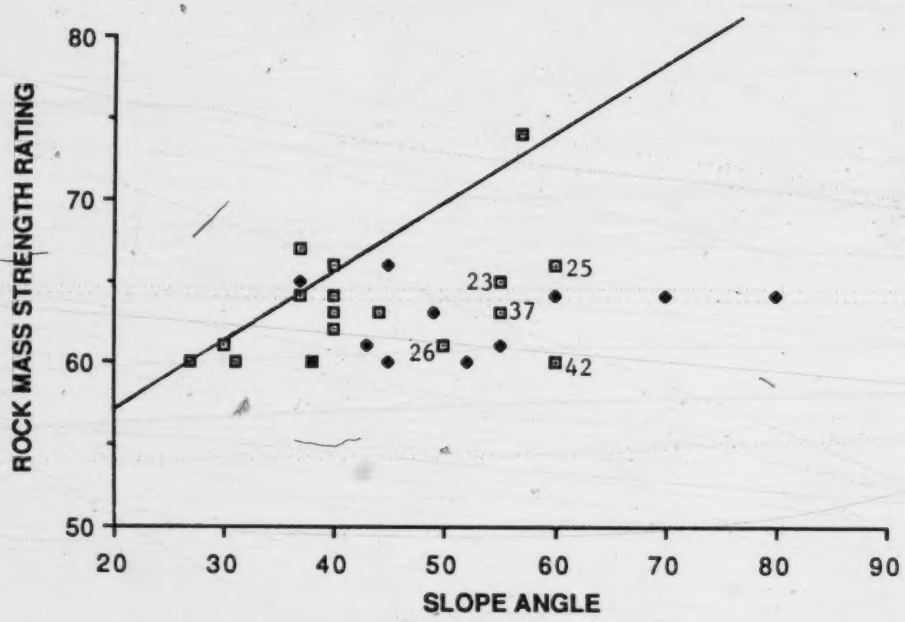

Figure 5.2 Relationship between the Rock Mass Strength Rating and the Slope Angle

considered as at the equilibrium state. From Fig. 5.2, we can see that some overdip slopes are close to the straight line but some are not.

Not considering the potential rockslides, those slopes not close to the line are Sites 23, 25, 26, 37 and 42. The bedding dips at Sites 23 and 25 are only 15° so the slope angles seem to be influenced mainly by the joints perpendicular to bedding. Also the slope at Site 23 was undercut by erosion. The overdip slope at Site 26 was formed by a small gully and the slope angle of the foot of the slope is larger than the value predicted from the rock mass rating. The reason is the slope is undercut by erosion. Site 42 was undercut by glacial processes because a cirque is below the slope. Site 37 is a overall dip slope so the slope angle is controlled by the bedding dip. The overall dip slope will be discussed below. Except Site 29, which is a convex slope, and Sites 27, 38 and 43, which are overall dip slopes, all the other slopes close to the line are planar. This indicates that the planar overdip slopes are controlled mainly by rock mass strength ratings.

On Figure 5.2, some potential rockslides and the overdip slopes obviously controlled by the structure also fall into the region of the equilibrium state. So the region is not exclusive.

Rocksliding is not a movement type for planar overdip slopes so no signs of earlier sliding can be seen. Toppling can occur on the joints perpendicular to bedding surfaces

(Cruden, 1987). An example of toppling is at Site 21. A thin layer of weathered rock debris generally covers the planar slope. If the rock mass strength rating does not change, the planar overdip slope can evolve parallel to the slope surface. Planar overdip slopes are found in the Fairhome Group, the Palliser Formation, the Banff Formation, the Rundle Group and the Rocky Mountain Group.

Figure 5.3 gives the relationship between the slope angle and the dip angle of the bedding surfaces at all the sites except the potential rockslides and Sites 5, 6, 17, 18, 24, 32 and 34. Sites 5, 6, 17, 18, 24 and 34 are around the hinges of the fold structures so the bedding dips are not constants at these sites. Site 32 is a rockslide site and the slope has become a dip slope because the sliding occured before. Of the 15 overdip slopes where the bedding dips are between 20° and 30° (including 20° and 30°), 12 are planar slopes. The other three are Site 27 which is an overall dip slope that is going to be discussed below, Site 29 which is a convex slope with a dip slope part and Site 26 which is obviously undercut by erosion. From Fig. 5.3, it can be seen that all the planar slopes except Site 42 occur where the bedding dip is between 20° and 30°. At Site 42, the roughness angle of the bedding surfaces is over 10° and this may account for the occurrence of the overdip slope where the bedding dips at 45°, which is much larger than the bedding dips of the other planar overdip slopes.

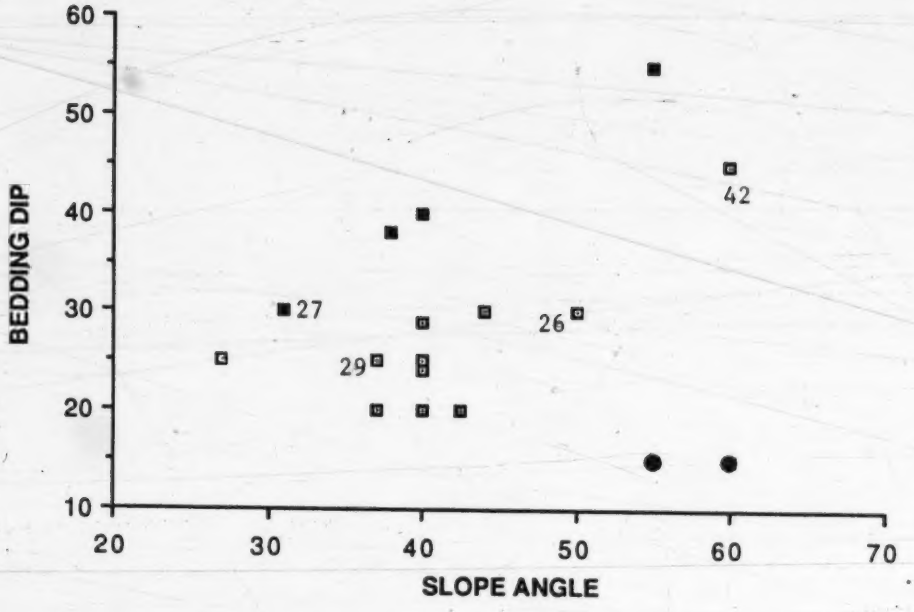

■ Overall dip slopes

● Overdip slopes developed from joints perpendicular to bedding surfaces

Figure 5.3 Relationship between the Slope Angle and the Bedding Dip

Besides the planar overdip slopes and the overdip slopes which are obviously undercut, the other overdip slopes are controlled mainly by the attitudes of the bedding surfaces and the joints.

When the dip angle of bedding surfaces is steep and much larger than the basic friction angle, the slope is an overall dip slope with only some thin layers on it to form overdip scarps. These thin layers are kept on the slope by the cohesion and maybe lateral restraints as well as the friction. Examples of this type of slope are Site 27, 37 and 38. The thicknesses of the thin layers on the slopes are generally less than 5m.

It was found that if the dip angle of the bedding surfaces is less than 20°, a steep slope with the slope angle in the range of 50-70° can form. This is because the overdip scarp can be developed from either of the joint sets perpendicular to bedding surfaces by toppling. These joint sets exist at all the sites. Examples are Site 23 and 25.

6 sites are around the hinge of the fold structures. The dip angle of the bedding surfaces around the fold hinge is generally smaller than that on the fold limbs and the bedding dips at these 5 sites are estimated as less than 15°. It is not likely that the potential rockslides can form. The access to these 5 sites is difficult.

6. Conclusions

1. Basic friction angles of carbonate rocks are controlled by mineralogy and grain sizes. For pure carbonate rocks, increasing dolomite contents decrease basic friction angles while big grain sizes increase basic friction angles. The basic friction angles vary from 22.8° to 41.4°. For impure carbonate rocks basic friction angles are generally less than 31.5° depending on clay mineral and quartz content. Basic friction angles of quartz sandstones in the study area are from 24.4° to 25.6°. The friction angles generally decrease with displacement for dolostones and quartz sandstones but there is no relationship between the friction angle and the displacement for limestones.
2. Lower bounds of apparent cohesion along bedding surfaces of carbonate rocks are generally between 30KPa and 50KPa. These correspond to less than 1% of apparent rock bridges along bedding surfaces.
3. If the bedding dip is greater than the basic friction angle, the overdip slope is a potential rockslide and the apparent cohesion prevents the potential sliding mass from sliding. But external forces can initiate sliding and cohesion can be worn away with time. The slope profiles of the potential rockslides are convex or steplike and 8 out of 13 slopes have a dip slope part or dip slope parts.
4. If the bedding dip is smaller than the basic friction

angle, the slope is not a potential rockslide. If the bedding dip is from 20° to 30° and the slope is planar, the slope angles can be predicted from the rock mass strength ratings. 12 out of 15 of the overdip slopes where the bedding dips are between 20° and 30° are planar. As the bedding dip increases and is much larger than the basic friction angle, overall dip slopes with only thin layers of rocks forming overdip scarps develop. If the bedding dip is less than 20°, overdip slopes with slope angles larger than 50 to 60° develop due to toppling from the joint sets prependicular to bedding surfaces.

Bibliography

Alberta Recreation and Parks, 1985a, The Map of Kananaskis Provincial Park Summer Trails.

Alberta Recreation and Parks, 1985b, The Map of Ribbon Creek/Spray Recreation Areas Summer Trails.

Alberta Government, 1981, Kananaskis Country Recreational Developement Planning Base Map. Department of Energy and National Resources, Alberta, Edition 5, Map.

Barton, N., 1971, A Relationship Between Joint Roughness and Joint Shear Strength, Proceedings, Symposium on Rock Fracture, Nancy, France, Paper 1-8.

Barton, N. R. and Choubey, V., 1977, The Shear Strength of Rock Joints in Theory and Practice, Rock Mechanics, 10, PP. 1-54.

Bayrock, L. A. and Reimchen, T. H. F., 1980, Surficial Geology, Alberta Foothills and Rocky Mountains, Alberta Research Council, 6 maps.

Beach, H. H., 1943, Moose Mountain and Morley Map-area, Alberta, Canada Geological Survey, Memoir 236, 74p.

Bielenstein, H. U., Price, R. A. and Jones, P. B., 1971, Geology of the Seebe-Kananaskis Area, Map in Halladay, I. A. R. and Mathewson, D. H., A Guide to the Geology of the Eastern Cordillera along the Trans Canada Highway between Calgary, Alberta and Revelstoke, British Columbia, Alberta Society of Petroleum Geologists, Calgary, 94p.

Bishop, A. W., 1973, The Stability of Tips and Spoil Heaps, Quarterly Journal of Engineering Geology, Volume 6, PP. 335-376.

Bruce, I. G., 1978, The field Estimation of Shear Strength on Rock Discontinuities, Ph. D. Thesis, University of Alberta, Edmonton, Alberta, Canada, 309p.

Bruce, I. G. and Cruden, D. M., 1980, Simple Rockslides at Jonas Ridge, Alberta, Canada, 3rd International Symposium on Landslides, New Delhi, Volume 1, pp. 185-190.

Carrara, A., 1983, Multivariate Models for Landslide Hazard Evaluation, Mathematical Geology, 15, No. 3, pp. 403-426.

Carrara, A., 1984, Landslide Hazard Mapping, Aims and Methods, Colloquium on Ground Movements, Caen Bureau de Recherches Géologiques et Minières, Document 83, pp. 142-151.

Carroll, D., 1970, Rock Weathering, Plenum Press, New York, 203p.

Cavers, D. S., 1981, Simple Methods to Analyze Buckling of Rock Slopes, Rock Mechanics, 14, pp. 87-104.

Cawsey, D. C. and Farrar, N. S., 1976, Simple Apparatus for Finding Rock Joint Friction, Geotechnique, 26, pp. 382-386.

Coulson, J. H., 1970, The effects of surface roughness on the shear strengths of joints, Ph.D. Thesis, University of Illinois, Urbana, Illinois, USA.

Coulson, J. H., 1972, Shear Strength of Flat Surfaces in Rock, Proceedings, 13th Symposium on Rock Mechanics, pp. 77-105.

Cruden, D. M., 1975, The Influence of Discontinuities on the Stability of Rock Slopes, in Mass Wasting, 4th Guelph Symposium on Geomorphology, Edited by E. Yatsu, A. J. Ward and F. Adams, Published by GEO ABSTRACTS LTD. University of East Anglia, Norwich, England, pp. 57-67.

Cruden, D. M., 1985, Rockslope Movements in the Canadian Cordillera, Canadian Geotechnical Journal, 22, pp. 528-540.

Cruden, D. M., 1987, Thresholds for Catastrophic Instabilities in Sedimentary Rockslopes, Some Examples from the Canadian Rockies, Symposium on the Dynamic System Approach to Natural Hazards, IASH, Vancouver, Canada, in press.

Cruden, D. M. and Eaton, T. M., 1985a, Reconnaissance of Rockslide Hazards in Kananaskis Country, Volume 1, Department of Civil Engineeirng, University of Alberta, Report to the Minister of Transportation, Government of Alberta, 133p.

Cruden, D. M. and Eaton, T. M., 1985b, Reconnaissance of Rockslide Hazards in Kananaskis Country, Volume 2, Department of Civil Engineering, University of Alberta, Report to the Minister of Transportation, Government of Alberta, 166p.

Dearman, W. R., 1974, Weathering Classification in the Characterisation of Rock for Engineering Purposes in British Practice. Bulletin of International Association

of Engineering Geology, 9, pp. 34-42.

Dearman, W. R., 1976, Weathering Classification in the Characterisation of Rock: A Revision. Bulletin of International Association of Engineering Geology, 13, pp. 123-127.

Deere, D. U., 1968, Geological Considerations, In: Rock Mechanics in Engineeirng Practice, Edited by O. C. Zienkiewicz and D. Stagg, Wiley, New York, pp. 1-20.

deWit, R. and Mclaren, D. J., 1950, Devonian Sections in the Rocky Mountains between Crowsnest Pass and Jasper, Alberta, Geological Survey of Canada, Paper 50-23.

Douglas, R.J.W., 1958, Mount Head map-area, Alberta, Geological Survey of Canada, Memoir 291.

Eaton, T. M., 1986, Reconnaissance of Rockslide Hazards in Kananaskis Country, M. Sc. Thesis, University of Alberta, Edmonton, 291p.

Environment Canada, 1981, Canadian Climate Normals, Temperature and Precipitation, Prairie Provinces, 1951-1980, Environment Canada, pp. 12, 21, 66, 91, 103, 104 and 161.

Fecker, E. and Renger, N., 1971, Measurement of Large Scale Roughness of Rock Planes by means of Profilograph and Geological Compass, Proceedings, International Symposium on Rock Fracture, Nancy, France, 1-18, 11p.

Fookes, P. G. and Higginbottom, I. E., 1975, The Classification and Description of Near-shore Carbonate sediments for Engineering Purposes, Geotechnique, 25, pp. 406-411.

Gardner, J. S., 1980. Frequency, Magnitude and Spacial Distribution of Mountain Rockfalls and Rockslides in the Highwood Pass Area, Alberta, Canada, Chapter 3 in Coates, D. R. and Vitek, J. D., Thresholds in Geomorphology, Allen and Unwin, Boston, pp. 267-295.

Gardner, J. S., 1982, Alpine Mass-wasting in Contemporary Time: Some Examples from the Canadian Rocky Mountains, Chapter 8 in Thorn, C. E., Space and Time in Geomorphology, Allen and Unwin, Boston, pp. 172-192.

Gardner, J. S., 1983, Rockfall Frequency and Distribution in the Highwood Pass Area, Canadian Rocky Mountains, Zeitschrift fur Geomorphologie, 27, pp. 311-324.

Goodman, R. E., 1980, Introduction to Rock Mechanics, John Wiley & Sons, United States of America, 478p.

Greenlee, G. M., 1981, Soil Survey of Designated Areas within Kananaskis Provincial Park, Alberta and Interpretation for Recreational use, Earth Sciences Report 80-5, Alberta Research Council, 58p.

Halladay, I. A. R. and Mathewson, D. H., 1971, A Guide to the Geology of the Eastern Cordillera along the Trans Canada Highway between Calgary, Alberta and Revelstoke, British, Columbia, Canadian Exploration Frontiers Symposium, Alberta Society of Petroleum Geologists, Calgary, 94p.

Hansen, A., 1984, Strategies for Classification of landslides, Chapter 1 in Brunsden, D. and Prior, D. B., Slope Instability, Wiley, Toronto, pp. 1-25.

Heim, A., 1932, Bergsturz und Menschenleben, Vierteljahrschrift der naturforsch, Gesellschaft, Zürich, 77.

Hencher, S. R., 1976, Discussion of " A Simple Sliding Apparatus for the Measurement of Rock Joint Friction", Geotechnique, 26, pp. 641-644.

Henkel, D. J., 1967, Local Geology and the Stability of Natural Slopes, Proceedings, American Society of Civil Engineers, 93, SM4, pp. 437-446.

Hillebrand, W. F., Lundell, G. E. F., Bright, H. A. and Hoffman, J. I., 1953, Applied Inorganic Analysis, John Wiley and Sons. Inc., New York, 1034p.

Hoek, E. and Bray, J., 1974, Rock Slope Engineeirg, Institute of Mining and Metallurgy, London, U.K., 402p.

Hoek, E. and Bray, J., 1981, Rock Slope Engineeirg, Institute of Mining and Metallurgy, London, U.K., 358p.

Ingram, R. L., 1954, Terminology for the Thickness of Stratification and Parting Units in Sedimentary Rocks, Bulletin, Geological Society of America, 65, pp. 937-938.

International Society for Rock Mechanics, 1973, Suggested Methods for Determining the Point-load Strength Index, ISRM Committee on Laboratory Tests, Document No. 1, pp. 8-12.

International Society for Rock Mechanics, 1978, Suggested Methods for the Quantitative Description of Discontinuities in Rock Masses, International Journal of Rock Mechanics and Mining Sciences and Geomechanics Abstracts, Vol. 15, No. 6, pp. 319-368.

Jackson, L. E., 1976, Surfacial Geology and Terrain Inventory Kananaskis Lakes 82-J (Alberta Protion), Geological Survey of Canada, Open file 924, 2 maps.

Jackson, L. E. Jr., 1981, Quarternary Stratigraphy of t Regoin between Calgary and the Porcupine Hills, In Thompson, R. I. and Cook, D. G., Field Guide to Geo and Mineral Deposits, Calgary, 1981, Annual Meeting Geological Association of Canada, pp. 79-99.

Jaeger, C., 1979, Rock Mechanics and Engineering, Cambr University Press, London, 523p.

Kohl, W. R., 1976, Map of Overdip Slopes that Can Affec Landsliding in Armstrong Country, Pennsylvania, U. Geological Survey, Map MF-730.

Lama, R. D. and Vutukuri, V. S., 1978, Handbook on Mechanical Properties of Rocks, Volume IV, Trans Te Publications, Clausthal, Germany, 515p.

Leighton, M. W. and Pendexter, C., 1962, Carbonate Rock Types, In Classification of Carbonate Rocks, A Symposium, Edited by William E. Ham, Published by t American Association of Petroleum Geologists. Tulsa Oklahoma, USA, pp. 33-61.

Locat, J. and Cruden, D. M., 1977, Major Landslides on Eastern Slopes of the Southern Canadian Rockies, Proceedings, 15th Symposium on Engineeirng Geology, University of Idaho, pp. 179-197.

Macqueen, R.W. and Bamber, E. W. , 1967, Stratigraphy o Banff Formation and Lower Rundle Group(Mississippia Southwestern Alberta, Geological Survey of Canada, 67-47, 37p.

Macqueen, R. W., Bamber, E. W. and Mamet, B. L., 1972, Carboniferous Stratigraphy and Sedimentology of the Southern Canadian Rocky Mountains, XXIV Internation Geological Congress, Montreal, Canada, 62p.

McGugan, A. and Rapson, J. E., 1962, Permo-Carboniferou Stratigraphy, Crowsnet Area, Alberta and British Columbia, Journal of the Alberta Society of Petrol Geologists, 10, pp. 352-368.

Middleton, G. V., 1963, Facies Variation in Mississipp Elbow Valley Area, Alberta, Canada, Bulletin of the American Association of Petroleum Geologists, 47, 1813-1827.

Mining Research and Developement Establishment, 1977, Cone Indenter, MRDE Handbook, No. 5, 12p.

Moye, D. E., 1955, Engineering Geology for the Snowy Mountains Scheme, Journal of Inst. of Engineers, Australia, 27, pp. 281-299.

Müller, L., 1959, The European Approach to Slope Stability Problems in Open Pit Mines, Proceedings of 3rd Symposium on Rock Mechanics, Colorado School of Mines Quarterly, 54, No. 3, pp. 116-133.

Norris, D. K., 1972, A Method for the Determination of Geographic Position, Geological Survey of Canada, Paper 72-1, Part B, pp. 124-125.

Ollerenshaw, N. C., 1968, Preliminary Account of the Geology of Limestone Mountain Map-area, Southern foothills, Alberta, Geological Survey of Canada, Paper 68-24, 37p.

Pachoud, A., 1975, Zones Exposées a des risques liès aux mouvements du sol, Cart Zermos, Bureau de Recherches Géologique et Minières, 2 maps, Paris, France.

Patton, F. D., 1966a, Multiple modes of shear failure in rock and related material, Ph. D. Thesis, University of Illinois, Urbana, Illinois, USA, 282p.

Patton, F. D., 1966b, Multuple Modes of Shear Failure in Rock, Proceedings of 1st International Congress of Rock Mechanics, Lisbon, 1, pp. 509-513.

Perkin-Elmer, 1976, Analytical Methods for Atomic Absorption Spectrophotometry, User's Manual.

Porter, S. C. and Orombelli, G., 1981, Alpine Rockfall Hazards, American Scientists, 69, pp. 67-75.

Protodyakonov, M. M., 1960, New Methods of Determining Mechanical Properties of Rock, Proceedings of International Conference on Strata Control, Paris, Paper C2, pp. 187-195.

Raymond, P. E., 1930, The Paleozoic Formations in Jasper Park, Alberta, American Journal of Science, 5th series, 20, pp. 289-300.

Rengers, N., 1970, Influence of the Surface Roughness on the Friction Properties of Rock Planes, Proceedings of 2nd Congress of the International Society of Rock Mechanics, Belgrade, 1, pp. 229-234.

Rutter, N. W., 1972, Geomorphology and Multiple Glaciation in the Area of Banff, Alberta, Geological Survey of Canada, Bulletin 206.

Ruxton, B. P. and Berry, L., 1957, The Weathering of Granite

and Associated Erosional Features in Hong Kong, Bulletin, Geological Society of America, 68, pp. 1263-1292.

Selby, M. J., 1980, A Rock Mass Strength Classification for Geomorphic Purposes: with Tests from Antactica and New Zealand, Zeitschrift fur Geomorphologie, 24, 1, pp. 31-51.

Selby, M. J., 1982, Hillslope Materials and Processes, Oxford University Press, New York, 264p.

Simmons, J. V., 1977, Observations of Translational Rockslides in the Eastern Foothills of the Rocky Mountains, 49° to 52° North Latitude,Report, Geological Survey Division, Alberta Research Council, 36p.

Tang, S. W. Y., 1986, Field Examples of Toppling Induced by External Forces, M. Eng. Report, University of Alberta, Edmonton, Canada, 62p.

Terry, R. D. and Chilingar, G. V., 1955, Summary of "Concerning Some Additional Aids in Studying Sedimentary Formations" by M. S. Shvestov, Journal of Sedimentary Petrology, Vol. 25, pp. 229-234.

Terzaghi, K., 1962, Stability of Steep Slopes on Hard Unweathered Rock, Geotechnique, 12, pp. 251-270.

Whitehouse, J. E. and Griffiths, G. A., 1983, Frequency and Hazard of Large Rock Avalanches in the central Southern Alps, New Zealand, Geology, 11, pp. 331-334.

Appendix

Test Results

The testing results from tilting table tests, chemical analyses of the carbonate samples and indentation tests are presented in this appedix.

Table A.1 Tilting table test results

Sliding Sample		Testing Sequence 1	2	3	4	5	6
1-1-1	φ_f	37.1	38.4	33.9	33.7	32.6	35.0
	φ_i	35.3	30.9	29.7	29.6	30.0	24.7*
1-1-2	φ_f	34.1	38.9	36.1	36.3	35.3	35.8
	φ_i	30.2	34.6	31.6	26.8	27.6	28.9
1-1-3	φ_f	32.9	34.2	38.9	32.2	35.0	37.2
	φ_i	23.7	27.6	29.7	23.9	29.5	29.2
1-2-1	φ_f	32.1	29.5	30.0	32.5	33.8	34.9
	φ_i	26.3*	28.9	26.8	27.1	33.6	33.9
1-2-2	φ_f	34.2	34.5	36.1	36.6	33.9	33.2
	φ_i	34.2	31.6	31.6	30.0*	29.7*	31.6*
2-1-1	φ_f	22.1	24.1	21.8	24.6	24.2	23.3
	φ_i	20.0	19.7	18.2	21.1	20.0	18.4*
2-1-2	φ_f	26.6	22.6	23.0	24.5	28.7	28.4
	φ_i	26.6	22.6	23.0	21.6	25.0	21.3
4-1-1	φ_f	23.7	24.6	21.8	23.2	25.0	25.8
	φ_i	20.5	22.9*	20.2*	18.7*	20.2*	22.6
7-1-1	φ_f	27.9	24.5	27.9	26.6	24.6	29.1
	φ_i	24.2	21.6	23.7	24.5	24.2	24.7

Sliding Sample		Testing Sequence 1	2	3	4	5	6
7-2-1	φ_f	31.3	30.8	30.8	30.7	29.6	
	φ_i	29.5	28.2	28.2	27.9	28.4	
7-2-2	φ_f	31.1	30.8	29.3	27.8	29.1	
	φ_i	28.9	30.5	23.9*	27.8	26.6	
7-3-1	φ_f	38.9	38.3	38.4	38.9	37.9	38.2
	φ_i	36.4	31.6	38.4	34.9	34.5	31.8
7-3-2	φ_f	38.4	35.9	36.2	40.1	37.9	37.0
	φ_i	33.9	33.7	36.1	35.9	32.9	36.8
8-1-1	φ_f	24.5	20.8	19.5	24.5	20.8	26.6
	φ_i	23.9	18.7	19.5	24.1	20.5	26.6
8-2-1	φ_f	32.6	31.3	41.2	43.4	34.9	36.8
	φ_i	24.7	31.3	36.8	38.9	29.7	36.8
8-2-2	φ_f	35.5	42.6	41.2	37.9	41.1	37.9
	φ_i	35.5	42.6	41.2	35.8	41.1	37.9
9-1-1	φ_f	32.0	32.0	32.1	28.3	32.1	36.1
	φ_i	32.0	29.0	26.1	28.3	29.2	31.6
9-1-2	φ_f	33.1	32.6	32.6	31.8	33.2	32.9
	φ_i	30.5	32.0	27.6*	31.1	30.5	29.5*

Sliding Sample		Testing Sequence 1	2	3	4	5	6
9-2-1	φ_f	43.8	38.4	38.2	40.8	45.8	
	φ_i	43.8	38.4	38.2	40.8	38.4	
9-2-2	φ_f	41.4	41.3	39.2	41.7	42.6	40.3
	φ_i	39.1	39.1	39.2	39.5	37.5	37.1
10-1-1	φ_f	33.9	31.8	32.1	33.9	34.5	31.8
	φ_i	33.9	28.9*	31.1*	28.9	29.2	27.1
10-1-2	φ_f	28.7	31.3	29.5	26.2	26.2	27.6
	φ_i	28.7	26.3	25.4	26.2	26.2	27.6
10-2-1	φ_f	34.6	34.1	30.3	28.9	30.3	29.3
	φ_i	34.6	34.1	30.3	28.9	30.3	29.3
10-2-2	φ_f	28.4	27.4	24.2	27.8	26.1	26.7
	φ_i	28.4	27.4	24.2	27.8	26.1	26.7
11-1-1	φ_f	25.8	22.9	22.1	22.2	22.4	22.9
	φ_i	24.2	21.8	18.7	19.5*	20.3*	20.0*
11-1-2	φ_f	26.8	27.6	26.3	25.3	23.4	24.6
	φ_i	25.8	24.7	22.6*	23.7*	21.6*	20.8*
12-1-1	φ_f	31.3	27.6	26.3	25.3	23.7	24.7
	φ_i	25.8	24.7	22.6*	23.7*	21.8*	20.8*

Sliding Sample		Testing Sequence 1	2	3	4	5	6	7
13-1-1	φ_f	31.8	27.4	21.4	21.4	21.8	19.7	
	φ_i	31.8	27.4	21.4	21.4	21.8	19.7	
13-1-2	φ_f	24.2	21.6	25.8	23.2	24.1	27.6	
	φ_i	24.2	18.2	23.9	23.2	18.4	27.6	
14-1-1	φ_f	25.9	23.4	23.2	23.2	23.9	23.7	
	φ_i	20.0*	18.7*	13.7*	16.8*	11.1*	10.5*	
15-1-1	φ_f	21.3	22.9	22.2	21.1	18.7	20.4	
	φ_i	18.4	19.2	17.6	19.6	15.5	16.3	
15-1-2	φ_f	23.4	22.1	21.2	22.1	22.9	20.4	
	φ_i	23.4	20.0	21.2	20.0	19.7	20.4	
16-1-1	φ_f	37.4	35.3	36.3	34.6	35.3	34.7	
	φ_i	37.4	33.7	36.3	34.6	35.3	34.5	
16-1-2	φ_f	32.4	31.8	32.4	30.0	30.8	30.0	
	φ_i	32.4	27.1*	31.3	27.6*	27.9	30.0	
20-1-1	φ_f	38.1	33.9	32.1	33.7	34.7	34.7	32.6
	φ_i	38.1	33.9	30.0	30.9	34.1	34.7	32.6
20-1-2	φ_f	40.0	38.4	33.7	36.3	33.9	42.9	34.7
	φ_i	40.0	38.4	33.7	36.3	33.9	42.9	34.7

Sliding Sample		Testing Sequence 1	2	3	4	5	6	7	8
25-1-1	φ_f	41.4	40.1	38.6	37.9	39.9	38.2		
	φ_i	39.5	34.7	33.7	35.8	34.5	35.0		
26-1-1	φ_f	33.7	33.7	39.5	30.8	36.8	32.9	35.8	
	φ_i	33.7	33.7	39.5	30.8	36.8	32.9	35.8	
27-1-1	φ_f	30.5	32.9	29.2	31.7	30.4	29.9	28.0	28.4
	φ_i	30.5	32.9	29.2	31.7	30.4	29.9	28.0	28.4
27-1-2	φ_f	32.9	33.7	31.1	32.1	30.9	29.1		
	φ_i	32.9	33.7	31.1	32.1	30.9	29.1		
27-2-1	φ_f	30.5	30.2	30.5	28.4	28.9	27.1		
	φ_i	30.5	28.7	26.3	26.3	27.4	26.4		
27-2-2	φ_f	31.6	28.2	27.0	26.3	26.1	24.2		
	φ_i	29.2	28.2	23.9*	26.3	26.1	24.2		
28-1-1	φ_f	36.6	30.0	27.6	27.6	29.5	26.3		
	φ_i	36.6	27.9	26.8	26.3	24.5*	22.1*		
28-1-2	φ_f	33.9	31.8	26.6	29.7	26.6	23.7		
	φ_i	27.4	31.8	26.6	23.9	24.7	22.1		
28-2-1	φ_f	33.9	33.3	31.4	30.7	29.9	29.6		
	φ_i	33.9	33.3	31.4	30.7	29.9	29.6		

Sliding Sample		Testing Sequence 1	2	3	4	5	6	7
29-1-1	φ_f	35.0	32.9	32.4	31.8	28.7	28.2	
	φ_i	35.0	32.9	32.4	31.8	26.6	28.2	
29-1-2	φ_f	36.6	40.9	31.1	26.6	32.2	27.1	26.3
	φ_i	36.6	40.9	29.5	26.6	32.2	27.1	24.5
30-1-1	φ_f	33.7	30.5	28.8	29.2	31.1	29.2	28.9
	φ_i	26.6	30.5	28.7	29.2	26.3	29.2	28.7
30-1-2	φ_f	33.4	34.1	30.8	29.2	28.4	28.7	27.6
	φ_i	31.3	33.9	30.8	26.3	28.4	28.7	27.6
31-1-1	φ_f	37.6	37.6	36.8	36.3	36.1	35.8	36.8
	φ_i	37.6	37.6	35.5	36.3	32.9	35.8	34.2
31-1-2	φ_f	38.4	36.1	31.3	26.6	27.1	37.6	32.9
	φ_i	38.4	36.1	31.3	26.6	27.1	37.6	32.9
35-1-1	φ_f	44.5	34.8	35.7	36.6	33.9	38.0	
	φ_i	37.4	26.3	34.5	33.4	30.8	38.0	
35-1-2	φ_f	40.5	41.6	40.0	40.8	40.8	40.0	
	φ_i	38.2	36.1	37.9	34.7	40.5	39.5	
42-1-1	φ_f	36.3	36.1	31.1	31.1	32.4	30.8	30.3
	φ_i	33.2*	35.8	25.0*	30.8	25.0*	25.5*	24.2*

Sliding Sample		Testing Sequence 1	2	3	4	5	6	7
42-1-2	φ_f	37.4	38.7	36.3	36.2	34.7	37.4	35.9
	φ_i	37.4	38.7	36.3	36.2	34.7	37.4	35.9
42-2-1	φ_f	39.1	33.8	34.5	35.5	34.3	36.1	33.9
	φ_i	36.1	29.5	32.5	35.1	33.0	32.1	27.9
42-2-2	φ_f	33.9	34.7	33.3	33.2	33.4	32.9	31.7
	φ_i	31.8	27.5	28.2	30.4	29.5	28.9	31.6

* : Creep occurred when testing the sample.

φ_f: Final sliding angle.

φ_i: Initial sliding angle.

Table A.2 Results of chemical analyses of the carbonates

Sample	$[Ca^{2+}]$ (ppm)	$[Mg^{2+}]$ (ppm)	W_{Ca} (mg)	W_{Mg} (mg)	M_{Ca} (millimole)	M_{Mg}	W_{Do} (mg)	W_{Ci} (mg)	W_R (mg)
1-1	12.7	2.58	158.75	32.25	3.9608	1.3265	244.62	263.67	0
1-2	11.9	2.80	148.75	35.00	3.7113	1.4396	265.48	227.37	0
2-1	16.7	0.15	208.75	1.88	5.2083	0.0771	14.22	513.58	7.2
4-1	9.0	0.13	112.50	1.62	2.8069	0.0668	12.32	274.26	199.4
7-1	12.2	2.37	152.50	29.62	3.8048	1.2185	224.70	267.88	0
7-2	6.0	1.95	75.00	24.38	1.8713	1.0026	184.89	86.95	222.4
7-3	14.2	0.74	177.50	9.25	4.4286	0.3805	70.17	405.17	27.5
8-1	15.6	0.56	194.38	6.94	4.8496	0.2854	52.63	456.83	0
8-2	15.9	0.34	198.75	4.25	4.9588	0.1748	32.23	478.83	0
9-1	13.8	0.87	172.50	10.88	4.3039	0.4473	82.49	386.01	21.5
9-2	15.6	0.20	195.00	2.50	4.8653	0.1028	22.28	476.68	6.5
10-1	10.4	3.65	130.00	45.62	3.2435	1.8766	346.06	136.81	15.8
10-2	15.9	0.10	198.75	1.25	4.9588	0.0514	9.48	491.18	0
13-1	7.0	4.05	87.50	50.62	2.1831	2.0823	384.00	10.09	92.6
14-1	8.5	4.90	106.25	61.25	2.6509	2.5193	464.58	13.17	6.8
15-1	8.5	4.96	106.25	62.00	2.6509	2.5502	470.28	10.08	0
16-1	13.8	1.21	172.50	15.12	4.3039	0.6221	114.72	368.51	18.2
20-1	16.1	0.40	201.25	5.02	5.0212	0.2066	38.09	481.90	0
25-1	15.6	0.12	195.00	1.50	4.8653	0.0617	11.38	480.79	9.0
26-1	10.8	3.43	135.00	42.88	3.3683	1.7635	325.21	160.62	16.0
27-1	15.0	0.15	187.50	1.88	4.6781	0.0771	14.22	460.51	22.6
27-2	2.2	1.45	27.50	18.12	0.6861	0.7455	137.48	0	371.9
28-1	11.1	0.12	138.75	1.50	3.4618	0.0617	11.38	340.31	144.8
28-2	6.9	3.55	86.72	44.35	2.1679	1.8253	336.58	34.26	138.4
29-1	12.6	0.61	157.50	7.63	3.9296	0.3136	57.83	361.92	70.6
30-1	15.0	0.23	187.50	2.88	4.6781	0.1183	21.82	456.39	19.3
31-1	14.2	0.84	177.50	10.50	4.4286	0.4319	79.65	400.03	10.5
35-1	15.4	0.11	192.50	1.38	4.8029	0.0566	10.44	475.06	20.5
42-1	10.0	2.27	125.00	28.38	3.1188	1.1671	215.22	195.35	101.2
43-1	13.8	0.69	172.50	8.62	4.3039	0.3548	65.43	395.26	27.6

$[Ca^{2+}]$ and $[Mg^{2+}]$ are concentrations of Ca^{2+} and Mg^{2+}.

W_{Ca} and W_{Mg} are weights of calcium and magnesium.

M_{Ca} and M_{Mg} are numbers of atomic milligrams of Ca and Mg.

W_{Do}, W_{Ci} and W_R are weights of dolomite, calcite and residual respectively.

Table A.3 Results of indentation tests

Sample	M_0(mm)	D_2(mm)	M_2(mm)	Pm(mm)	Im	σ_c(MPa)
1-1	9.820	1.27	11.290	0.20	6.35	227
7-1	11.725	1.27	13.225	0.23	5.52	198
8-1	10.205	1.27	11.760	0.285	4.46	160
10-2	11.545	1.27	12.055	0.24	5.29	189
11-1	11.620	1.27	13.015	0.125	10.16	364
14-1	11.560	1.27	13.000	0.17	7.47	267
20-1	11.190	1.27	12.650	0.19	6.68	239
28-1	11.725	1.27	13.190	0.195	6.51	233
30-1	11.960	1.27	13.410	0.18	7.06	253
35-1	11.870	1.27	13.340	0.20	6.35	227

M_0 is the initial reading of the micrometer.

D_2 is the spring deflection.

M_2 is the reading of the micrometer corresponding to D_2.

Pm is the penetration of the cone into the sample.

Im is the modified cone indenter number.

σ_c is the uniaxial compressive strength.